NEW CONTROL METHODS FOR A CLASS OF NONLINEAR SYSTEMS WITH CONSTRAINED INPUT

By

ATIF ALI

A DISSERTATION

Submitted to

National University of Sciences and Technology

in partial fulfillment of the requirements for the degree of

DOCTOR OF PHILOSOPHY

Supervised by

DR MOHAMMAD BILAL MALIK

College of Electrical and Mechanical Engineering

National University of Sciences and Technology, Pakistan

2016

In the name of Allah, the most Merciful and the most Beneficent

DECLARATION

I certify that the research work titled "NEW CONTROL METHODS FOR A CLASS OF NONLINEAR SYSTEMS WITH CONSTRAINED INPUT" has been carried out by me and it's entirely my own research effort. The research work presented in this thesis has not been submitted anywhere else for appraisal. Also, any data taken from primary or secondary sources has been properly cited and acknowledged.

Signature of Student

(Atif Ali)

(2008-NUST-DirPhD-EE-14)

ABSTRACT

NEW CONTROL METHODS FOR A CLASS OF NONLINEAR SYSTEMS WITH CONSTRAINED INPUT

By

ATIF ALI

Conventional nonlinear feedback control tools include linearization, gain scheduling, integral control, feedback linearization, sliding mode control, Lyapunov redesign, back stepping, passivity based control etc. Each of these techniques is designed to deal with a specific nature of problem. None of these methods are universal in the sense that it can be applied to all classes of nonlinear control problems. The realm of nonlinear control systems encounters theoretical and practical problems that do not fit into existing frameworks. This demands development of novel and innovative methods that go beyond conventional philosophy of control systems. This thesis also deals with such class of problems that is difficult to deal due to usual nonlinear control techniques. The core issue is hard constraints on the input of the system, that restrict the freedom of a control designer to incorporate control methods based on continuous stabilization, cancellation, compensation and/or adjustment of control parameters.

The thesis starts with a discussion on sampled data tracking problem for a class of multi-input multi-output (MIMO) nonlinear systems. The nature of system is generic enough to handle many theoretical and practical problems. However, the thesis broadly focuses on a challenging example of the two-axis orientation control of a gyroscopic system with constrained input. During a single sample period, only a fixed amplitude pulse of variable position and width can be applied as a single control input. The example also falls in the

category of under actuated systems due to single control of two axes. Alternately, pulse width and position can be construed as two inputs of the system. The output is also assumed to be available at only the sampling instants. All these restrictions result in a complex problem whose exact solution is not possible and thus we have to resort to approximate methods.

The thesis begins with exploration of classical techniques. Firstly, a more conventional pulse width modulation approach based on principle of equivalent areas is proposed. This is followed by an error minimized control technique which is based on optimal control. The solution minimizes a cost function so as to obtain optimal values of pulse width and position. The problems of local minima and non-causality have to be addressed in order to solve the problem. The main contribution of the thesis is a particle controller for the class of systems under discussion. The classical theory of particle filters is adapted in order to solve the global optimization problem. A deterministic problem is solved using stochastic tools. The idea is to associate the cost function to be minimized with a probability density function (pdf). Input samples are drawn according to this pdf which are subsequently assigned weights using simulations of the system. The process includes steps like generation, refinement, regeneration, resampling etc. some of which are familiar in the realm of particle filters. This unconventional control philosophy has the potential to address a variety of control problems that are difficult to handle using available tools.

Extensive Monte Carlo simulations have been performed for each of the above techniques. Where applicable, performance comparisons have also been made. The suggested techniques are computationally heavy and require fast processing. However, they suit parallel computing and can thus be embedded using FPGAs or ASICs.

To

My Parents and my Family

ACKNOWLEDGEMENTS

I would like to express my sincerest gratefulness for the guidance and support of all my teachers whose intense efforts have made possible the efficacious completion of this work. The knowledge that I obtained from them proved advantageous throughout the path of my studies. I would like to express gratitude to my supervisor, Dr Mohammad Bilal Malik, , both for accommodating me as his PhD student and for imparting beneficial guidance, counseling and support over the years leading towards the completion of this thesis.

I would like to convey my earnest appreciation to Dr Mohammad Ali Maud, Dr Fahad Mumtaz Malik, Dr Muwahida Liaquat, Dr Muhammad Salman Masood, Dr Valiuddin, Dr Shahzad Amin Sheikh, Muhammad Usman Akhtar, Rahat Ali, Asghar Ali, and Iftikhar Ali for their valuable time, consideration and encouragement. I gratefully acknowledge the assistance I received from Nauman Anwer, Zeeshan, Noman Razzak and Muhammad Asim Ejaz and all officers attached with EME College.

I am thankful to my father Dr. Wajahat Ali whose belief in me helped me to remain focused in difficult times and to my mother for her guidance, support and prayers. I am obliged to my sister Dr. Sadia Fatima and my brother Adil Ali who have been sources of encouragement and inspiration for me and their prayers have complemented me throughout my life. I am indebted to my wife and children Umer, Zainab and Usman who have been very compliant and supportive and have shown remarkable patience all the way along.

I would also like to thankfully acknowledge National University of Sciences and Technology (NUST) for the financial assistance they provided for my studies and research.

TABLE OF CONTENTS

LIST OF FIGURES

LIST OF TABLES

CHAPTER 1

INTRODUCTION

The focal point of this dissertation is to discover new methods to control a class of nonlinear systems under constrained input. To drive such systems generally two types of actuators are utilized namely servo and on-off type. This restriction makes it inconvenient to apply the classical or conventional control schemes such as linearization, gain scheduling, integral control, feedback linearization, sliding mode control, Lyapunov redesign, back stepping, passivity based control etc to control such systems. These proven techniques have also matured with time and offer limited gaps for improvements. After a thorough literature review, it becomes slightly difficult to decide the start point for the research. Therefore a multi-pronged approach was adopted. In which pure classical techniques based on optimization as well as latest concepts to use particle filter in control theory was carried out. A brief pictorial overview of the proposed approach is shown in the figure 1-1.

1.1 Research Objectives

The overall objective of the thesis is to develop new methods for a class of nonlinear systems under constrained input. Following are three specific objectives that must be satisfied in order to satisfy the overall objective:

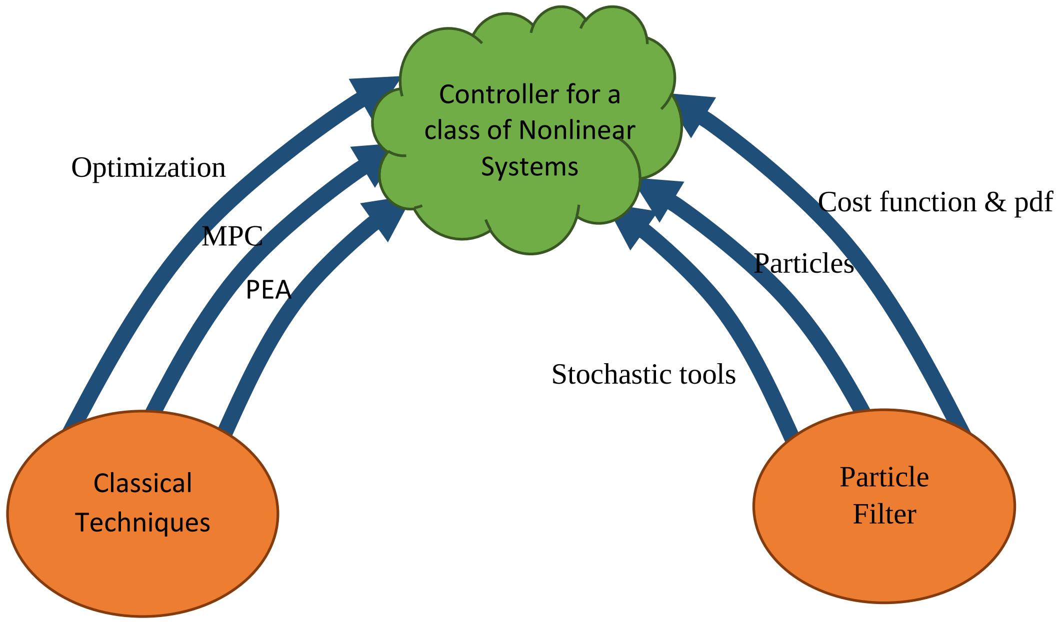

Figure1.1: Evolution of new Methods

- Develop a framework for modeling a class of MIMO nonlinear system with constrained input. This model includes an error model for the design of control law that guarantees asymptotic tracking.

- Based on literature review, explore conventional techniques as well as latest particle filter theory for development of new methods and their comparison with the existing techniques.

- Discuss mathematical model for the class of nonlinear systems with constrained input under consideration.

- Design a control law under given constraints for suitable tracking of reference signal by employing the developed control techniques.

1.2 Particle Filter – Introduction

Sequential Monte Carlo method or the particle filter [1] was presented as a numerical approximation to the nonlinear Bayesian filtering problem in 1993. It is mainly used to deal nonlinear and non-Gaussian problems and based on the concept of Bayesian theory and sequential importance sampling [2]. The basic idea of this sequential Monte Carlo methodology is the recursive computation of relevant probability distributions with discrete random measures known as particles. These particles are actually the samples from the space of the unknowns. It approximates probability distributions with these particles and their associated weights. Using the concepts of sampling and approximated pdf (through particles), the particle filter approximates relevant distributions. To be concise, particle methods are a set of powerful and versatile simulation-based methods to execute optimal state estimation in nonlinear non-Gaussian state-space models.

The benefit of particle filtering over other methods is that the approximation does not involve linearization around current estimates but instead approximations in the representation of the desired distributions by discrete random measures.

1.3 Literature review

Greenfield [3] was among the initial researchers who utilizes the concept of Particle filter in control theory. He proposed a method for finite horizon control that approximates the expected cost of a given control sequence using a finite number of samples. Andrieu, and Doucet in their famous research contribution [4] used particles to approximate the value function and its gradient in an optimal stochastic control problem, and use a gradient search method to find a locally optimal solution. Blackmore [5] applied the concept of

Particle Filter in control theory for state estimation. Interestingly, most of the researchers use the particle filters for state estimation as evident from [6,7,11,12,51-53]. They used particle filter exclusively as a state estimator by computing a point estimate from the particle cloud. This point estimate is then used in the usual Model Predictive Control (MPC) optimization procedure. In fact, the application of particles filter theory has allowed the MPC methodology to be extended to nonlinear non-Gaussian problems. Hol and Schon [10] made a comparison between four frequently encountered resampling algorithms for particle filters. Kantas [9] presented Sequential Monte Carlo (SMC) as the computational engine for general stochastic MPC problems. It shows how SMC methods can be used to find global optimizers of non-convex problems for solving open-loop stochastic control problems in case of receding-horizon implementation of MPC and thus allowing the MPC methodology to be extended to nonlinear non-Gaussian problems. De villers [8] explored sequential and batch Monte Carlo techniques to solve the Nonlinear MPC problem with stochastic system dynamics and noisy state observations. He has used Maximum A-posteriori (MAP) for control estimate and considered it as the optimal control sequence. Dominik Stahl [1] developed MPC by using two particle filters , one for the state estimation and the other for estimation of control input for the system. The authors have claimed that their technique is superior to other techniques developed so far. However they have used trivial methods for drawing of control input's transition pdf. In tracking applications control input has significant changes. If it is not given due considerations, then system performance will degrade significantly, and may even degrade the stability of the system.

1.4 Research Overview

Conventionally, the concept of weighted particles has addressed the problem of state estimation for nonlinear dynamical systems under the influence of non-Gaussian process/observation noises. Recently, the research focus has shifted towards designing of control law for nonlinear feedback systems using particle filter concepts. However, the focus of these researchers has been restricted to a class of optimal control problems related to :-

- Nonlinear stochastic systems
- Discrete-time systems

There are some gaps / weak areas which need attention in order to carry forward the work of these researchers, such as following :-

- Inter sample behavior in discrete systems is not covered as physical systems are continuous time models and their discrete time equivalent model results in loss of information. Sample data nonlinear system models are required if these methods are to be applied to physical systems.

- Following Optimization considerations are not covered :-

    - Existence of local minima should be considered. Otherwise, there is a possibility that the algorithm gets trapped in local minimum.

    - Search of global extremum is based on maximum weight particle, which estimate the mode of pdf under consideration. However, the sparsity of particles may compromise the accuracy of the estimate of mode.

- Theory of Particle filter has been extended to use in MPC. However, particular considerations for MPC or nonlinear control are not focused in above mentioned research. The specific nature of issues related to nonlinear systems has been left unaddressed.

- These methods inject stochastics features into the system which convert a deterministic system into its stochastic counterpart. This step is necessary if the conventional particle filter theory is directly adapted to solve the optimal control problem. Furthermore, in many physical systems the observations may be accurate enough, where observation noise is negligible.

- The example used by some of the authors can be solved by conventional control theory. Application of particle filter theory may not be computationally feasible. On the other hand, the example quoted in this thesis, cannot be handled by conventional methods.

- Some of the methods are iterative and hence are computationally intensive. De villers [8] used simulated annealing method which is computationally intensive as well as impractical too.

1.5 Under actuated systems

Control of under actuated systems has attracted a lot of attention from the researchers mainly because they are economically efficient. The applications of under actuated mechanical designs have shown significant improvement in the robust operating performance [39,40,41,48,49]. This also finds application in spin stabilized flying bodies, under actuated ships and satellite control schemes. The control of such under actuated systems has its limitations and is a challenging problem. To drive such systems, generally two types of actuators are utilized namely servo and on-off type [42,43 and the references therein]. The consequent design of control systems for such actuators involves nonlinear analysis and design. Various techniques such as the Principle of Equivalent Areas (PEA) for Pulse Width Modulation (PWM) [44,45,46,47,50] are used to design the linear control systems having on-off actuation mechanism. In addition they can be solved through optimal control theory and model predictive control techniques also.

1.6 Example of under actuated systems

The orientation control of a special drill machine specifically designed for drilling soft materials was presented in [13,14]. This special drill machine [13] is a typical example of an under actuated spinning system. The magnitude and phase of the actuation pulse are controlled by a discrete time controller. The underlying model of the controller is the discrete-time equivalent model of the plant. The plant is actuated for a short duration i.e., during a complete revolution of the bit and is unactuated otherwise. This leads to an under actuated control problem. The solution provided by [13] is effective in controlling the orientation, but has a major practical limitation. The pulse width of control input is fixed while its magnitude is proportional to the amount of control force required. In physical system such high amplitude may leads to saturation. On the other hand, limiting the maximum amplitude of the control signal restricts the overall movement and leads to stability issues.

The limitation of unlimited amplitude can be overcome by assuming the actuation pulse to be of fixed amplitude and variable duration. Adjusting the pulse width and delay of such control input is first carried out through the Principle of Equivalent Areas (PEA) .The main advantage of PEA is that it is practically implementable, but is based on approximation. Thus, for high modulation frequency, the averaging response becomes closer to the given control signal and consequently the higher model formulas are more difficult to convert using the PEA concept. The minimum pulse width which cannot be ignored is also a major limitation for developing exact PEA signal. This led to designing a more complex algorithm where the control input leads to non-closed form time variant solution. The controller design for such systems is a real challenge (where the orthodox control theory is not applicable). To overcome this limitation, an output feedback optimization algorithm based on the minimization of the error signal is proposed. The resultant actuating signal is generated based on the optimized values of pulse width and delay. It is shown via simulations that the presented scheme provided a smooth control for precise movement and overcome the limitations on the control effort. The cost function, however, appears to be ill behaved, resulting in multiple local minima. The elimination of local minima and the estimation of unique global minima is carried out through reference phase algorithm and multiple initial point algorithm (MIP) [15,16]. Global minimization plays an effective role in many real problems such as science, engineering and economy [17]. The causality is also assured by employing a sliding adjustment technique. However the real time application of this technique is not possible due to heavy computation which is required for the exhaustive search algorithms. This limitation was overcome through particle controller which is based on Bayesian philosophy.

1.7 Thesis Outline

The thesis is organized in six chapters including the introduction. The problem statement and main frame work is described in Chapter 2. In addition it describes the model of the under actuated drill machine. The various techniques which will be developed in subsequent chapters will be applied on this problem. Chapter 3 presents the control law based on PWM and PEA techniques for tracking problem of an under actuated and input constrained problem. Various results along with their limitations are also discussed. Chapter 4 presents the Error minimization control algorithm, which is based on MPC and optimal control theory. It highlights the local minima issues and presents novel techniques for searching algorithm of global minima. It also covers the causality issues and methods to avoid system becoming non- casual. Chapter 5 covers the literature review of particle filter theory and development of Particle controller for a class of non-linear systems. Chapter 6 is the last chapter which concludes the thesis and suggests few ideas for future research work.

CHAPTER 2

PROBLEM DEFINATION

2.1 Continuous-time Nonlinear System

Consider the following class of multi-input, multi-output nonlinear system

$$\begin{aligned} \dot{x} &= f(x) + G(x)u \\ y &= H(x) \end{aligned} \tag{2.1}$$

where $x \in R^n$ is the state, $u \in R^m$ and $y \in R^m$ are the m-dimensional input and output respectively. The dimension of input and output is considered the same for convenience. The vector field f is considered smooth. The $n \times m$ matrix $G(x) = [g_1(x) \quad \dots \quad g_m(x)]$ where $g_1(x) \quad \dots \quad g_m(x)$ are smooth vector fields. Similarly the $m \times m$ matrix $H(x) = [h_1(x) \quad \dots \quad h_m(x)]^T$ where $h_1(x) \quad \dots \quad h_m(x)$ are smooth function.

The system is assumed to have a vector relative degree $\{\rho_1, ...\rho_m\}$ such that $\rho_1 + \rho_2 + \dots \rho_m \le n$. Consequently, the model (2.1) can be transformed into the normal form with a diffeomorphism as follows

$$
\begin{aligned}
&\dot{\eta} = f_0(\eta,\xi) \\
&\dot{\xi}_1^1 = \xi_2^1 \\
&\dot{\xi}_2^1 = \xi_3^1 \\
&\vdots \\
&\dot{\xi}_{\rho_1}^1 = b_1(\xi,\eta) + a_{11}(\xi,\eta)u_1 + a_{12}(\xi,\eta)u_2 + \cdots + a_{1m}(\xi,\eta)u_m \\
&\dot{\xi}_1^2 = \xi_2^2 \\
&\dot{\xi}_2^2 = \xi_3^2 \\
&\vdots \\
&\dot{\xi}_{\rho_2}^2 = b_2(\xi,\eta) + a_{21}(\xi,\eta)u_1 + a_{22}(\xi,\eta)u_2 + \cdots + a_{2m}(\xi,\eta)u_m \\
&\vdots \\
&\dot{\xi}_1^m = \xi_2^m \\
&\dot{\xi}_2^m = \xi_3^m \\
&\vdots \\
&\dot{\xi}_{\rho_m}^m = b_m(\xi,\eta) + a_{m1}(\xi,\eta)u_1 + a_{m2}(\xi,\eta)u_2 + \cdots + a_{mm}(\xi,\eta)u_m
\end{aligned}
$$

and

$$
y = \begin{bmatrix} y_1 \\ y_2 \\ \vdots \\ y_m \end{bmatrix} = \begin{bmatrix} \xi_1^1 \\ \xi_1^2 \\ \vdots \\ \xi_1^m \end{bmatrix}
$$

where $\xi^i \in R^{\rho_i}$ represent the dynamic relationship of output $y_i(t)$, for $1 \le i \le m$ with input $[u_1, u_2, \ldots, u_m]^T$ and $\eta \in R^{n-\rho}$ are the zero dynamics of the system. The maps $a_{ij}(\eta,\xi) = L_{g_i} L_f^{\rho_j - 1}(h_j(x))$ and $b_i(\eta,\xi) = L_f^{\rho_i}(h_i(x))$ respectively for $1 \le i, j \le m$.

It may be noted here that at least one of $a_{ij}(\eta,\xi) = L_{g_i} L_f^{\rho_j - 1}(h_j(x))$ is nonzero in last state equation for each relative degree indicating connection of every output with at least one of the inputs.

The system can be written in the compact vector form (2.2) as

$$\begin{aligned} \dot{\eta} &= f_0(\eta,\xi) \\ \dot{\xi} &= A_c\xi + B_c\phi(\eta,\xi,u) \\ y &= C_c\xi \end{aligned} \tag{2.2}$$

where $A_c = \text{block diag}\left[A_1,......,A_m\right],\ A_i = \begin{bmatrix} 0 & 1 & \cdots & \cdots & 0 \\ 0 & 0 & 1 & \cdots & 0 \\ \vdots & & & & \vdots \\ 0 & \cdots & \cdots & 0 & 1 \\ 0 & \cdots & \cdots & \cdots & 0 \end{bmatrix}_{\rho_i \times \rho_i}$,

$B_c = \text{block diag}\left[B_1,......,B_m\right],\ B_i = \begin{bmatrix} 0 \\ 0 \\ \vdots \\ 0 \\ 1 \end{bmatrix}_{\rho_i \times 1}$,

$C_c = \text{block diag}\left[C_1,......,C_m\right],\ C_i = \begin{bmatrix} 1 & 0 & \cdots & 0 & 0 \end{bmatrix}_{1 \times \rho_i}$, and

$$\phi(\eta,\xi,u) = \begin{bmatrix} \phi_1(\eta,\xi,u) \\ \phi_2(\eta,\xi,u) \\ \vdots \\ \phi_m(\eta,\xi,u) \end{bmatrix}$$

with $\phi_i(\eta,\xi,u) = b_i(\xi,\eta) + a_{i1}(\xi,\eta)u_1 + a_{i2}(\xi,\eta)u_2 + \cdots + a_{im}(\xi,\eta)u_m$.

2.2 Asymptotic Tracking Problem

The objective is to asymptotically track the reference signal $r(t) = \left[r_i(t).....r_m(t)\right]^T$ such that $\lim_{t\to\infty}\|e(t)\| \to 0$ where *e(t)* is the tracking error defined as

$$e(t) = y(t) - r(t)$$

The reference signal is sufficiently smooth. Moreover, it is assumed that the reference signal and derivative of its components up to the respective relative degree, i.e. $r_i^{(\rho_i)}$ for $1 \le i \le m$ are available online.

Considering the normal form representation of the nonlinear system (2.2), the tracking error can be elaborated as

$$\begin{aligned}
e_1^i &= \xi_1^i - r_i \\
e_2^i &= \xi_2^i - r_i^{(1)} \\
e_3^i &= \xi_3^i - r_i^{(2)} \\
&\vdots \\
e_{\rho_i}^i &= \xi_{\rho_i}^i - r_i^{(\rho_i - 1)}
\end{aligned}$$

for $1 \le i \le m$. The tracking error dynamics are therefore represented by

$$\begin{aligned}
\dot{e}_1^i &= \dot{\xi}_2^i - \dot{r}_1^{(1)} = e_2^i \\
\dot{e}_2^i &= e_3^i \\
&\vdots \\
\dot{e}_{\rho_i}^i &= \dot{\xi}_{\rho_i}^i - r_i^{(\rho_i)} = \phi_i(\eta, \xi, u) - r_i^{(\rho_i)}
\end{aligned} \tag{2.3}$$

$$
\begin{aligned}
&\dot{e}_1^1 = e_2^1 \\
&\dot{e}_2^1 = e_3^1 \\
&\vdots \\
&\dot{e}_{\rho_1}^1 = b_1(\xi,\eta) + a_{11}(\xi,\eta)u_1 + a_{12}(\xi,\eta)u_2 + \cdots + a_{1m}(\xi,\eta)u_m - r_1^{(\rho_1)} \\
&\dot{e}_1^2 = \xi_2^2 \\
&\dot{e}_2^2 = \xi_3^2 \\
&\vdots \\
&\dot{e}_{\rho_2}^2 = b_2(\xi,\eta) + a_{21}(\xi,\eta)u_1 + a_{22}(\xi,\eta)u_2 + \cdots + a_{2m}(\xi,\eta)u_m - r_2^{(\rho_2)} \\
&\vdots \\
&\dot{e}_1^m = \xi_2^m \\
&\dot{e}_2^m = \xi_3^m \\
&\vdots \\
&\dot{\xi}_{\rho_m}^m = b_m(\xi,\eta) + a_{m1}(\xi,\eta)u_1 + a_{m2}(\xi,\eta)u_2 + \cdots + a_{mm}(\xi,\eta)u_m - r_m^{(\rho m)}
\end{aligned}
$$

$$
\begin{aligned}
&\dot{e}_{\rho_1}^1 = b_1(\xi,\eta) + a_{11}(\xi,\eta)u_1 + a_{12}(\xi,\eta)u_2 + \cdots + a_{1m}(\xi,\eta)u_m - r_1^{(\rho_1)} \\
&\dot{e}_{\rho_2}^2 = b_2(\xi,\eta) + a_{21}(\xi,\eta)u_1 + a_{22}(\xi,\eta)u_2 + \cdots + a_{2m}(\xi,\eta)u_m - r_2^{(\rho_2)} \\
&\vdots \\
&\dot{e}_{\rho_m}^m = b_m(\xi,\eta) + a_{m1}(\xi,\eta)u_1 + a_{m2}(\xi,\eta)u_2 + \cdots + a_{mm}(\xi,\eta)u_m - r_m^{(\rho m)}
\end{aligned}
$$

$$
\dot{e} = B(\eta,\xi) + A(\eta,\xi)u - r^{(\rho)}
$$

$$
A(\eta,\xi) = \begin{bmatrix} a_{11}(\eta,\xi) & a_{12}(\eta,\xi) & \cdots & a_{1m}(\eta,\xi) \\ a_{21}(\eta,\xi) & a_{22}(\eta,\xi) & \cdots & a_{2m}(\eta,\xi) \\ \vdots & \vdots & \vdots & \vdots \\ a_{m1}(\eta,\xi) & a_{m2}(\eta,\xi) & \cdots & a_{mm}(\eta,\xi) \end{bmatrix}
$$

$$
B(\eta,\xi) = \begin{bmatrix} b_1(\eta,\xi) \\ b_2(\eta,\xi) \\ \vdots \\ b_m(\eta,\xi) \end{bmatrix} \quad r^{(\rho)} = \begin{bmatrix} r_1^{(\rho_1)} \\ r_2^{(\rho_2)} \\ \vdots \\ r_m^{(\rho_m)} \end{bmatrix} \quad v = \begin{bmatrix} v_1 \\ v_2 \\ \vdots \\ v_m \end{bmatrix} \quad u = \begin{bmatrix} u_1 \\ u_2 \\ \vdots \\ u_m \end{bmatrix} \quad \dot{e} = \begin{bmatrix} \dot{e}_1 \\ \dot{e}_2 \\ \vdots \\ \dot{e}_m \end{bmatrix}
$$

for $1 \le i \le m$, which can be written in the matrix notation described earlier as

$$\dot{e} = Ae + B\begin{bmatrix} \phi_1(\eta,\xi,u) - r_1^{(\rho_1)} \\ \phi_2(\eta,\xi,u) - r_2^{(\rho_2)} \\ \vdots \\ \phi_m(\eta,\xi,u) - r_m^{(\rho_m)} \end{bmatrix} \tag{2.4}$$

2.2.1 The Classical Tracking Controller

For a minimum phase system with continuous-time state feedback and unconstrained input, design of control law that guarantees asymptotic tracking becomes trivial, such as discussed in [19]. For example, defining

$$u = A^{-1}(\eta,\xi)[-B(\eta,\xi) + v + r^{(\rho)}] \tag{2.5}$$

Where $$A(\eta,\xi) = \begin{bmatrix} a_{11}(\eta,\xi) & a_{12}(\eta,\xi) & \cdots & a_{1m}(\eta,\xi) \\ a_{21}(\eta,\xi) & a_{22}(\eta,\xi) & \cdots & a_{2m}(\eta,\xi) \\ \vdots & \vdots & \vdots & \vdots \\ a_{m1}(\eta,\xi) & a_{m2}(\eta,\xi) & \cdots & a_{mm}(\eta,\xi) \end{bmatrix},$$

$$B(\eta,\xi) = \begin{bmatrix} b_1(\eta,\xi) \\ b_2(\eta,\xi) \\ \vdots \\ b_m(\eta,\xi) \end{bmatrix}, \qquad r^{(\rho)} = \begin{bmatrix} r_1^{(\rho_1)} \\ r_2^{(\rho_2)} \\ \vdots \\ r_m^{(\rho_m)} \end{bmatrix}, \qquad v = \begin{bmatrix} v_1 \\ v_2 \\ \vdots \\ v_m \end{bmatrix}.$$

The tracking error dynamics of the resulting closed loop system are represented by

$$\begin{aligned} \dot{e}_1^i &= e_2^i \\ \dot{e}_2^i &= e_3^i \\ &\vdots \\ \dot{e}_{\rho_i}^i &= v_i \end{aligned},$$

which can be written in the compact vector form as

$$\dot{e} = Ae + Bv \qquad (2.6)$$

Choosing $v = Ke$ such that eigenvalues of $A + BK$ are in the left half plane [21] guarantees asymptotic tracking.

2.2.2 Output feedback tracking controller

In case of output feedback with the non-availability of system states ξ_j^i, $1 \le i \le \rho_j$ and $1 \le j \le m$ for feedback, a suitable observer can be used for state estimates $\hat{\xi}_j^i$ with $1 \le i \le \rho_j$ and $1 \le j \le m$ [19]. The tracking problem for a nonlinear system without zero dynamics using the estimated system states is defined as follows

$$\begin{aligned}
\hat{e}_1^i &= \hat{\xi}_1^i - r_i \\
\hat{e}_2^i &= \hat{\xi}_2^i - r_i^{(1)} \\
\hat{e}_3^i &= \hat{\xi}_3^i - r_i^{(2)} \\
&\vdots \\
\hat{e}_{\rho_i}^i &= \hat{\xi}_{\rho_i}^i - r_i^{(\rho_i - 1)}
\end{aligned}$$

with the tracking controller as discussed above, modified as

$$u = A^{-1}(\hat{\xi})[-b(\hat{\xi}) + v + r^{(\rho)}] \text{ and } v = K\hat{e}$$

2.2.3 **Sampled-data Output Feedback Control**

The compactness and robustness of digital electronics has prompted wide spread application of sampled data control systems. There are two aspects of sampled-data output feedback control

Sampled Output: In case of availability of sampled output for feedback, the following nonlinear observer is used to estimate system states

$$\hat{\xi}[k+1] = A_d\hat{\xi}[k] + B_d\phi(\hat{\xi}[k],u[k]) + H_p[k](y[k] - \hat{\text{y}}[\text{k}])$$

where A_d and B_d are discretized system and input matrices respectively and the gain $H_P[k]$ is chosen such that the estimation error asymptotically decays to zero. One such observer is the Sampled-data High Gain Observer discussed by Khalil and Dabroom [35].

The observable part ξ of (2.2) is written as

$$\dot{\xi}(t) = A\xi(t) + B\phi(\xi(t),u(t)) \tag{2.7}$$

$$y[k] = C[k]\xi[k] \tag{2.8}$$

Where $\xi \in R^p$ continuous time observable state vector. $\phi(\xi,u) \in R^m$ is the continuous time plant input and only sampled output $y[k] \in R^m$ is available for measurement.

The sampled output and continuous-time plant input is utilized for the reconstruction of system states of (2.7) with impulsive observer. The reconstruction of the system states is carried out in two steps. In the first step, open-loop estimation of continuous-time system states is carried out within the sampling interval by integrating (2.7). In the second step impulsive correction is introduced in the estimated states. The prediction impulsive observer for (2.7) &(2.8) is given as [54]

$$\dot{\hat{\xi}}(t) = A\hat{\xi}(t) + B\phi(\xi(t),u(t)) \qquad \text{kT} \le \text{t}<(\text{k}+1)\text{T} \tag{2.9}$$

$$\hat{\xi}[k+1] = \hat{\xi}(t^-) + H_p[k](y[k] - \hat{y}[k]) \qquad t = (k+1)T, \quad k = k_o,\ k_o+1,\ \ldots \tag{2.10}$$

Where $\hat{\xi} \in R^p$ is the prediction observer state and $H_p[k] \in R^{p \times m}$ is the time varying prediction observer gain matrix. The initial state of the observer is $\hat{\xi}(t_o) = \hat{\xi}_o$. Impulsive observer (2.9) and (2.10) function in two steps as explained above. It falls under a well-known predictor-corrector observer structure.

Discrete Control Decision: The second aspect of sampled-data control is the decision of the control input for the sampling interval at discrete points in time, i.e.

$$u(t) = \gamma(u[k]) \quad t \in [kT, (k+1)T)$$

where k is an integer and T is the sampling time. A typical representation of the above equation is the zero-order-held input, in which case

$$u(t) = u[k] \quad t \in [kT, (k+1)T)$$

2.3 Sampled-data output feedback tracking with constrained input

The definition of control law (2.5) in the previous section, to achieve asymptotic tracking is implicitly based on the assumption of availability of entire m-dimensional space for the input. However almost every practical applications is in contradiction with this assumption due to physical or design constraints. In such a case the input signal can only belong to the space of *admissible* inputs i.e. $u[k] \in U$. With such constraints the asymptotic tracking may become intractable in some cases. In this case the tracking problem can be cast as an optimization problem with the objective of minimizing the following scaler cost function over the sampling interval :-

$$J_K = \int_{kT}^{(K+1)T} \left(\xi(t) - r(t)\right)^2 dt \qquad (2.11)$$

As already discussed in the previous section, for the case of sampled-data control, the state $\xi(t)$ is not available, instead its discrete-time estimates $\hat{\xi}[k]$ are obtained using the observer. Using these discrete-time estimates, the estimated state $\hat{\xi}(t)$ over the sampling interval can be obtained by open loop integration as follows :-

$$\dot{\hat{\xi}} = A\xi + B\phi(\xi, u)$$

The control objective then becomes the minimization of the following cost function

$$\hat{J}_K = \int_{kT}^{(K+1)T} \left(\hat{\xi}(t) - r(t)\right)^2 dt$$

which can be elaborated as $\hat{J}_k = \hat{J}_{k1} + \hat{J}_{k2} + \cdots + \hat{J}_{kn}$

such that

$$\begin{aligned}
\hat{J}_{k1} &= \sum_{i=1}^{\rho_1} \int_{kT}^{(k+1)T} \left(\hat{\xi}_i^1(t) - r_1^{(i-1)}(t)\right)^2 dt \\
\hat{J}_{k2} &= \sum_{i=1}^{\rho_2} \int_{kT}^{(k+1)T} \left(\hat{\xi}_i^2(t) - r_2^{(i-1)}(t)\right)^2 dt \\
&\vdots \\
\hat{J}_{km} &= \sum_{i=1}^{\rho_m} \int_{kT}^{(k+1)T} \left(\hat{\xi}_i^m(t) - r_m^{(i-1)}(t)\right)^2 dt
\end{aligned}$$

2.4 Types of constraint on input signal

- **Direct Constraints**. Here the input signal can only belong to the space of *admissible* inputs i.e. $u \in U$.

  Where $u_{\min} \leq u \leq u_{\max}$

- **Parameterized Constraints**. The input signal has some parameters and those parameters belong to some admissible space :-

  $u = u(\theta)$
  where $\theta \in \Theta \mid \Theta \subseteq R^{p\times 1}$

- **Constraint on Sampling Time.**

  $u = u(\theta_s)$
  where θ_s may be dependent on T_s
  and $T_s \geq T_{\min}$ or may be fixed

- **Dynamic Constraints**. The input signal is constrained by the performance of the system. For example, backlash and coulomb friction.

  $u(x) \in U$ where $x \in \Theta$
  Θ is the region in which system is operating

2.5 Case Study (Under-actuated Drill Machine)

Use of drill Machine on multiple axis is very common in industry [14]. Precise drilling on fine and curved surfaces requires precise control. Here the challenge is to keep the axis of the drill bit precisely aligned so that it is normal to the surface where the hole is made. This orientation or alignment is required in two axes i.e. the vertical and horizontal axis, for clarity of understanding we can call them as pitch and yaw axes and thus requires two independent actuators for orientation. It is worth mentioning here that drilling on the soft material experiences negligible lateral resistance thus when the bit is orientated to some desired location the required change in control effort is negligible. Therefore drilling on soft surfaces requires orientation control rather than full compliance control. The control mechanism for orientation control of a special drill machine which is required to drill on the soft surfaces is considered here. Due to mounting limitations, the actuation mechanism of the drill is based on single pair of electromagnetic poles. The rotor is the drill bit itself and a permanent magnet is installed on it. When the magnetic field produced by the single pair of electromagnets interacts with that of the rotor, a torque is produced, which is used for the orientation control of the drill bit. The electromagnet installed on the stator are excited for short duration at specific points during the spinning of the drill bit and thus controls their orientation.

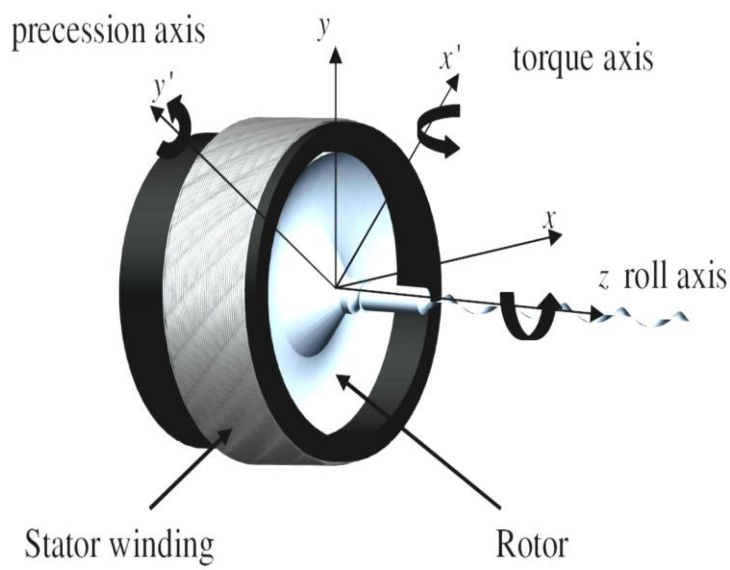

Figure 2.1 : Under Actuated Drill Machine [13]

2.5.1 Construction

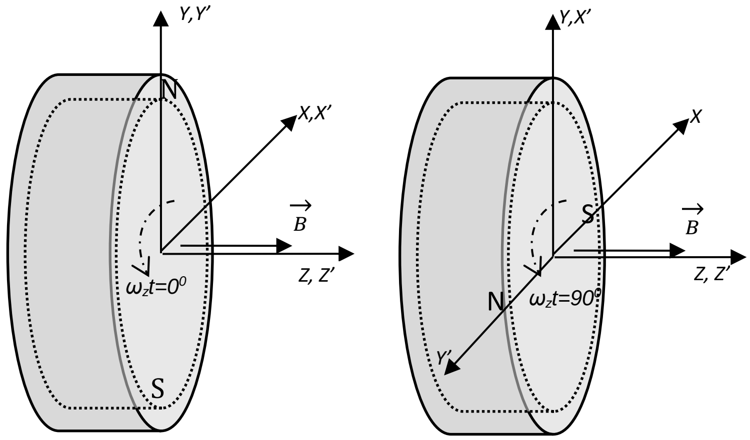

Figure 2.2 : Direction of Actuation

The construction is shown in the Figure 2.1. The rotor is a ring shaped permanent magnet and is mounted on a shaft which is connected with a universal joint. It spins or rotates about its z-axis, while right & left and up & down movements are about x-axis and y-axis respectively. A single coil is wound over the stator and excitation of the coil is responsible for the change of orientation of the rotor. The magnetic field produced by these electromagnetic poles interacts with that of permanent magnet mounted on the spinning shaft produces a torque which in turns is used for changing orientation of the drill bit. Since shaft is rotating, therefore both axes can be excited. But due to single pair of poles only one axis can be excited at one time, thus the fully actuated system converts into an under actuated system. The electromagnetic poles are excited for a specific duration at specific roll phase to orient the device in the desired direction.

2.5.2 Notations

X, Y, Z System of rectangular body fixed axes

X', Y', Z'	System of rectangular axes fixed to housing
H_z	Angular momentum along Z axis
τ_x, τ_y, τ_z	Torque vector along X, Y, Z axis
θ'_x, θ'_y	Angular positions about X'&Y' axes
$\omega_x, \omega_y, \omega_z$	Angular spin velocity along X, Y, Zaxis in radians per second
$\vec{B}$	Magnetic field due to stator winding
J_x, J_y, J_z	Moment of inertia along X, Y, Z axes
b	Coefficient of friction

2.5.3 Theorem 2.1

The time derivative of a vector $\vec{v}$ with respect to the inertial frame is related to the time derivative with respect to a rotating coordinate frame by [23]

$$\frac{d}{dt_I}\vec{v} = \frac{d}{dt_{rot}}\vec{v} + \vec{\omega}_{rot} \times \vec{v} \tag{2.12}$$

Where $\vec{\omega}_{rot}$ is the angular velocity of the rotating coordinate frame and subscript 'I' indicates that the derivative must be obtained with respect to inertial frame with its time derivative with respect to body axes.

2.5.4 Rotational dynamics

The frame of reference attached with the rotor is (X, Y, Z) and the other attached with the stator is (X', Y', Z') as shown in the Figure 2.2. The magnetic field produced by rotor magnet is always along rotor's Y axis.Therefore the torque produced will always be along rotor's X axis. As the rotor is spinning, therefore when $\omega_z t = 0^o$, the direction of torque is along stator's X'axis and when $\omega_z t = 90^o$, the direction of torque is along stator's Y' axis and so on.

It must be appreciated that a single actuation signal is controlling two degrees of freedom motion of the drill bit, which is the reason of under-actuation phenomenon of the drill machine. Also the actuation pulse is applied for a specific roll instant, when the field of rotor's permanent magnet and the unit vector of the projection of the desired position of the bit are perpendicular to each other. The duration is considered as a fraction of the time when compared with the time for a complete rotation of the drill bit. Moreover the actuation pulse can be applied only once in a complete revolution of the bit and the system will remain unactuated during the remaining time of a revolution.

According to Newton's second law the net moment acting on a body is equal to the time rate of change of angular momentum $\vec{H}$ and mathematically as:-

$$\vec{\tau} = \frac{d}{dt_I}\vec{H} \tag{2.13}$$

Where

$$\vec{H} = J_x\omega_x\hat{i} + J_y\omega_y\hat{j} + J_z\omega_z\hat{k} \tag{2.14}$$

Subscript "I" in (2.13) indicates that derivative should be obtained with respect to inertial frame. As the stator axis is non-inertial frame therefore (2.14) after employing (2.13) becomes

$$\vec{\tau} = \frac{d}{dt_r}\vec{H} + \left(\vec{\omega}_r \times \vec{H}\right) \tag{2.15}$$

Subscript "r" in (2.15) indicates rotor frame. The Euler equations in the rotor frame of reference are given as below :-

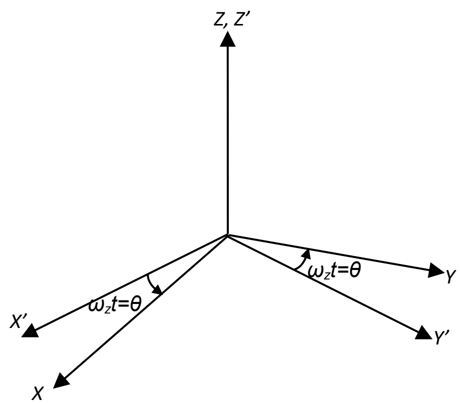

Figure 2.3 : Frame transformation [24]

$$
\begin{aligned}
\tau_x &= J_x \frac{d\omega_x}{dt} - \left(J_y - J_z\right)\omega_y\omega_z \\
\tau_y &= J_y \frac{d\omega_y}{dt} - \left(J_z - J_x\right)\omega_z\omega_x \\
\tau_z &= J_z \frac{d\omega_z}{dt} - \left(J_x - J_y\right)\omega_x\omega_y \\
\tau &= \tau_x\hat{i} + \tau_y\hat{j} + \tau_z\hat{k}
\end{aligned}
\tag{2.16}
$$

The torques and angular velocities in the rotor frame need to be transformed into stator frame. Using Figure 2.3, the relation between the torques and angular velocities in two frames is given as below

$$
\begin{aligned}
\begin{bmatrix} \tau_x \\ \tau_y \end{bmatrix} &= \begin{bmatrix} \cos\theta & \sin\theta \\ -\sin\theta & \cos\theta \end{bmatrix} \begin{bmatrix} \tau'_x \\ \tau'_y \end{bmatrix} \\
\begin{bmatrix} \omega_x \\ \omega_y \end{bmatrix} &= \begin{bmatrix} \cos\theta & \sin\theta \\ -\sin\theta & \cos\theta \end{bmatrix} \begin{bmatrix} \omega'_x \\ \omega'_y \end{bmatrix}
\end{aligned}
\tag{2.17}
$$

Letting $J_x = J_y = J$ due to axis symmetry, after some algebraic manipulations in (2.16) and (2.17), we get torques fixed with housing as :-

$$\begin{aligned} \tau'_x &= J\dot{\omega}'_x + J_z\,\omega_z\omega'_y \\ \tau'_y &= J\dot{\omega}'_y - J_z\,\omega_z\omega'_x \\ \tau'_z &= \tau_z = J_z\dot{\omega}_z \end{aligned} \tag{2.18}$$

No torque is applied to the spin axis as it coincides with Z axis therefore $\tau'_z = 0$. The angular momentum along Z axis is $H_z = (J_z - J)\omega_z$. The presence of damping forces due to friction etc. will cause a damping torque about $X'$and Y'axis [25]. Therefore (2.18) reduces to (2.19):-

$$\begin{aligned} \tau'_x &= J\dot{\omega}'_x + b\omega'_x + H_z\omega'_y \\ \tau'_y &= J\dot{\omega}'_y + b\omega'_y - H_z\omega'_x \end{aligned} \tag{2.19}$$

Due to single pole mounted on the rotor, the torque will be available only in one channel i.e.,$\tau_x = \alpha \text{ and } \tau_y = 0$ and (2.17) reduces as:-

$$\begin{aligned} \tau'_x &= \alpha\cos\omega_z t \\ \tau'_y &= \alpha\sin\omega_z t \end{aligned} \tag{2.20}$$

the dynamics of the system in the stator frame are given as :-

$$\begin{aligned} J\ddot{\theta}'_x + b\dot{\theta}'_x + H_z\dot{\theta}'_y &= \alpha\cos\omega_z t \\ J\ddot{\theta}'_y + b\dot{\theta}'_y - H_z\dot{\theta}'_x &= \alpha\sin\omega_z t \end{aligned} \tag{2.21}$$

To represent (2.21) in state space form, $\dot{\theta}'_x$, $\dot{\theta}'_y$, θ'_x , θ'_y , $\alpha\cos\omega_z t$ *and* $\alpha\sin\omega_z t$ are denoted as x_1, x_2, x_3, x_4, u_1 and u_2 respectively. It is assumed that ω_z is constant which is quite typical in spinning systems. The angular positions are obtained by integrating angular velocities, which can be accurately calculated using Euler angle transformations [25]. Finally the state space representation in stator frame of reference is given in (2.22).

$$\begin{aligned} \dot{x_1} &= -\frac{b}{J}x_1 - \frac{H_z}{J}x_2 + \frac{u_1}{J} \\ \dot{x_2} &= \frac{H_z}{J}x_1 - \frac{b}{J}x_2 + \frac{u_2}{J} \\ \dot{x_3} &= x_1 \\ \dot{x_4} &= x_2 \end{aligned} \tag{2.22}$$

The (2.22) can be written in matrix form (2.23). The output vector $y(t)$ comprises angular positions θ_x and θ_y in stator frame of reference and the input $u(t)$ is given by (2.24).

$$\begin{aligned} \dot{x}(t) &= A\,x(t) + B\,u(t) \\ y(t) &= C\,x(t) \end{aligned} \tag{2.23}$$

$$u(t) = \begin{bmatrix} u_1 \\ u_2 \end{bmatrix} \tag{2.24}$$

$$\text{Where } \bar{A} = \begin{bmatrix} -\frac{b}{J} & -\frac{H_z}{J} & 0 & 0 \\ \frac{H_z}{J} & -\frac{b}{J} & 0 & 0 \\ 1 & 0 & 0 & 0 \\ 0 & 1 & 0 & 0 \end{bmatrix}, \ \bar{B} = \begin{bmatrix} \frac{1}{J} & 0 \\ 0 & \frac{1}{J} \\ 0 & 0 \\ 0 & 0 \end{bmatrix}, \ \bar{C} = \begin{bmatrix} 0 & 0 & 1 & 0 \\ 0 & 0 & 0 & 1 \end{bmatrix} \tag{2.25}$$

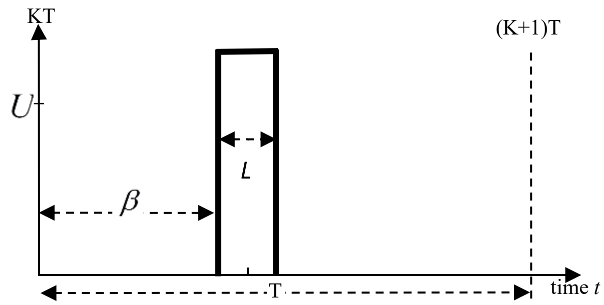

Figure 2.4 : Constrained Actuation Signal – Type I

2.5.5 Actuation Constraints

The actuation in control scheme [13] is rectangular pulses of fixed duration L and variable amplitude as shown in Figure 2.4. The actuation cycle of period T applied for a complete revolution is constant. The center of the actuation pulse is the point where the magnetic field of the rotor and the precession axis are precisely aligned. In each actuation cycle, the input pulse is applied after a time delay β and the system remains unactuated for the rest of cycle i.e., $T - L$ The requirement of pulse width having unlimited amplitude is restricted to maximum amplitude.

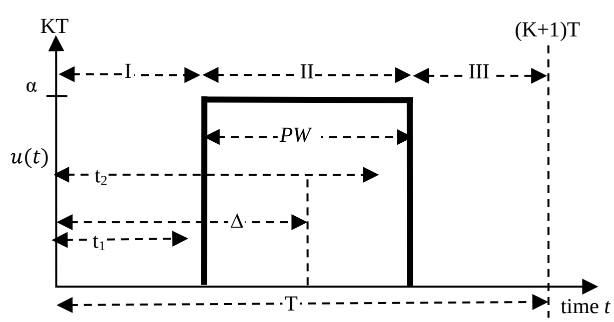

Figure 2.5 : Constrained Actuation Signal – Type II

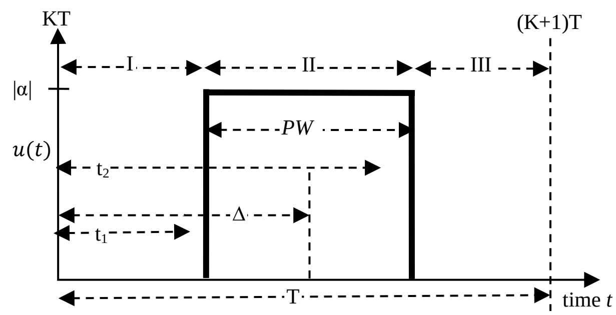

Figure 2.6 : Constrained Actuation Signal – Type III

This limitation was overcome by assuming the actuation pulse having fixed amplitude with variable duration. The modified actuation cycle of period T applied for a complete revolution is shown in the Figure 2.5. The phase of actuation Δ represents the shift of the center of the rectangular pulse from the start of the revolution. The amplitude α of the pulse is fixed however it is allowed to change its polarity, whereas PW varies according to the requirement of the control signal magnitude. This marks the difference in approach from [13] where a pulse having fixed width with varying amplitude was used for the actuation. Therefore PW and Δ are to be estimated subject to the following constraints:-

$$\left.\begin{array}{l} t_1 \le |PW| \le t_2 \\ 0 \le \Delta \le T \\ |u(t)| = \pm\alpha \end{array}\right\} \qquad \text{where } (t_2 - t_1) \le \frac{T}{2} \tag{2.26}$$

In case of type III signal (Figure 2.6) the polarity of amplitude α of the pulse cannot be changed. Thus the actuation is unidirectional.

$$\left.\begin{array}{l} t_1 \le |PW| \le t_2 \\ 0 \le \Delta \le T \\ |u(t)| = \alpha \end{array}\right\} \qquad \text{where } (t_2 - t_1) \le \frac{T}{2} \tag{2.27}$$

CHAPTER 3

PULSE EQUIVALENT AREA – CLASSICAL TECHNIQUE

In this chapter, a discrete-time control algorithm is presented for a class of under-actuated linear systems. This model is developed for both unconstrained and constrained input signals. This continuous-time system is actuated through a single pulse having short duration for a fixed interval of time (equation(2.26)). This time signal is termed as actuation cycle. The system will be actuated only for duration of pulse and remains unactuated during the rest of actuation cycle. The equivalent model is developed by considering a complete actuation cycle as a single discrete step.

The Discrete-time controller calculates the phase and amplitude of the actuation pulse by using sampled state feedback. A state feedback control law finds out the amplitude of actuation pulse. A fully actuated, time invariant discrete-time equivalent model of the continuous-time system forms the basis for the designing of a state feedback control law by considering a complete actuation cycle as a single discrete step.

Two techniques are discussed in this chapter. One is the amplitude modulation technique which is the same as developed by Fahad et. al [13] while the other is the pulse equivalent area technique. Both techniques will be using on state feedback control law and complying constraints presented in (2.26).

3.1 Discrete Time Equivalent Model (Figure 2.4)

The discrete-time equivalent model is derived using Figure 2.4. The time interval $\left[KT, (K+1)T\right]$ is considered as one revolution in the rotor frame. The equivalent discrete model is developed in following two steps:

Interval I: $t \in \left[KT+\beta, KT+L+\beta\right]$

In the first interval, the system (2.23) is actuated

$$x\left(KT+L+\beta\right) = A_{d1}x\left(KT\right) + B_{d1}u\left(KT+\beta\right)$$

Where, $A_{d1} = e^{A(L)}$, $\quad B_{d1} = B\int_{KT+\beta}^{KT+\beta+L} e^{A(KT+\beta+L-\sigma)}d\sigma$

Interval II: $t \in \left[KT+\beta+L, KT+T+\beta\right]$

The system remains unactuated in this interval and the states are given by

$$x(KT+T+\beta) = e^{A(T-L)}x(KT+\beta+L)$$

by substituting value of $x\left(KT+L+\beta\right)$ in above equation we have

$$x(KT+T+\beta) = A_d x\left(KT+\beta\right) + B_d u\left(KT+\beta\right) \tag{3.1}$$

Where, $A_d = e^{A(T-L)}A_{d1}$, $\quad B_d = e^{A(T-L)}B_{d1}$

3.2 Discrete Time Equivalent Model (Figure 2.5)

The discrete-time equivalent model for actuation signal under constraints (2.26) is derived using Figure 2.5. The time interval $\left[KT,(K+1)T\right]$ is considered as one revolution in the rotor frame. The time period T is divided into three separate intervals i.e., interval I, II and III. It must be noted that during interval I and III the system is un-actuated.

Interval I : $t \in \left[KT, KT+\Delta-\frac{PW}{2}\right]$

The system (2.23) is unactuated and the states are given as

$$x\left(KT+\Delta-\tfrac{PW}{2}\right)=e^{A\left(KT+\Delta-\frac{PW}{2}\right)}x\left(KT\right)$$

Interval II : $t \in \left[KT+\Delta-\frac{PW}{2}, KT+\Delta+\frac{PW}{2}\right]$

The system (2.23) is actuated and the states are given as

$$x\left(KT+\Delta+\tfrac{PW}{2}\right)=e^{APW}e^{A\left(\Delta-\frac{PW}{2}\right)}x\left(KT\right)+\int_{-PW/2}^{PW/2}e^{A\left(\frac{PW}{2}-\sigma\right)}Bu(\sigma)d\sigma \tag{3.2}$$

Interval III : $t \in \left[KT+\Delta+\frac{PW}{2},(K+1)T\right]$

The system (2.23) is unactuated during this interval and the states are given as

$$x\left((K+1)T\right)=e^{A\left(T-\Delta-\frac{PW}{2}\right)}x\left(KT+\Delta+\tfrac{PW}{2}\right) \tag{3.3}$$

Substituting values from (3.2) into (3.3) we get:-

$$x\left((K+1)T\right)=e^{AT}x\left(KT\right)+e^{A(T-\Delta)}\int_{-PW/2}^{PW/2}e^{-A\sigma}\ Bu(\sigma)d\sigma \tag{3.4}$$

Although the integral in (3.4) is solvable but the closed form becomes inconveniently lengthy to handle. By using Taylor series [26] an approximate non-closed form expression is obtained. The approximate states at time (T+1) for a specific PW and Δ are given in (3.5) . The control techniques presented in [13] is not applicable for systems that are not convenient to express in closed form. Due to this limitation we resort to use non-conventional method derived from theory of pulse equivalent area.

$$x\left(\left(K+1\right)T\right)\cong e^{AT}x\left(KT\right)+e^{A(T-\Delta)}\left(PW+\frac{A^{2}PW^{3}}{24}+\frac{A^{4}PW^{5}}{1920}\right)Bu \tag{3.5}$$

3.3 Amplitude Modulation Scheme

The amplitude modulation technique is developed by Fahad [13]. Using the discrete time equivalent model (3.1), a state feedback controller is designed which calculates the amplitude of the input signal, while the phase of the signal is calculated by following equation :-

$$\beta[i]=\tan^{-1}\left(\frac{u_2[\mathrm{i}]}{u_1[\mathrm{i}]}\right) \tag{3.6}$$

This technique cannot be directly applied under the constraints (2.26). Therefore the amplitude calculated from state space model is restricted to a fixed vale of "α" to comply with the constraints (2.26) while the phase angle calculated from (3.6) can be used directly.

3.4 PEA Based Control Scheme

Another approach for such a system is to use the Principle of Equivalent Areas (PEA) [44] for Pulse width modulation (PWM) scheme [46,47,50]. The PEA implies that even when two input signals have different waveforms, they can still results in the similar outputs if they have the same areas [45]. When this concept is applied to a PWM signal whose pulse width is to be modified to achieve a PEA equivalent of a given control signal the relationship is governed by :-

$$\int_{KT}^{(K+1)T} u(t)dt = U\sigma_k$$

U is pulse amplitude, T is the PEA interval, $u(t)$ is given control signal to be converted into pulse signal and α_k is pulse-width to be determined.

As evident from (3.4), that the exact solution through discrete time equivalent model cannot be obtained under constraints (2.26). Therefore, the constrained actuation signal type I will be transformed into type II signal through PEA scheme to comply constraints 2.26. Therefore the solution found in (3.1) will be transformed to comply constraints mentioned in (2.26) as :-

$$PW = \frac{LU}{\alpha} \quad , \quad \Delta = \beta + \frac{L}{2} \tag{3.7}$$

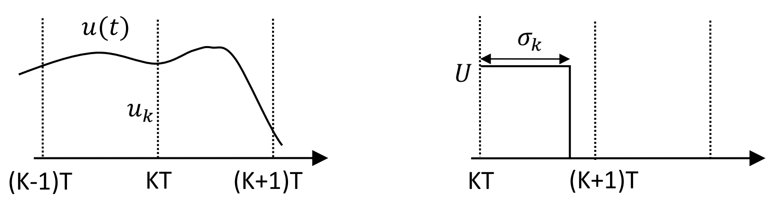

Figure 3.1 : PEA based Pulse width Determination [45]

3.5 Controller Design

The overall control scheme is shown in Figure 3.2. Controller is based on the discrete equivalent model given by (3.1). The standard pole placement technique is utilized for this purpose [21]. The control input is

$$u[k] = -Fx[k] + Nr \tag{3.8}$$

The matrix F is chosen such that the eigenvalues of $(A_d - B_d F)$ are within the unit circle. The reference signal is $(r_x, r_y) \in R^2$, where the matrix N = $C\left[\left(I - A_d + B_d F\right)^{-1} B_d\right]^{-1}$.

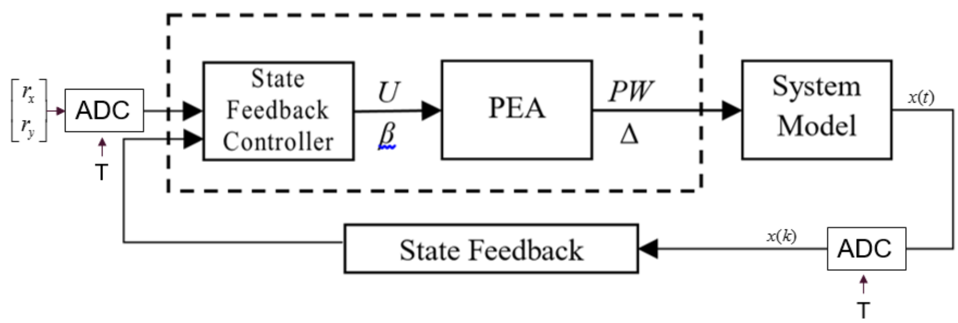

Figure 3.2 : PEA based Control Scheme

3.6 Simulations and Performance

Simulations were carried out in MATAB and SIMULINK. The parameters used are $\omega_z = 400\,\pi$, $b = 400$, $J = 4kgm^2$, $J_z = 5kgm^2$ and F = [0.992, 0.995+.9j, 0.99, 0.99+.9j] . The time interval to complete one revolution is taken to be 0.05 sec. Figure 3.3 &3.4 shows the comaprison of results with and without PEA transformation under application type II constraints. Figure 3.3(a) and Figure 3.4(a) shows the performance when the reference to be tracked is constant. It can be seen that both techniques show satisfactory results. However, when subjected to time varying reference signals as shown in Figure 3.3(b) and Figure 3.4(b), PEA based technique tracks the varying reference whereas, other technique (without PEA transformation) could not track the desired trajectory.

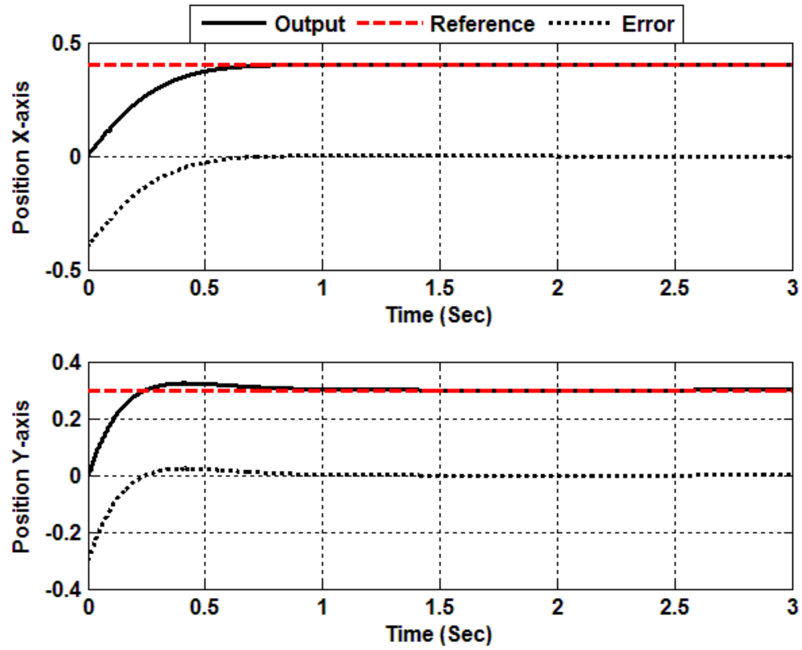

(a) Fixed Reference

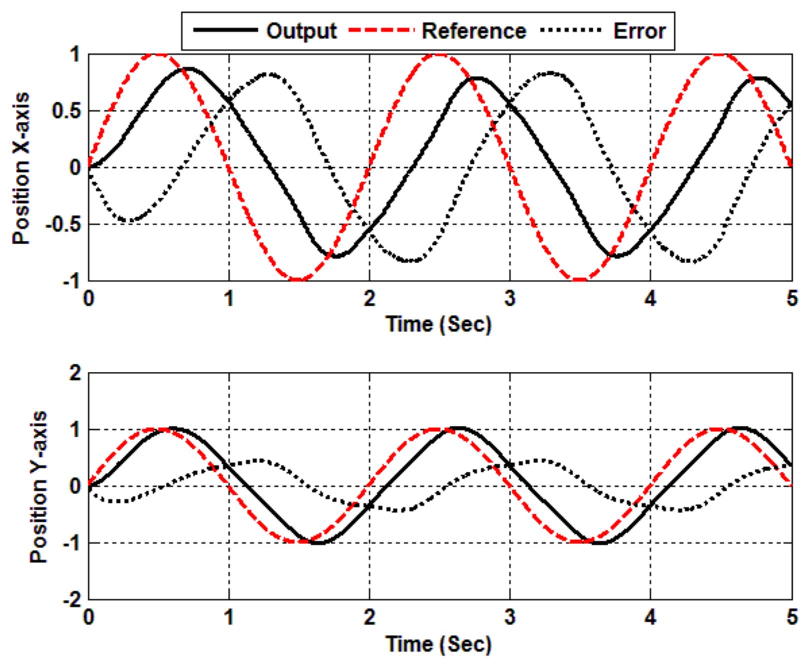

(b) Time Varying Reference

Figure 3.3 : Stabilization without PEA transformation

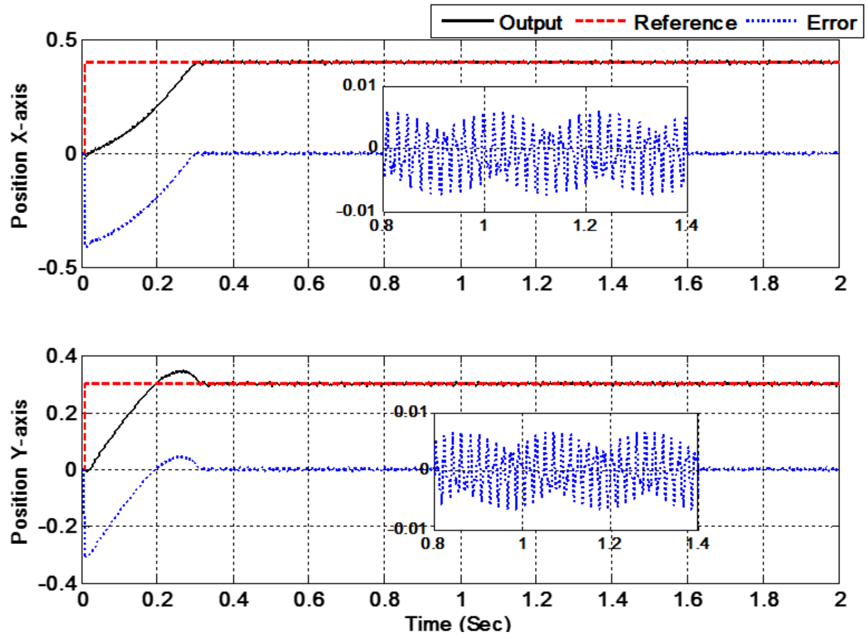

(a) Fixed Reference

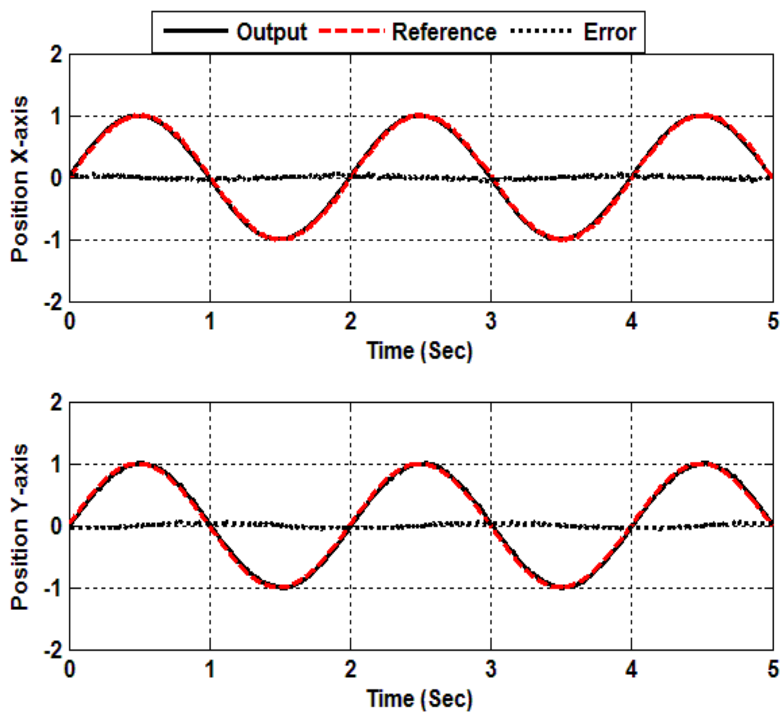

(b) Time Varying Reference

Figure 3.4 : PEA based Stabilization

3.7 Parametric Variation Simulations

The parametric variation simulation is performed to verify the robustness of proposed technique. A variation of 10% and 25 % was made in the nominal values of the plant by introducing random disturbances in parameters of (2.25). The system is simulated 10000 times by simultaneously introducing the random disturbances in parameters. The controller is designed for nominal system parameters. As seen from the results in Figure 3.5 that the system remains stable with minor variations in settling time. The transient performance deteriorates at 25% parametric variations but still remains stable. To sum up the overall system performance with PEA based technique is robust enough to handle perturbations in plant parameters.

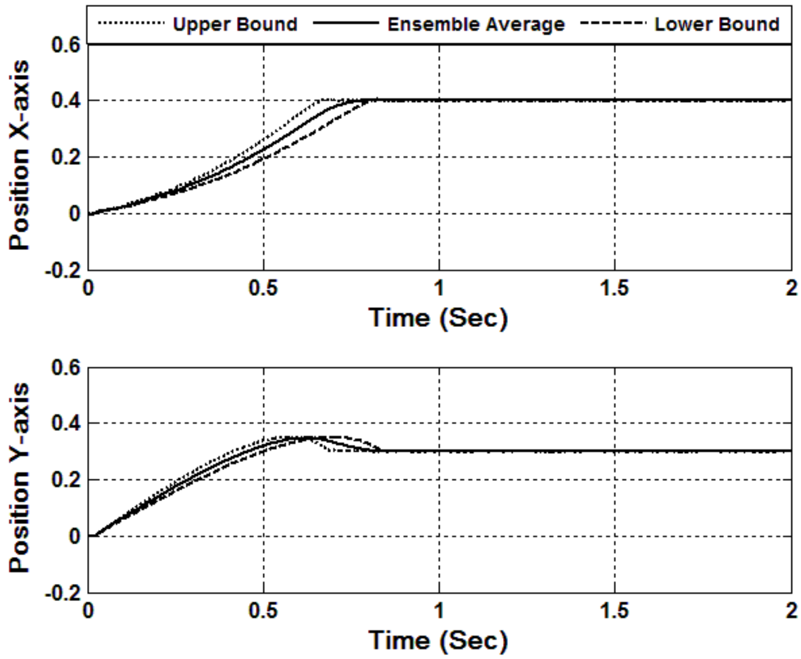

(a) Under 10% Parametric variation

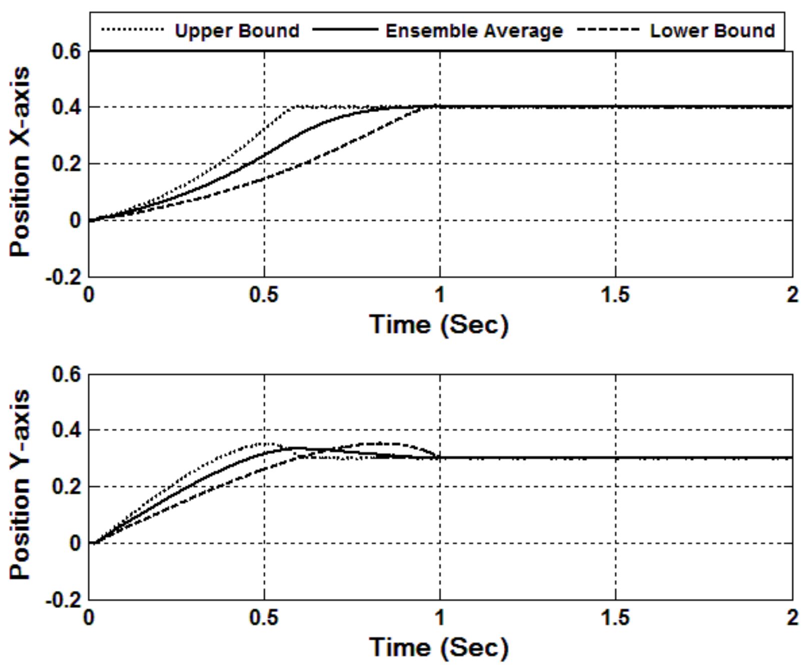

(b) Under 25% Parametric variation

Figure 3.5: PEA based Stabilization

3.8 Discussion

The solution provided by [13] has a major practical limitation as the pulse width of control input is fixed while its magnitude is proportional to the amount of control force required and is unlimited. To overcome this limitation two constraints are applied on actuating signal of fixed amplitude with adjustable pulse width. Due to the given constraints the exact solution of discrete time equivalent model was not possible. Therefore control signal generated by technique [13] is transformed into a PEA signal which ensures that the control signal is produced to meet the constraints. The proposed technique [27] has shown satisfactory results in achieving the desired orientation for the nominal as well as for the perturbed system with 10% and 25% variation in parameters.

CHAPTER 4

ERROR MINIMIZED CONTROL

PEA based scheme discussed in last chapter has few limitations as it is based on approximation and thus not suitable for precise tracking. There is a need to evolve a novel technique which can generate an input signal that can minimize the tracking error by complying with constraints (2.26). The complexity level is also increased by posing it as an output feedback control as opposed to the state feedback control used for techniques developed in previous chapter.

4.1 Error Minimized Control (EMC)

Based on the theory of Model predictive control (MPC), a novel algorithm is presented which is based on the optimization of the error signal. The discrete-time equivalent model given at (3.4) is reproduced here as (4.1)

$$x\left(\left(K+1\right)T\right)=e^{AT}x\left(KT\right)+e^{A(T-\Delta)}\int_{-PW/2}^{PW/2}e^{-A\sigma}\,Bu(\sigma)d\sigma \tag{4.1}$$

The integral in (4.1) is solvable but the closed form becomes inconveniently lengthy to handle. The Pulse equivalent technique discussed in last of chapter and amplitude modulation technique [13] are not applicable for such systems that are not convenient to express in closed form. These techniques utilize exact solution (3.1) under constraints (2.26) , and the desired tracking results are not produced. Due to this limitation we resort to use non-conventional method derived from optimal control and Model predictive control theory.

Therefore, an output feedback optimization algorithm based on the minimization of the error signal is developed in this chapter. The resultant actuating signal is generated based on the optimized values of pulse width and delay. It is shown via simulations that the presented scheme provided a smooth control for precise movement and overcame the limitations on the control effort. The cost function, however, appears to be ill behaved, resulting in multiple local minima. The elimination of local minima and the estimation of unique global minima is carried out through reference phase algorithm and multiple initial point algorithm (MIP) [28]. Global minimization plays an effective role in many real problems such as science, engineering and economy [29]. The causality is also assured by employing a sliding adjustment technique. This technique has no relevance or connection with the famous “Sliding Mode Control” theory.

4.2 Control Law

The input signal comprises two variables i.e. pulse width PW and the position Δ. The values of these parameters can be controlled under constraints (2.26). The Figure 4.1 presents the proposed scheme. The control signal is generated by searching optimized values of PW and Δ based on the minimization of error. The error is the difference between the reference signal and the observer feedback (4.2). The cost function $J(u)$ is given by (4.3)

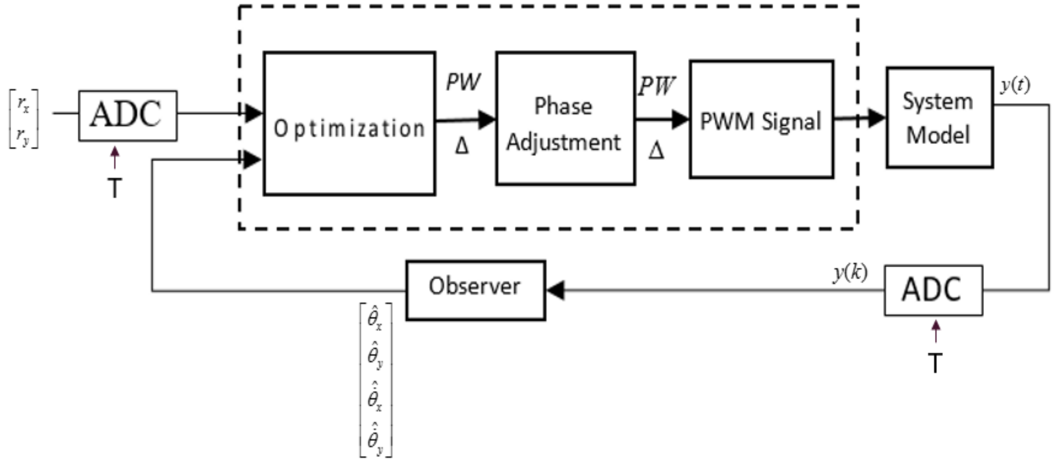

Figure 4.1 : Error Minimized Control Scheme

$$e(t) = \begin{bmatrix} e_1 \\ e_2 \\ e_3 \\ e_4 \end{bmatrix} = \begin{bmatrix} r_x - \hat{\theta}_x \\ r_y - \hat{\theta}_y \\ \dot{r}_x - \dot{\hat{\theta}}_x \\ \dot{r}_y - \dot{\hat{\theta}}_y \end{bmatrix} \tag{4.2}$$

$$J(u) = e_1^{\,2} + e_2^{\,2} + \eta \left\{ e_3^{\,2} + e_4^{\,2} \right\} \tag{4.3}$$

where variable η is the weighting function. Minimization of (4.3) based on the constraints (2.26) is a non-linear least square problem [30]. This can be solved via interior-reflective Newton method [31]. The algorithm is a subspace trust-region method and finds optimized values of PW and Δ

$$\min_{(Pw,\Delta)} \left\| J(u) \right\|_2^2 = \min_{(Pw,\Delta)} \left\{ e_1^{\,2} + e_2^{\,2} + \eta \left\{ e_3^{\,2} + e_4^{\,2} \right\} \right\} \tag{4.4}$$

Trust region methods mainly depends on the initial guess, therefore, only for 1st iteration, random values of PW and Δ were selected and for subsequent iterations their previous values were taken as initial guess, as explained below :-

$$
\begin{aligned}
\Delta_i &= \begin{cases} \dfrac{T}{2} & i = 0 \\ \Delta_{i-1} & i > 0 \end{cases} \\
PW_i &= \begin{cases} PW_0 & i = 0 \\ PW_{i-1} & i > 0 \end{cases}
\end{aligned} \qquad (4.5)
$$

For the proposed optimization algorithm, two problems were encountered. One is the problem of local minima. This problem can be effectively neutralized through two different algorithms discussed in detail in section 4.4. The other problem is that the actuation may become non-causal. This non-causality was denied through phase adjustment technique given in section 4.5.

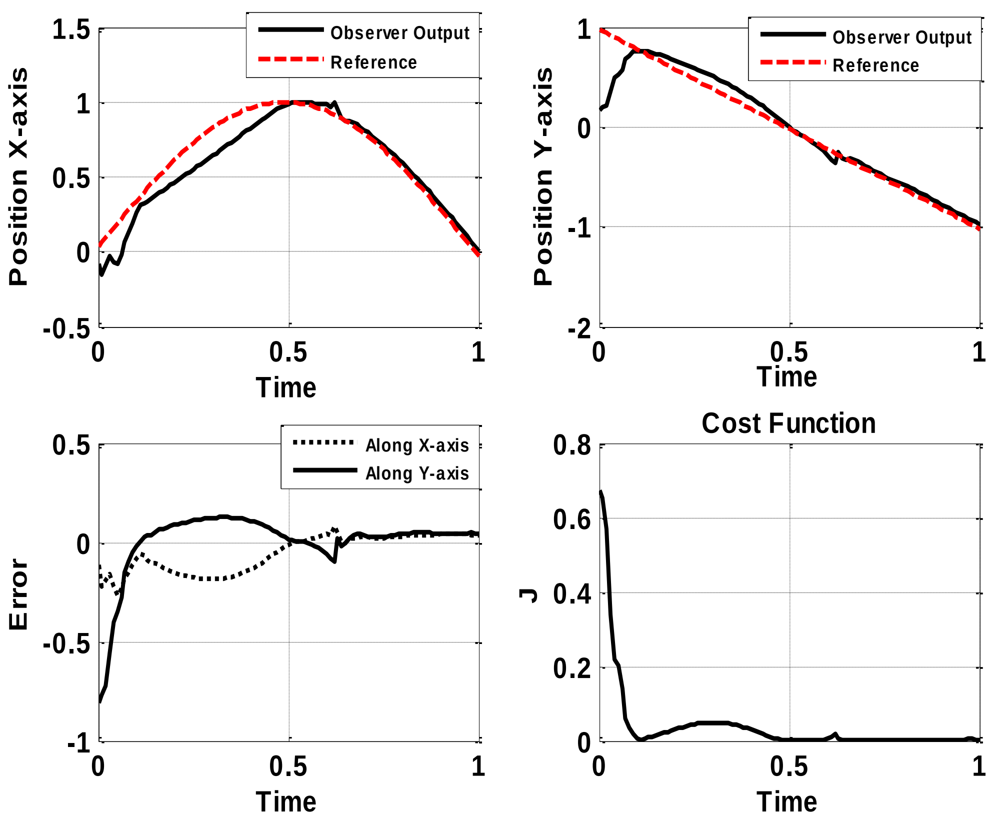

Figure 4.2 : EMC Based Control

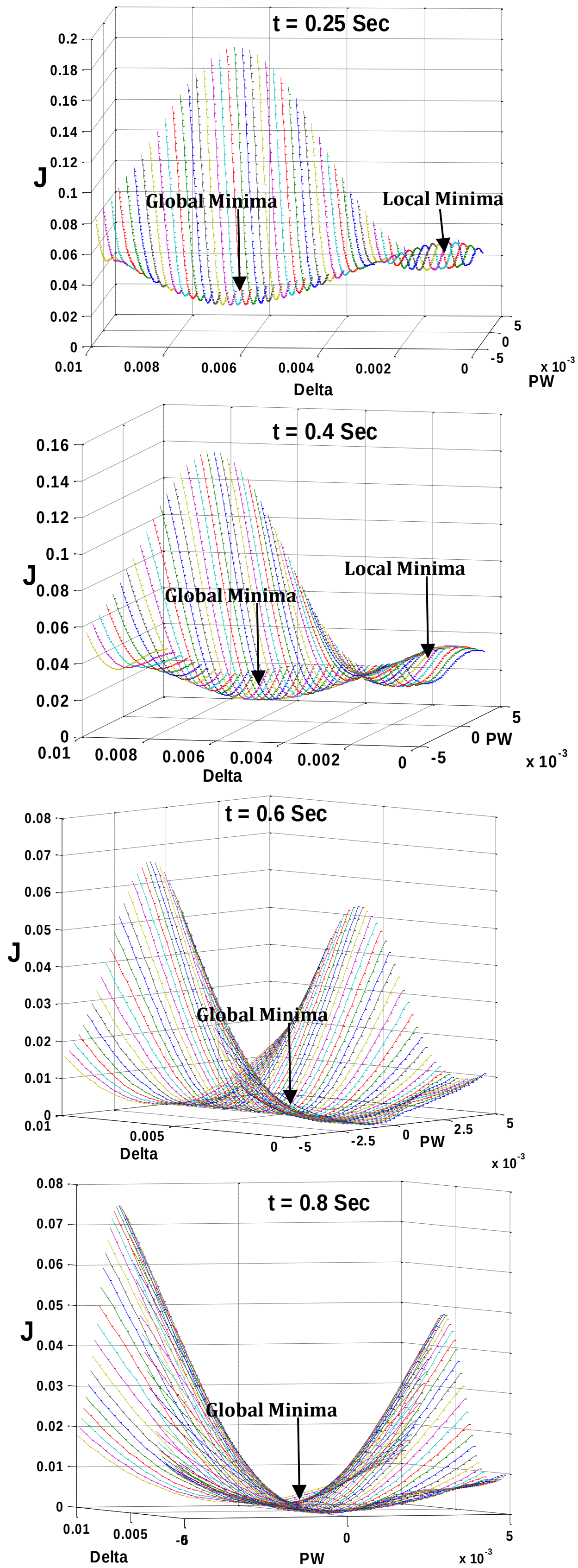

Figure 4.3 : Local and Global Minima Search

4.3 Observer Design

The observer is designed via the standard pole placement technique [32,33] for EMC. The observer gain $Lo = \begin{bmatrix} -531 & -531 & -414 & -414 \end{bmatrix}$ is designed for such eigenvalues that error (4.6) asymptotically converges to zero.

$$\begin{aligned} \dot{e}_o(t) &= \left[\bar{A} - L\bar{C} \right] e_o(t) \\ e_o(t) &= x(t) - \hat{x}(t) \end{aligned} \tag{4.6}$$

4.4 Local Minima Issues

The performance of the proposed EMC based control for the position control of X and Y axis is shown in Figure 4.2. The system shows poor tracking response for the time interval 0.1 sec to 0.5 sec. This is due to the existence of at least two minima in addition to global minima. Hence, the optimizer cannot differentiate between local and global minima and consequently the cost function could not be minimized. This problem was investigated through exhaustive search for global minima at different time intervals Figure 4.3. The values for the optimized cost function at 0.25 sec are $(J(u), PW, \Delta) = (90.044, -0.0012, 0.0013)$ but this is a local minimum. The global minimum exists at $(J(u), PW, \Delta) = (0.01, 0.0032, 0.0065)$. Similarly the same phenomenon of local minima is also observed at 0.4 sec. However, the situation is improved at 0.55 sec and 0.8 sec where the optimizer was able to converge to global minima effectively (because of the absence the local minima). In order to avoid local minima, two approaches in following sub-sections were used. Both the methods were able to avoid local minima and show satisfactory results.

4.4.1 Reference Phase Algorithm (RPA)

For each iteration, the initial guess for Δ and PW is fed to the search algorithm. This initial guess for Δ is calculated from the phase of the reference signal (4.7). The last value of PW is taken as initial guess for the next iteration.

$$
\begin{aligned}
\Delta_i \quad &= \begin{cases} \dfrac{T}{2} & i = 0 \\ \dfrac{T}{2\pi}\tan^{-1}\left(\dfrac{r_y}{r_x}\right) & i > 0 \end{cases} \\
PW_i &= \begin{cases} PW_0 & i = 0 \\ PW_{i-1} & i > 0 \end{cases}
\end{aligned}
\tag{4.7}
$$

4.4.2 Multiple Initial Point (MIP) Algorithm

This algorithm is a comprehensive search technique for global minimization. It is initiated through multiple equi-spaced n data sets. The values of Δ and PW are selected based on the lowest value of the cost function J. Mathematically, the algorithm is explained in (4.8).

$$
\begin{aligned}
PW_i &= \begin{cases} \dfrac{T}{2} & i = 0 \\ PW_{i-1} & i > 0 \end{cases} \\
\Delta_i \quad &= \left\{\Delta \rightarrow \min\left\{J\left(u_{pk}\right)\right\}\right\} \qquad i \geq 0 \\
where \quad u_p &= \begin{pmatrix} PW_i \\ (sk-1)\dfrac{T}{nr} + iT \end{pmatrix} \qquad \begin{matrix} nr \in N \;\; but \;\; nr \neq 0\;,1 \\ nr \geq sk \leq 0 \\ pk = 1, 2, \ldots\ldots, (nr\text{ -}1) \end{matrix}
\end{aligned}
\tag{4.8}
$$

4.5 Phase Adjustment

Case	Condition	ith Rotation	(i + 1)th Rotation
I	$\Delta - \left\|{Pw}/{2}\right\| < th_s$	$\gamma = th_s - \Delta + \left\|{PW}/{2}\right\|$ $t_{end(i)} = t_{end(i)} - \gamma$	$\begin{Bmatrix} t_{start(i+1)} = t_{end(i)} \\ t_{end(i+1)} = t_{start(i+1)} + T \end{Bmatrix}$
III	$\Delta + \left\|{PW}/{2}\right\| > th_e$	$\gamma = \Delta + \left\|{PW}/{2}\right\| - th_e$ $t_{end(i)} = t_{end(i)} + \gamma$	
II	Otherwise	$t_{end(i)} = t_{end(i)}$	

Table I : Possible Scenarios for Phase Adjustment

The system's actuation becomes non-causal due to the use of PWM control signal. The center of the pulse Δ is to be determined at the end of each rotation; this might lead to the actuation becoming non-causal for some values of Δ. Because when Δ is very close either to start of actuation or end of actuation, there is the possibility that either the pulse starts before the reference point or ends after the reference point as shown in cases I &III in Figure 4.4. To counter this a phase adjustment is introduced to effectively produce a causal actuation. An arbitrary threshold zone "ths or the" is chosen such that the actuation should not fall within this zone. The observation is always taken at the start of the zone, which slides to deny the actuation to fall within "ths or the". Table I summarizes the three possible cases. The Figure 4.4 shows that for the cases I & III, when the reference is changed for (i+1) rotation, the next observation is so placed as to avoid the system becomes non-causal and align the center of actuation with the reference, but in doing so the actuation time is also changed.

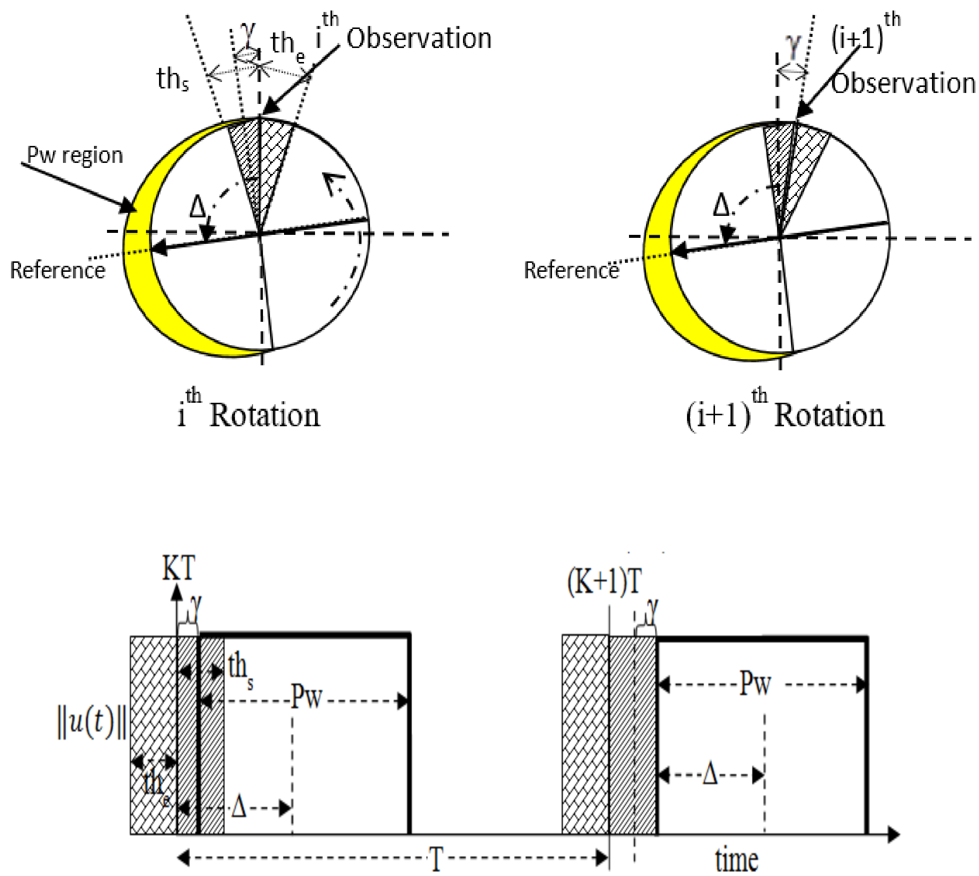

Case I - Sliding Adjustment (Actuation time reduced)

Figure 4.4a : Phase Adjustment Scenarios

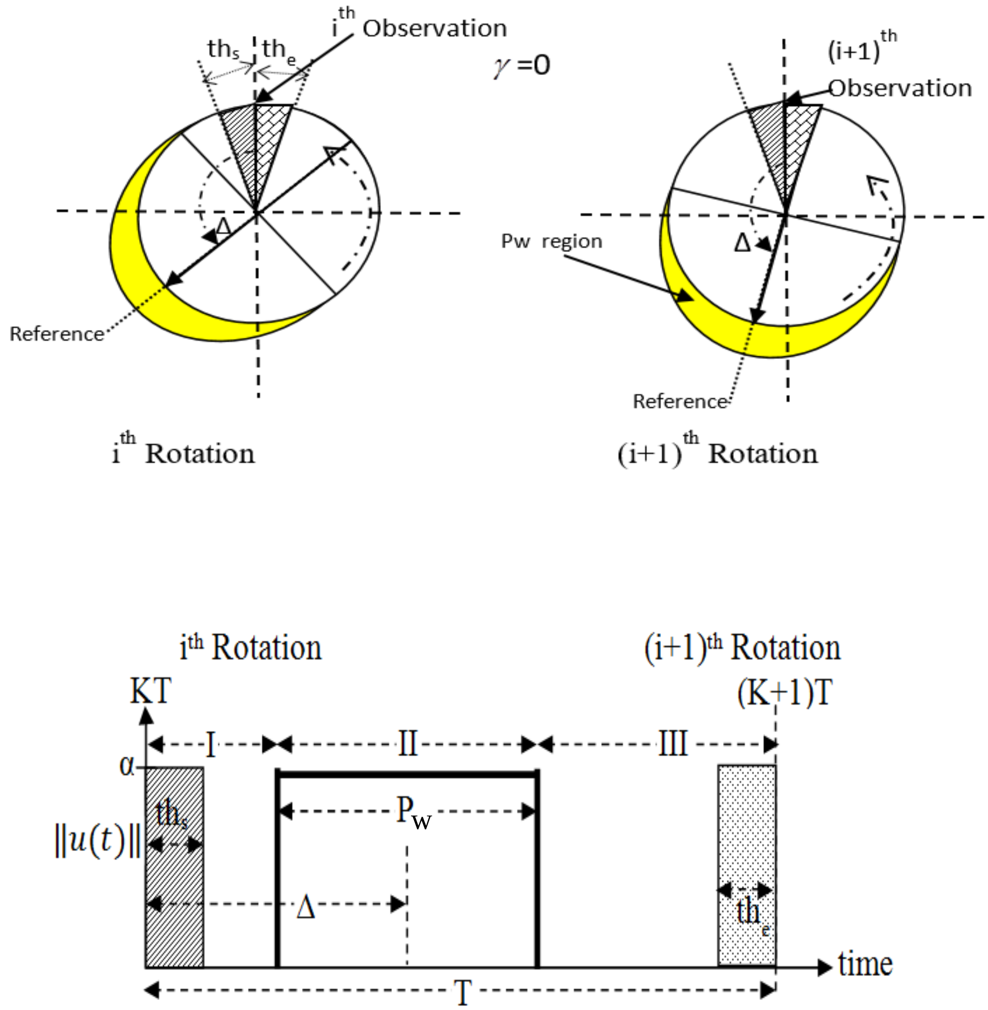

Case II - Sliding Adjustment (Actuation time unchanged)

Figure 4.4b : Phase Adjustment Scenarios

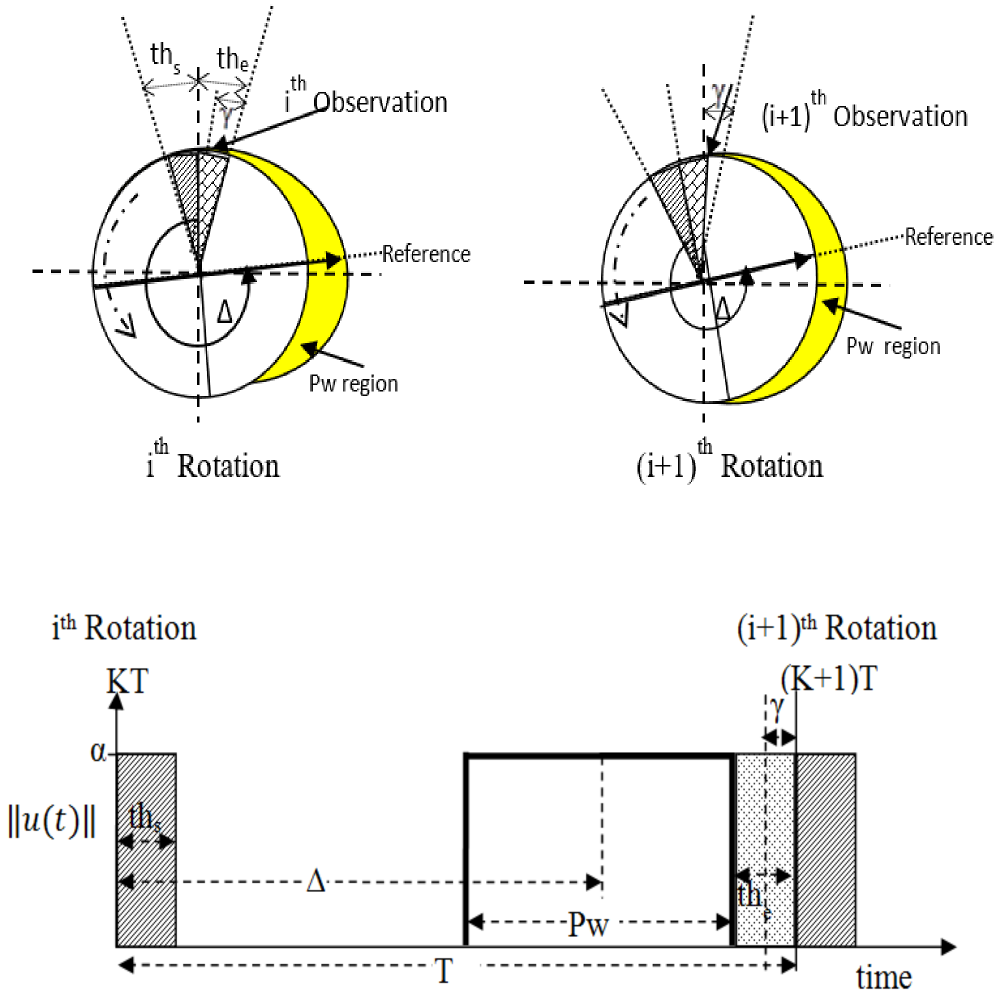

Case III - Sliding Adjustment (Actuation time increased)

Figure 4.4c : Phase Adjustment Scenarios

4.6 Simulations and Performance Analysis

Simulations were carried out in MATLAB and SIMULINK. The parameters used are $\omega_z = 400\ \pi$, $b = 400,\ K_i = 1,\ J = 4\ kgm,\ J_z = 5\ kg$. The time interval to complete one revolution is 0.05 sec. The values of parameters are kept same as in previous chapter, so that fair comparison between the techniques can be made. The PEA based approach though complying constraints (2.26) shows poor transient response. PEA based technique tracks a time varying signal but with errors and thus not suitable for precise tracking as shown in Figure 4.5. On the other hand EMC technique has good transient response as well as precisely follows moving reference too. The superior performance of EMC as compared to other techniques can be seen in Figure 4.6 and Figure 4.7. The MIP & RPA overcome local minima issues where as phase adjustment technique overcomes the causality problem. EMC achieves better settling time for constant reference and is able to track a moving reference effectively. However, the amount of computation required to implement MIP is much more than required in RPA.

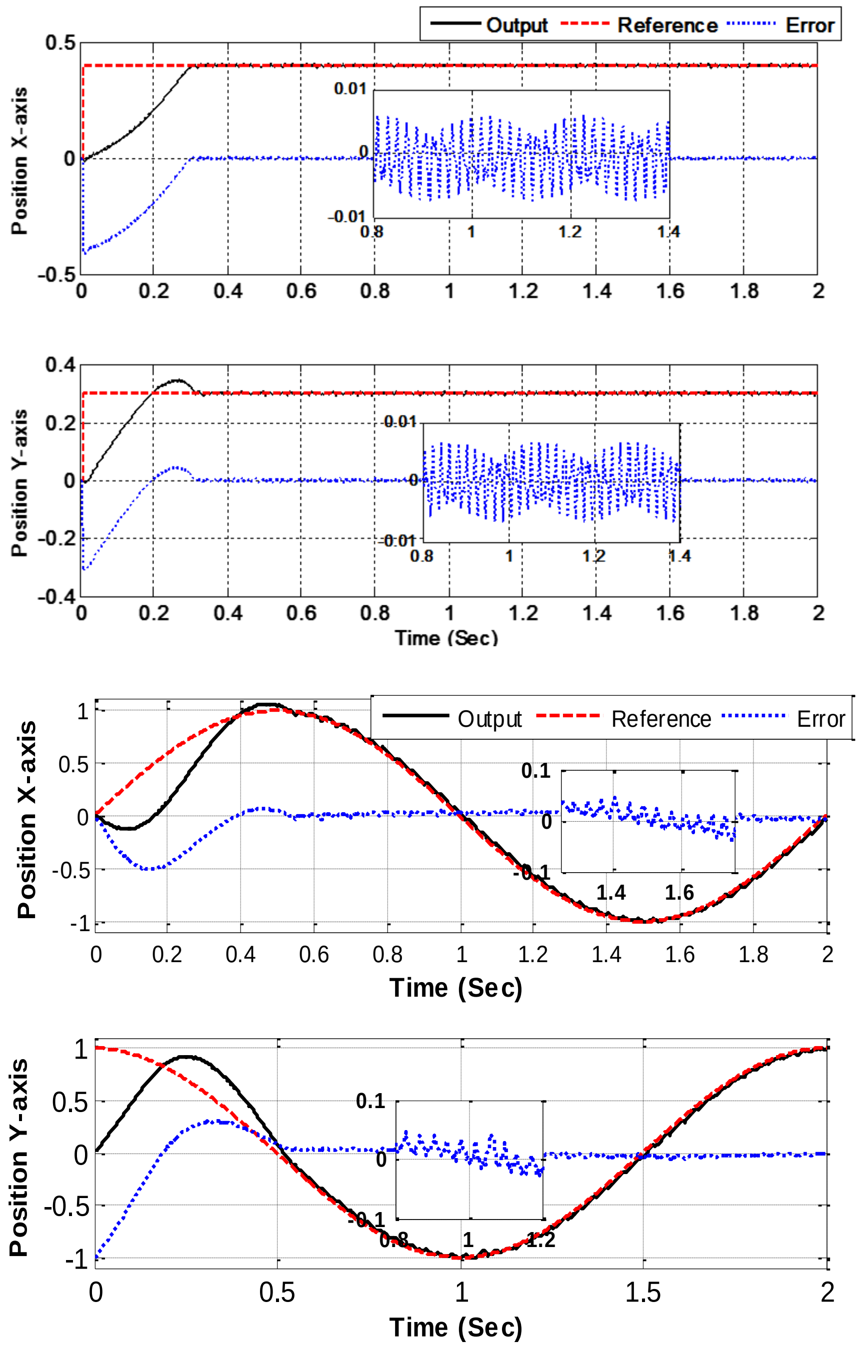

Figure 4.5 : PEA based Stabilization under Fixed and Time varying Reference

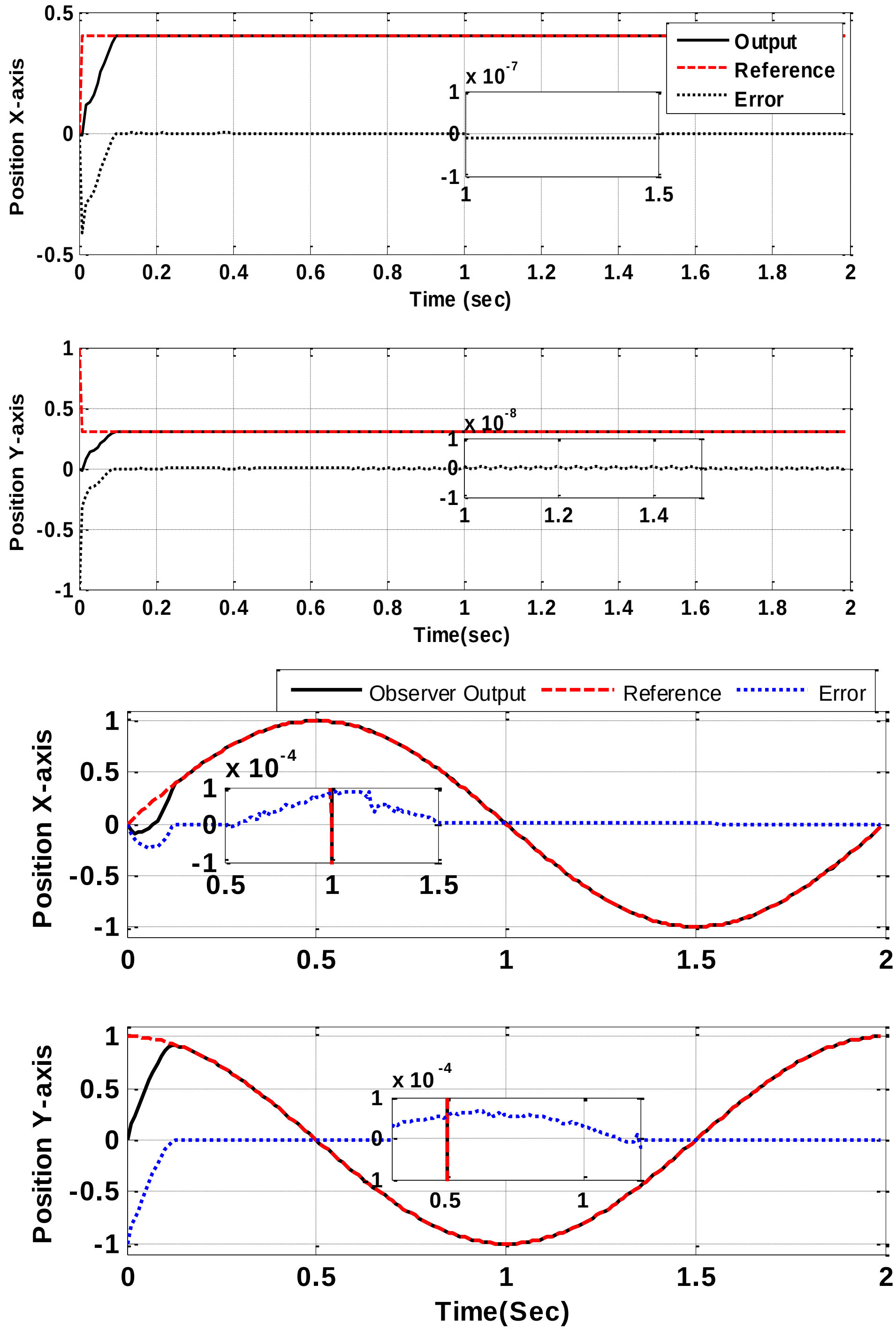

Figure 4.6 : Stabilization under Fixed & Varying Reference by MIP-EMC

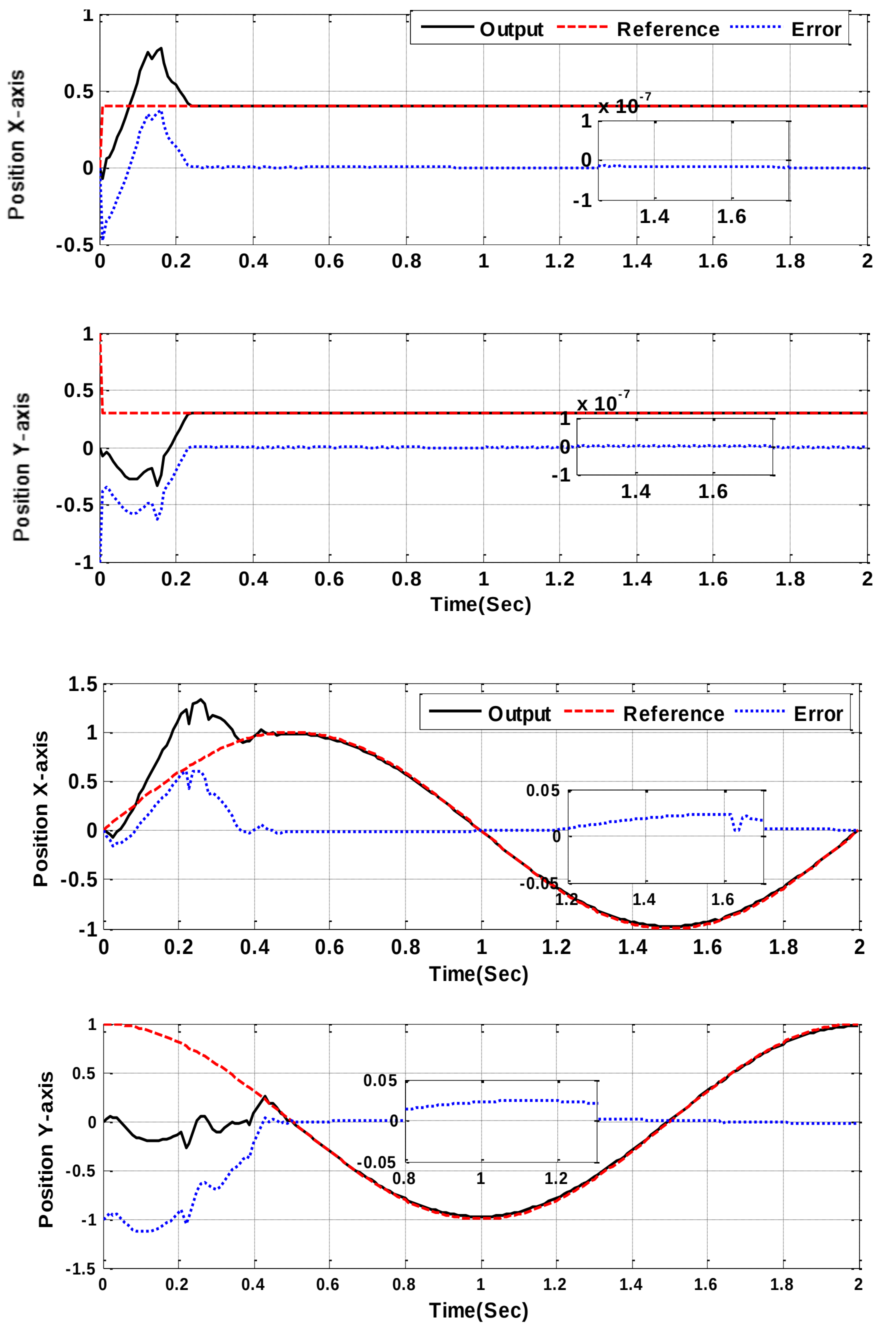

Figure 4.7 : Stabilization under Fixed & Varying Reference by RPA-EMC

4.7 Monte Carlo Simulations

The robustness of the EMC based control technique is verified by introducing parametric variations in the system model. Based on the results of over 5000 monte-carlo simulations, both RPA-EMC (Figure 4.8) and MIP-EMC (Figure 4.9) remained stable with minor variations in settling time and the tracking target was achieved. MIP-EMC showed better settling time as compared to RPA-EMC as they withstand up to 25% of parametric perturbation.

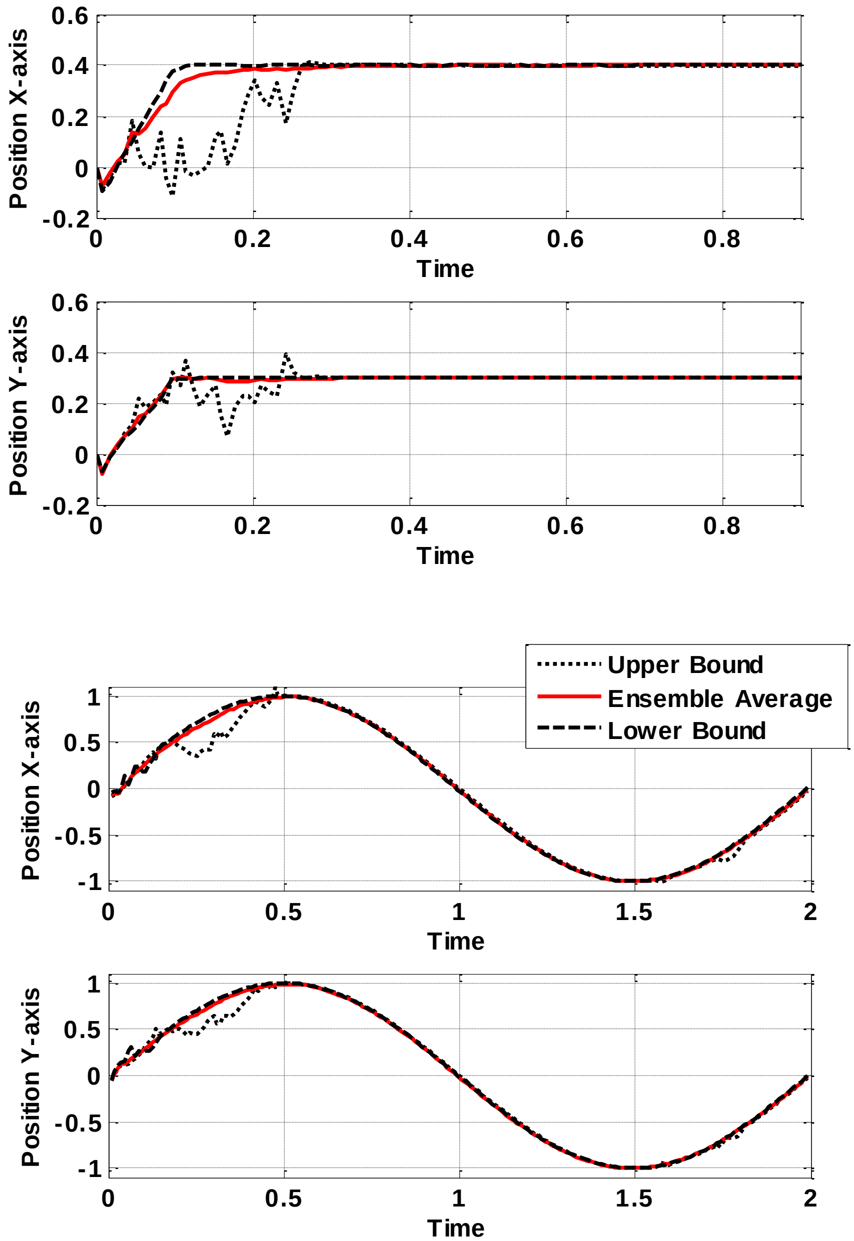

Figure 4.8 : Orientation Control through RPA-EMC Under 10% Parametric Variation

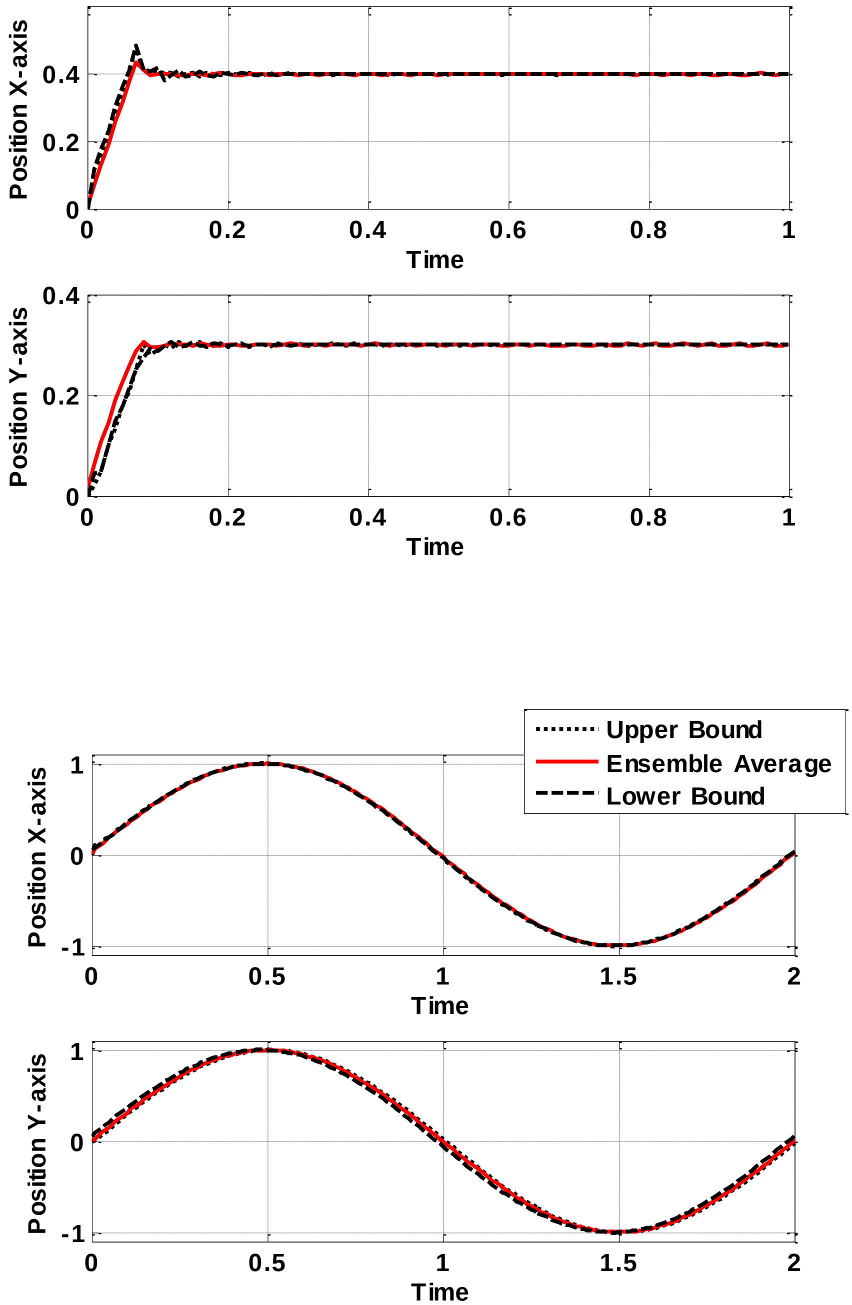

Figure 4.9 : Orientation Control through MIP-EMC Under 25% Parametric Variation

4.8 Real time implementation

So far real time implementation of presented algorithms is challenging due to high computational load which is required for exhaustive search algorithm of global minima. However the presented algorithms can be implemented for slow sampling systems through present day fast processing hardware. Similarly for system with high sampling rate, the presented algorithms can be implemented as offline controllers based on learning control design techniques.

4.9 Discussion

An error minimized control derived from the theory of MPC is proposed for the orientation control of an under actuated spinning system under constraints with application on a small drill machine. The scheme is presented to generate the required actuating signal of fixed amplitude and variable duration. It is based on the discrete equivalent model of the plant. Controller design is improved by introducing an output feedback error minimizing control based on PWM. The algorithm is a subspace trust-region method and finds optimized values of pulse width and amplitude of the control input. The problems of trapping in local minima have been handled by designing two methods which ensure that search algorithm does not traps into local minima. The non-causality issue was also addressed by sliding adjustment technique. The scheme is very effective for fixed references as well as for tracking problems, because of following reasons :-

- Tracking error is very less and better transient response when compared with PEA thus suitable for precise movements.
- Does not get trapped in Local minima.

- Non-causality is avoided.
- The minimum pulse width which cannot be avoided in case of PEA has been overcome by this technique.
- The scheme is effective for fixed references as well as for tracking problems

The PEA based technique of chapter 3 has shown satisfactory results under given constraints, but not suitable for precise movements. The monte-carlo simulations show that the EMC technique gives satisfactory performance under both nominal and parameter variations. EMC-MIP technique even outclasses EMC-RPA under high parametric variations. However, the real time implementation is difficult due to heavy computational load required for exhaustive search of global minima in each iteration. Therefore, smart optimization techniques for reduction in run time, based on particle filter approach is proposed in the next chapter.

CHAPTER 5

PARTICLE CONTROLLER

5.1 Sequential Monte Carlo – An introduction

The particle filtering method has emerged as an alternative to the extended Kalman filter. Based on Bayesian theory, it can handle non-Gaussian as well as nonlinear problems [18]. It is a sequential Monte Carlo methodology, where the basic idea is the recursive computation of underlying probability distributions with discrete random measures known as particles.

Particle filtering has the ability to track a variable of interest with non-Gaussian and multi modal pdf having two or more modes. A sample based representation is built for complete pdf, where the state of the variable of interest is represented with some model. Multiple copies (on random basis) of variable of interest are generated and termed as particles. Each particle is assigned with some weight. In fact, the quality of particle is indicated by its weight. Weighted sum or some other approximate measure of all the particles gives an estimate of variable of interest. The algorithms of particle filter are recursive in nature and are divided into two phases "Prediction and update". In prediction stage, after every iteration, each particle is modified as per existing model. Whereas, during the update stage, the particles are reassessed based on the observation. During resampling the heavy weight particles are replaced with a cluster of multiple lighter weight particles to avoid degeneracy. Particles having smaller weights are ignored. Prediction phase simulate the effect on the set of particles by using the model after adding suitable noise.

For example at time $t = k$, pdf of the system at previous instant of $t = k - 1$ is available. This is followed by finding apriori pdf at time $t = k$ by modeling the effect on particles. In update phase, weights of the particles are updated based on the observation to precisely define the pdf.

5.2 Sequential Monte Carlo Methods in Control Systems

Conventionally, the concept of weighted particles has addressed the problem of state estimation of nonlinear dynamical systems under the influence of non-Gaussian process/observation noise. Recently some researchers have developed methods to use similar philosophy in designing control effort for nonlinear feedback systems [1,3,4,5,8,9]. However, the focus of these researchers has been restricted to a class of optimal control problems related to:-

- Nonlinear stochastic systems
- Discrete-time systems

There are some gaps / weak areas which need attention in order to carry forward the work of these researchers, such as:-

- Inter sample behavior in discrete systems is not covered as physical systems in general. Conversion of continuous time models into their discrete time equivalent model results in loss of information. Sample data nonlinear system models are required if these methods are to be applied to physical systems.

- Following Optimization considerations are not covered :-

- Existence of local minima should be considered. Otherwise, there is a possibility that the algorithm gets trapped in local minimum.

- Search of global extremum is based on maximum weight particle, which estimate the mode of pdf under consideration. However the sparsity of particles may compromise the accuracy of the estimate of mode.

- Theory of Particle filter is been extended to use in MPC. However, particular considerations for MPC or nonlinear control are not focused in above mentioned research. The specific nature of issues related to nonlinear systems has been left unaddressed.

- These methods inject stochastics into the system to convert a deterministic system into its stochastic counterpart. This step is necessary if the conventional particle filter theory is directly adapted to solve the optimal control problem. Furthermore, in many physical systems the observations may be accurate enough, where observation noise is negligible.

- The example used by some of the authors can be solved by conventional control theory. Application of particle filter theory may not be fully computationally feasible. On the other hand, the example quoted in this thesis, cannot be handled by conventional methods.

- Some of the methods are iterative and hence are computationally intensive. Engine. De villers [8] used simulated annealing method which is computationally intensive as well as impractical too.

5.2.1 Our Approach

Conventional weighted particle approach assumes availability of underlying probability density functions (including transition probability density function) of the system. In case, this information is not accurately known, the performance of the algorithm may significantly degrade. Whereas, our technique uses particles to characterize the probability density function (opposite to existing techniques, which draw particles from the presumed probability density function). This way the problem remains deterministic and not converted into a stochastic problem. Our theme is to somehow directly associate cost function to some probability density function. The concept will be discussed in section 5.3. By adopting this approach, we are able to utilize stochastic tools like re-sampling etc while addressing the specific attention demanded by nonlinear systems.

By virtue of our perspective, we have the facility to directly estimate particle weights. This in turn is based on Weight Assignment Process (WAP) which is discussed in section 5.4. Our approach is therefore, fundamentally different from conventional weight update through transition probability density function. Albeit both the idea fall within sequential monte carlo methods.

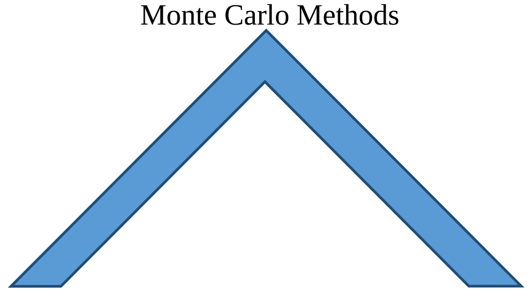

Figure 5.1 : Difference in Approach – Monte Carlo Methods

5.2.2 Sampled Data Tracking Problem

We address sampled data tracking problem for a class of nonlinear systems with due consideration given to the issue related to nonlinear nature of the system. This is our major contribution as compared to the authors who simplify the problem by considering discrete time systems only.

5.3 Cost function and its association with a pdf

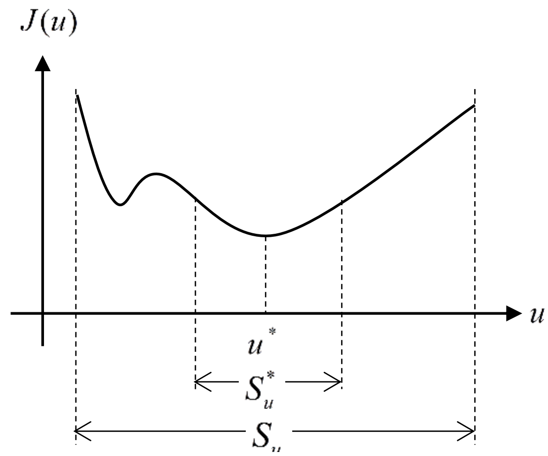

Figure 5.2 : Relation between Cost function and Input signal

Let $J(\mathrm{u})$ be the cost function that is minimized to solve the optimal control problem of chapter 4. u^* is assumed to be the global minimum and Su^* is the global minimum region such that every point has lower cost than any other local minimum. Let $p(u)$ be a distribution that is related with $J(u)$ in the following sense. Since our interest is finding the global minimum, $p(u)$ has the form such that it attains maximum value at u^*. This would indicate the highest probability of finding u^*. In case such information is not available we may opt for non-information distribution over the whole set S_u. Uniform distribution can be used in this case.

In particle theory, continuous distributions are approximated by some suitable discrete measures. The advantage is that samples of later type can easily be generated using discrete random particles. Let the following random measures approximate $p(u)$

$$p(u) \approx \sum_{m=1}^{M} w^{(m)} \delta(u - u^{(m)}) \tag{5.1}$$

Where $\delta(\bullet)$ is the dirac delta function, and $u^{(m)}$ are the M particles with respective assigned weights $w^{(m)}$

$$u = \{u^{(m)}, w^{(m)}\}_{m=1,2,....M} \tag{5.2}$$

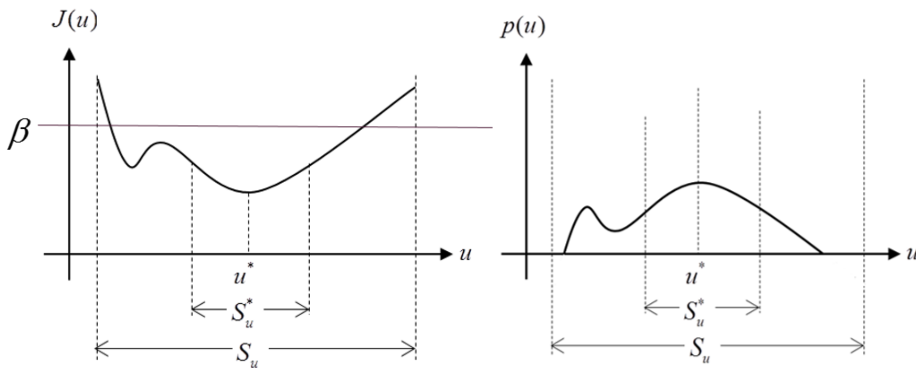

Figure 5.3 : Conversion of Cost function into pdf

5.3.1 Relation between $J(u)$ and $p(u)$

An important concept is to establish a relation between $J(u)$ and $p(u)$. Both of the functions are opposite in the sense of minima and maxima respectively. This relation can be defined by a function that defines $p(u)$ such that:-

- $p(u)$ has the same support as $J(u)$
- $p(u)$ attains its maximum at u^*, where $J(u^*)$ is the minimum value over a set S_u

- $p(u)$ decreases when $J(u)$ increases

$p(u)$ may be of zero value for values of $J(u)$ greater than a threshold β. A suitable candidate for β is the mean:-

$$m_J = \frac{\int_{S_u} J(u)}{\int_{u} S_u} \tag{5.3}$$

where $\int_{S_u} (\bullet) S_u$ is inegral over set S_u

Let $$q(u) = \begin{cases} 0 & J(u) > \beta \\ \beta - J(u) & otherwise \end{cases}$$

and $$p(u) = \begin{cases} \dfrac{q(u)}{\int_{S_u} q(u)} & u \in S_u \\ 0 & otherwise \end{cases}$$

$\int_{S_u} q(u)$ is the weighting so that $\int_{S_u} p(u) = 1$

5.4 Weight assignment process (WAP)

Conventionally particles are weighted based on the prior knowledge available in the form of probability density function. However, in our technique, each particle has been assigned a weight on the basis of the cost function. Figure 5.4 describes the weight assignment procedure in which every set of particle generates an output which is compared with the reference signal and respective cost is calculated. Samples of J_i obtained from u_i are obtained through following equation:-

$$\hat{J}_i = \int_{kT}^{(k+1)T} \left\| \hat{y}(t) - \hat{r}(t) \right\| dt \qquad (5.4)$$
$$\hat{y}(t) = h(\hat{x})$$

Just to remind that we are dealing with a multidimensional problem with $u \in R^m$, $r \in R^m$ and $y \in R^m$

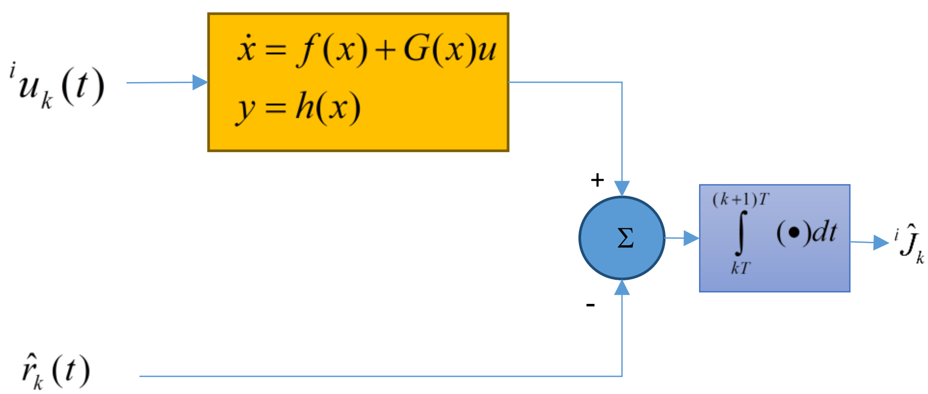

Figure 5.4: Weight Assignment Procedure (WAP)

In figure 5.4, a signal $^{i}u_k(t)$ over interval $[kT,(k+1)T]$ corresponding to a particle $^{i}u_k$ is applied to a simulated model of the physical system. The output is then compared with the reference $r_k(t)$ and integrated over interval $[kT,(k+1)T]$ to obtain $^{i}J_k$ (cost of particle $^{i}u_k$).

$\hat{x}(t)$ is obtained from the observer. For particles u_i , assign cost to each particle as per (5.5) as c_i, where as weight of each particle is assigned as follows :-

$$w_i^* = \begin{cases} 0 & c_i > \beta \\ \beta - c_i & otherwise \end{cases} \tag{5.5}$$

The weights are then normalize by following equation:-

$$w_i = \frac{w_i^*}{\sum w_i^*} \tag{5.6}$$

which will result in $\sum w_i^* = 1$

5.5 Refine Sampling

In order to calculate the mode, we choose the heaviest $\bar{u}_k$ (which is in fact has the minimum cost). Due to sparsity of particles, $\bar{u}_k$ is expected to be only suboptimal in the vicinity of global minima. A cluster of the P particles centered at $\bar{u}_k$ is generated. $\bar{u}_k^*$ is the refined mode after addition of new particles, as shown in Figure 5.4. $\bar{u}_k^*$ is expected to be a better estimate of u_k^*.

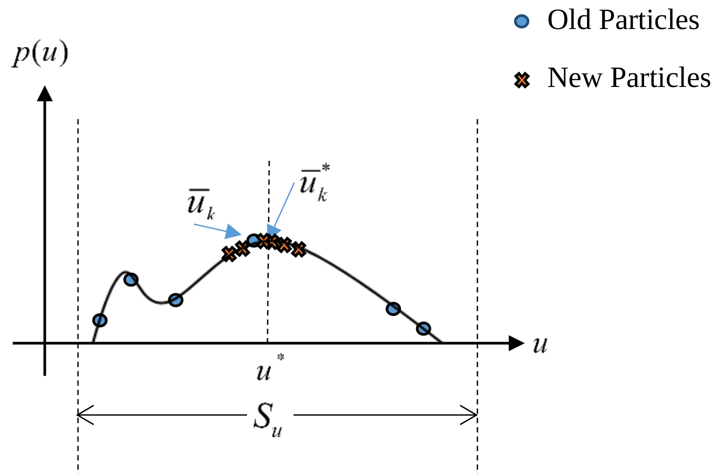

Figure 5.5 : Refine Sampling

5.6 Resampling

The main purpose of resampling is to avoid degeneracy and keep the complete search area S_u available for generation of new particles. Let η be the particles having low weight values. Resampling will be carried out and $(1-\eta)$ particles are replicated as the heavy weight particles according to distribution and weak particles are eliminated. $\beta(u)$ will be in general a narrow variance distribution with mean equal to u_i. After resampling, we have a new set of particles of equal weight. Weight assignment process (WAP) also requires particles to be equally weighted.

$$\eta = \{u_i', w_i\} \quad i = 1,...., M$$
$$\text{where } w_i = \frac{1}{M} \tag{5.7}$$

The heavy weight particles are replaced by a cluster of multiple lighter weight particles as shown in Figure 5.6. η particles are regenerated according to $p(u)$. The particles make sure that the algorithm recovers if it falls in a local minimum. These particles may be termed as guard particles.

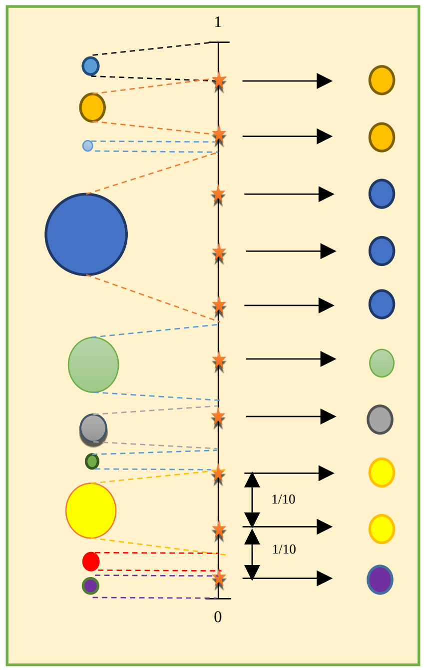

Figure 5.6: A schematic description of Resampling [18]

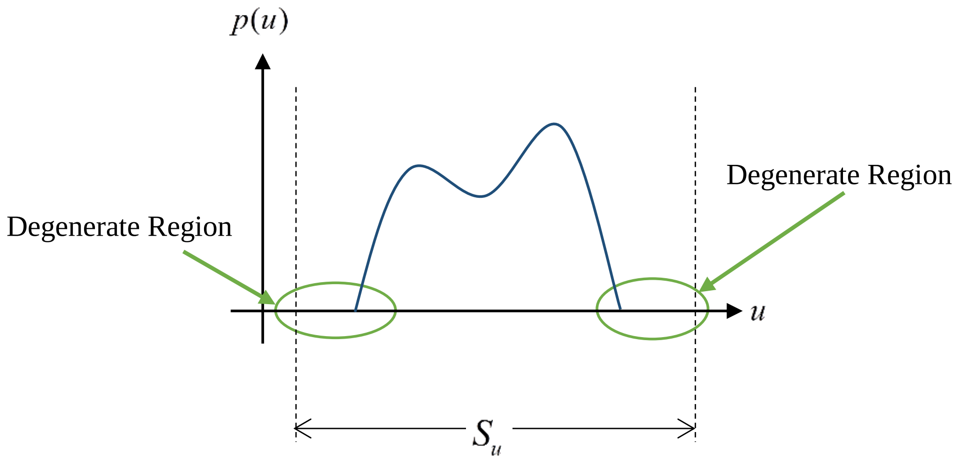

Figure 5.7 : Degenerate Region

5.7 Degenerate regions and Regeneration

Resampling has a side effect that it may create degenerate regions as shown in Figure 5.7. Based on the prior knowledge it is known that global minima exists within essential support S_{uE} .Therefore a non- information probability density function called as guard pdf is used. This guard pdf has support S_{uE} and not complete support S_u. Since there is a possibility that global minima might exists within the region, therefore we fuse the pdf with a guard pdf, so that the resulting pdf has support for entire S_{uE}. This process is called regeneration.

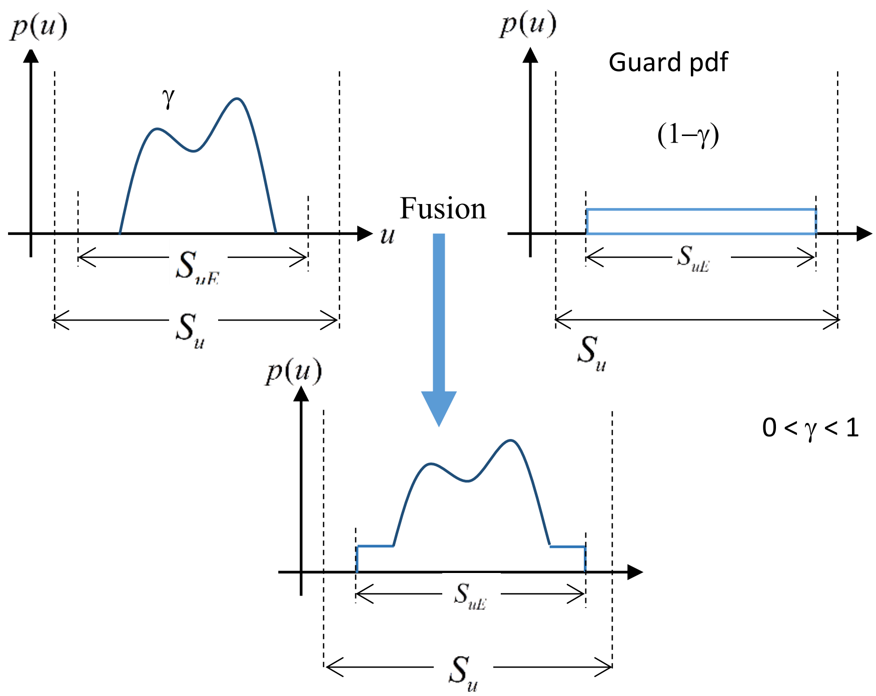

Figure 5.8 : Regeneration

5.8 Particle Controller

Following two algorithms have been proposed for designing control law for the class of nonlinear systems under consideration.

5.8.1 Algorithm –I (Current Control)

Before time k, assume availability of a set of equally weighted M particles characterizing $p(u_k \mid u_{k-1}, y_{k-1}, r_{k-1})$.

At time k, y_k and r_k are available.

Step 1 : Estimate $p(u_k | u_{k-1}, y_k, r_k)$ by WAP

Step 2 : Find mode $\overline{u}_k$ of $p(u_k | u_{k-1}, y_k, u_k)$

Step 3 : Refine sampling about $\overline{u}_k$

- Generate L particles in vicinity of $\overline{u}_k$ based on Gaussian distribution with mean at $\overline{u}_k$
- Assign weights using WAP
- Replace lowest cost L particles with these new particles

Step 4 : Find refine mode $\overline{u}_k^*$ which estimates u_k^*

Step 5 : Apply $\overline{u}_k^*$ to the actual system

Step 6 : Resampling of $p(u_k | u_{k-1}, y_k, u_k)$ to get $p'(u_k | u_{k-1}, y_k, u_k)$. (This is required for WAP). Resample only $M - M_G$ particles, where M_G are the number of particles to be discarded.

Step 7 : Predict $\hat{y}[k+1]$ using $u[k]$, $\hat{r}[k+1]$, where $\hat{r}[k+1]$ and system model is generated using model of system generator for reference r

Step 8 : Run WAP for interval $[(k+1)T\ ,\ (k+2)T]$ to get $\hat{p}(u_{k+1} | u_k, y_k, r_k)$

Step 9 : Resampling of $\hat{p}(u_{k+1} | u_k, y_k, r_k)$ to get $\hat{p}'(u_{k+1} | u_k, y_k, r_k)$. Resample only $M - M_G$ particles, where M_G are the number of particles to be discarded.

Step 10 : Fusion of guard pdf (non-information) with $\hat{p}'(u_{k+1} | u_k, y_k, r_k)$. In this step, guard particles equal to number of M_G particles are generated.

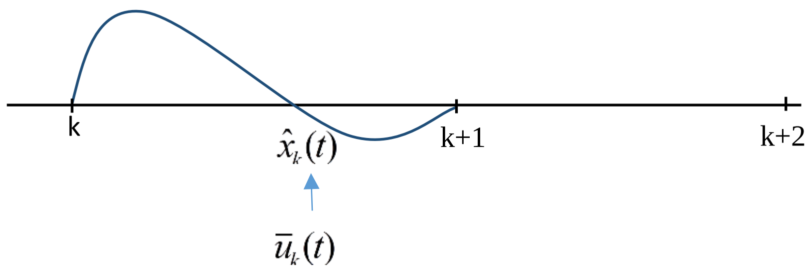

Figure 5.9 : Transition from $K \rightarrow K+1$

Transition from $K \rightarrow K+1$

u_k becomes u_{k-1} and $y_k \rightarrow y_{k+1}, r_k \rightarrow r_{k+1}, u_{k+1} \rightarrow u_k$

5.8.2 Algorithm –II (Predictive Control)

Before time k, we have set of equally weighted M particles characterizing $p(u_k | u_{k-1}, y_{k-1}, r_{k-1})$. Mode of $p(u_k | u_{k-1}, y_{k-1}, r_{k-1})$ is also available as $\bar{u}_k^*$.

At time k, y_k and r_k are available.

Step 1 : Apply $\bar{u}_k^*$ to the actual system

Step 2: Predict $\hat{y}_{k+1}, \hat{x}_{k+1}, \hat{r}_{k+1}$ on the basis of $\bar{u}_k^*, y_k, r_k$ and plant / exosystem models

Step 3 : Apply WAP for $[(k+1)T, (k+2)T]$ to obtain M particles (of unequal weights) that characterize $p(u_{k+1} | u_k, y_k, r_k)$

Step 4 : Find mode of $p(u_{k+1} | u_k, y_k, r_k)$. The heaviest particle will be the mode and call it $\bar{u}_k$

Step 5 : Refine sampling about $\bar{u}_k$

- Generate L particles in vicinity of $\bar{u}_k$ based on Gaussian distribution with mean at $\bar{u}_k$
- Assign weights using WAP
- Replace lowest cost L particles with these new particles

Step 6 : Find the new refined mode and call it $\bar{u}_k^*$

Step 7 : Resampling the $p(u_{k+1} | u_k, y_k, r_k)$ to get $p'(u_{k+1} | u_k, y_k, r_k)$ represented by M particles of equal weights. Resample only $M - M_G$ particles, where M_G are the number of particles to be discarded.

Step 8 : Carryout regeneration process. Fusion of guard pdf (non-information) with $p'(u_{k+1} | u_k, y_k, r_k)$ to avoid degeneration. In this step, guard particles equal to number of M_G particles are generated.

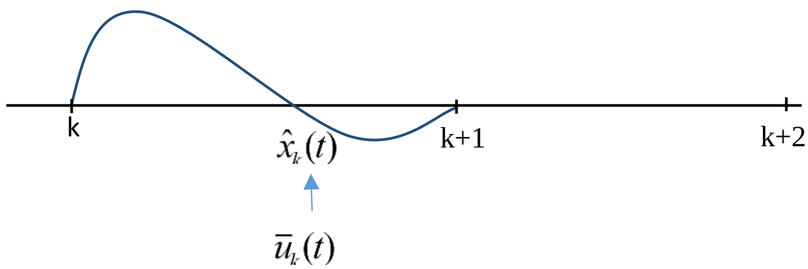

Figure 5.10 : Transition from $K \to K+1$

Goto Step1 Transition from $K \to K+1$

u_k becomes u_{K-1}

k+1 becomes k

k become k-1

5.9 Example

From chapter two, the dynamics of the system in the stator frame are given as :-

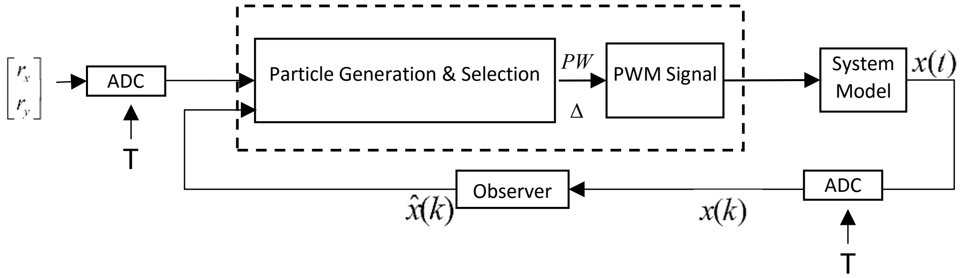

Figure 5.11 : Particle Controller based Scheme

$$J\ddot{\theta}_x' + b\dot{\theta}_x' + H_z\dot{\theta}_y' = \tau\cos\omega_z t$$
$$J\ddot{\theta}_y' + b\dot{\theta}_y' - H_z\dot{\theta}_x' = \tau\sin\omega_z t \quad (5.8)$$

To represent (5.8) in state space form, $\dot{\theta}_x'$, $\dot{\theta}_y'$, θ_x' , θ_y' , $\tau\cos\omega_z t$ *and* $\tau\sin\omega_z t$ are denoted as x_1, x_2, x_3, x_4, u_1 and u_2 respectively. The state space representation in stator frame of reference is given as under :-

$$\dot{x_1} = -\frac{b}{J}x_1 - \frac{H_z}{J}x_2 + \frac{u_1}{J}$$

$$\dot{x_2} = \frac{H_z}{J}x_1 - \frac{b}{J}x_2 + \frac{u_2}{J}$$

$$\dot{x_3} = x_1 \quad (5.9)$$

$$\dot{x_4} = x_2$$

Or in the matrix form as :-

$$\dot{x}(t) = A\,x(t) + B\,u(t)$$

$$y(t) = C\,x(t) \quad (5.10)$$

$$u(t) = \begin{bmatrix} u_1 \\ u_2 \end{bmatrix} \quad (5.11)$$

$$\text{Where } \bar{A} = \begin{bmatrix} -\frac{b}{J} & -\frac{H_z}{J} & 0 & 0 \\ \frac{H_z}{J} & -\frac{b}{J} & 0 & 0 \\ 1 & 0 & 0 & 0 \\ 0 & 1 & 0 & 0 \end{bmatrix},\ \bar{B} = \begin{bmatrix} \frac{1}{J} & 0 \\ 0 & \frac{1}{J} \\ 0 & 0 \\ 0 & 0 \end{bmatrix},\ \bar{C} = \begin{bmatrix} 0 & 0 & 1 & 0 \\ 0 & 0 & 0 & 1 \end{bmatrix} \quad (5.12)$$

Here the difficulty level is further increased and the actuation of type III is considered in this chapter. Thus under constraints (2.27), the pulse width PW and the position Δ are the two controllable parameters i,e., $u = [PW \quad \Delta]^T$. The control signal (Figure. 5.11) is generated by searching optimized values of PW and Δ based on the minimization of error. The Figure 5.11 presents the proposed scheme. The error is the difference between the reference signal and the observer feedback. The cost function $J(u)$ is given by (5.14)

$$e(t) = \begin{bmatrix} e_1 \\ e_2 \\ e_3 \\ e_4 \end{bmatrix} = \begin{bmatrix} r_x - \hat{\theta}_x \\ r_y - \hat{\theta}_y \\ \dot{r}_x - \dot{\hat{\theta}}_x \\ \dot{r}_y - \dot{\hat{\theta}}_y \end{bmatrix} \tag{5.13}$$

$$J(u) = e_1^{\,2} + e_2^{\,2} + e_3^{\,2} + e_4^{\,2} \tag{5.14}$$

In this example the each particle will have two parameters i.e., PW and Δ. First of all the M particles are generated based on uniform random distribution having equal weights. Figure 5.12 shows status of particles at different stages during the simulation. Figure 5.12a shows particles have been assigned weights through WAP. These weights are based on the cost function of tracking error. Figure 5.12b shows the top view of Figure 5.12a. It is clear that it is a multi modal pdf. The refined sampling will be performed in the vicinity of the possible global minima. The particles after refined sampling are shown in the Figure 5.12c and two minima are visible in the top view in Figure 5.12d. This is followed by resampling which replaces the heavy weight particles with a cluster of multiple lighter weight particles as shown in Figure 5.12e. Due to resampling, the degenerate regions are created. In the regeneration process, guard particles are generated as shown in figure 5.12f.

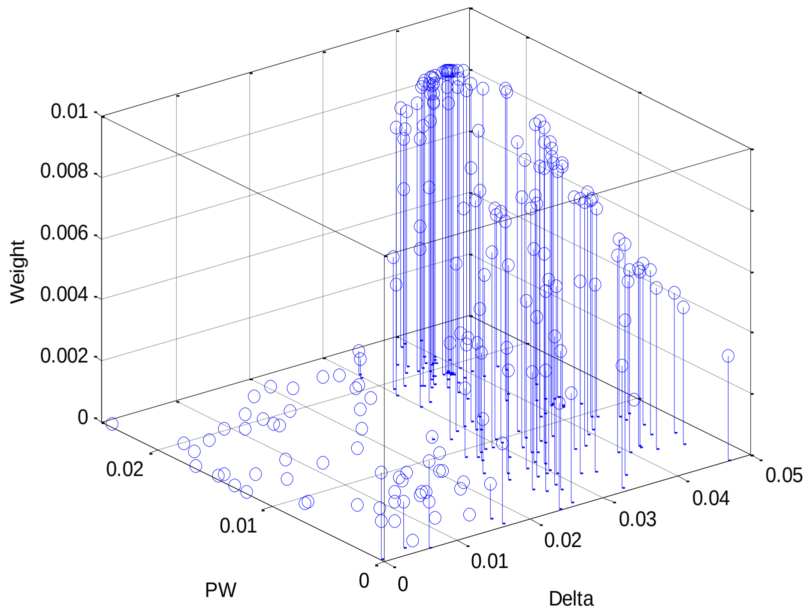

Figure 5.12a : Particle Spread after WAP

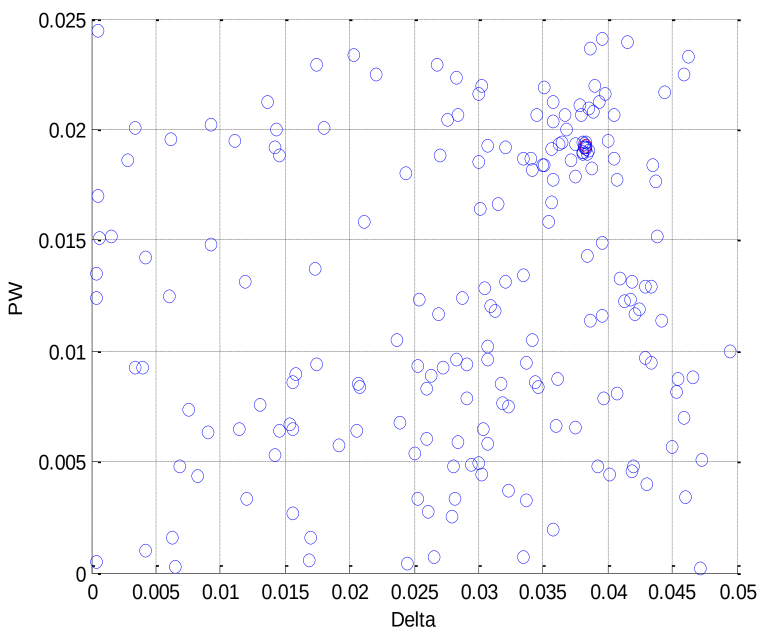

Figure 5.12b : Particle Spread after WAP

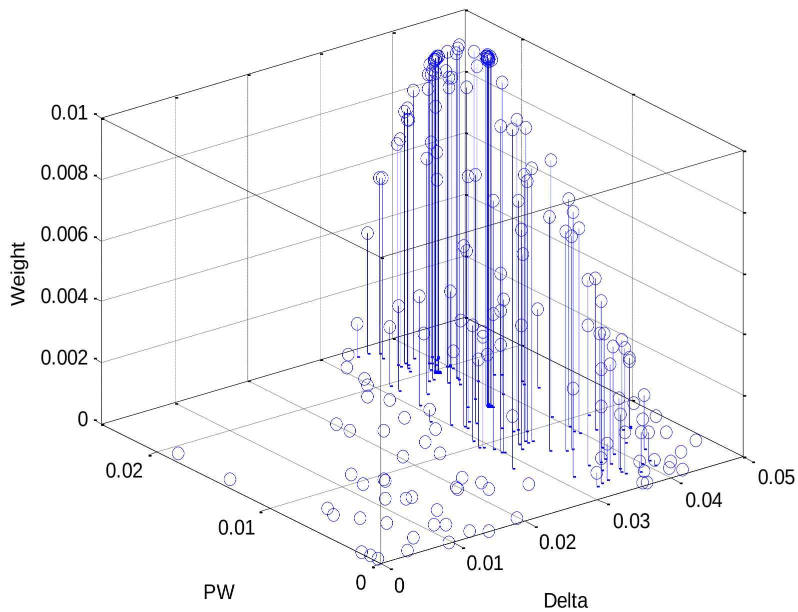

Figure 5.12c : Particle Spread After Refine Sampling

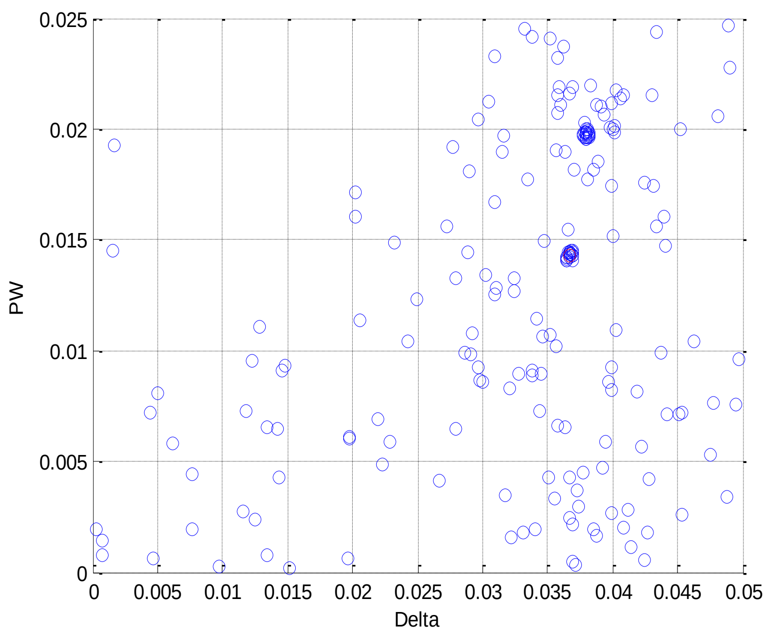

Figure 5.12d : Particle Spread After Refine Sampling

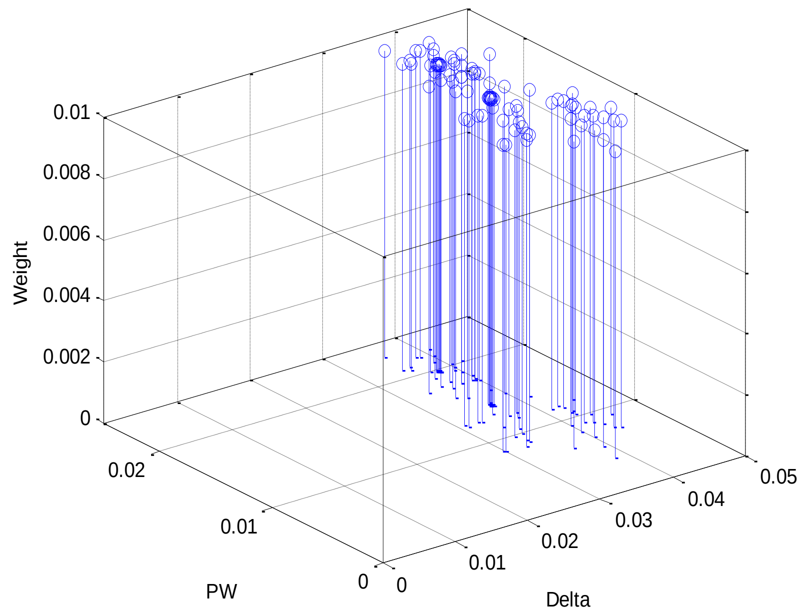

Figure 5.12e : Particle Spread After Resampling

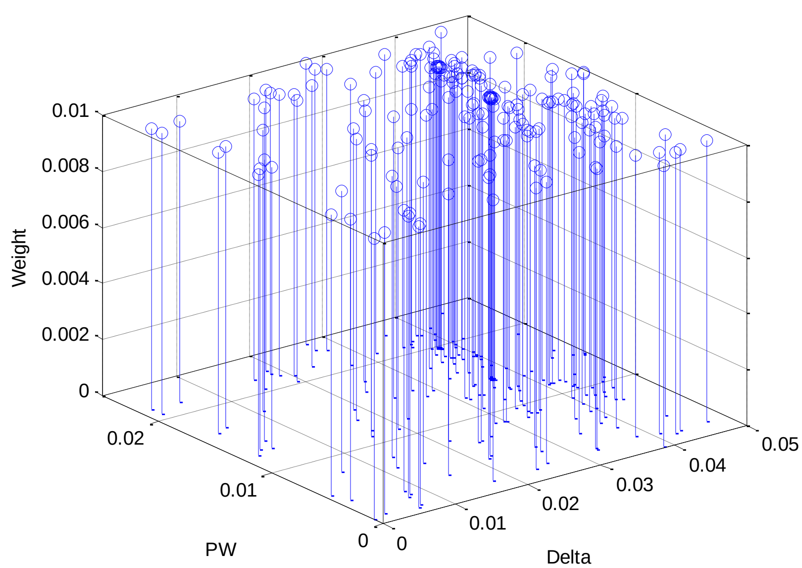

Figure 5.12f : Particle Spread after addition of Guard Particles

5.10 Simulations and Performance Analysis

Simulations were carried out in MATAB and SIMULINK. The parameters used are $\omega = 400\,\pi\,\frac{rad}{\sec}$, $b = 400$, $K_i = 1$, $J = 4\,kgm$, $J_z = 5\,kg$. The time interval to complete one revolution is 0.05 sec. The simulated performance of closed loop system for both the algorithms is shown Figure 5.13 and Figure 5.14 respectively. The particle controller tracks a fixed and varying time signal. It must be appreciated that the transient response is also very smooth. The tracking error has been shown in Figure 5.13b and Figure 5.13d for algorithm 1 and those for algorithm 2 are shown in Figure 5.14b and Figure 5.14d respectively. The pattern of delta and PW for both the algorithms (for time varying reference) is shown in Figure 5.13e and Figure 5.14e respectively. The cost function and the observer estimation error are shown in Figure 5.13f and Figure 5.13g respectively for algorithm 1. Similarly, the observer estimation error for algorithm 2 is shown in Figure 5.14f and Figure 5.14g respectively.

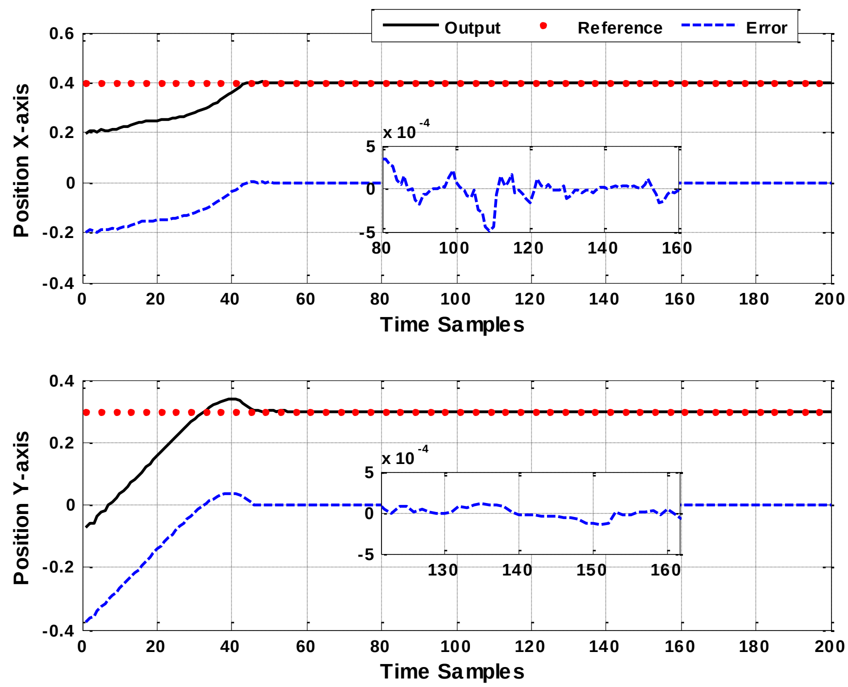

Figure 5.13a : Stabilization under Fixed Reference – Algorithm 1

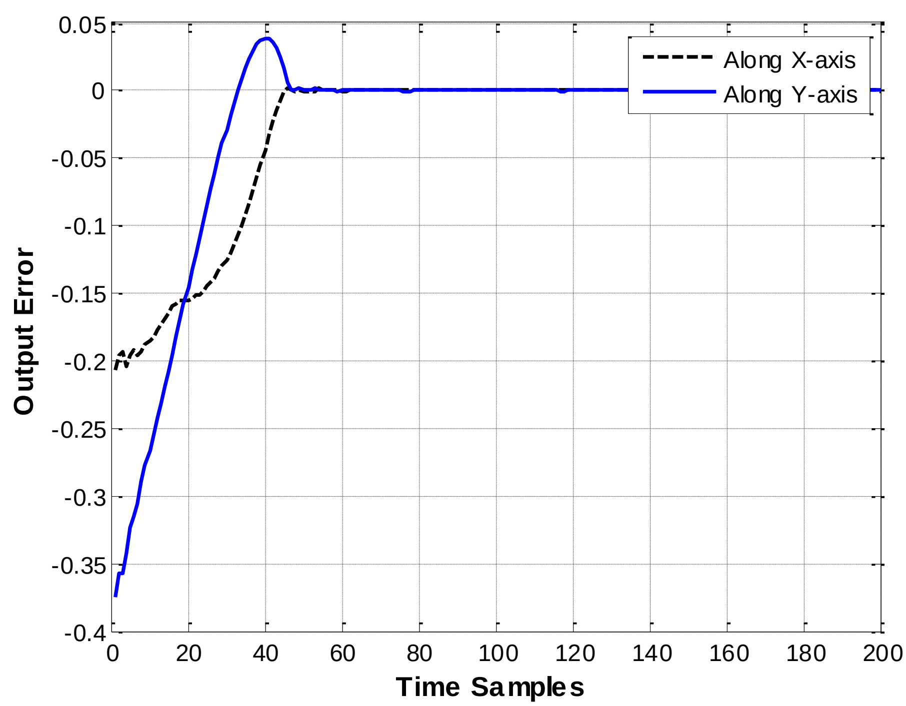

Figure 5.13b : Output Error under Fixed Reference – Algorithm 1

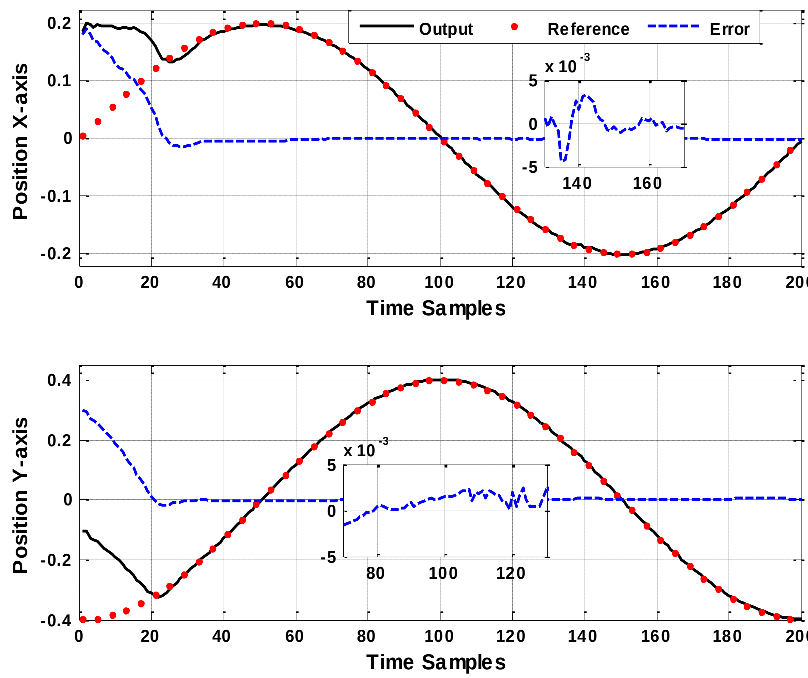

Figure 5.13c : Stabilization under Varying Reference – Algorithm 1

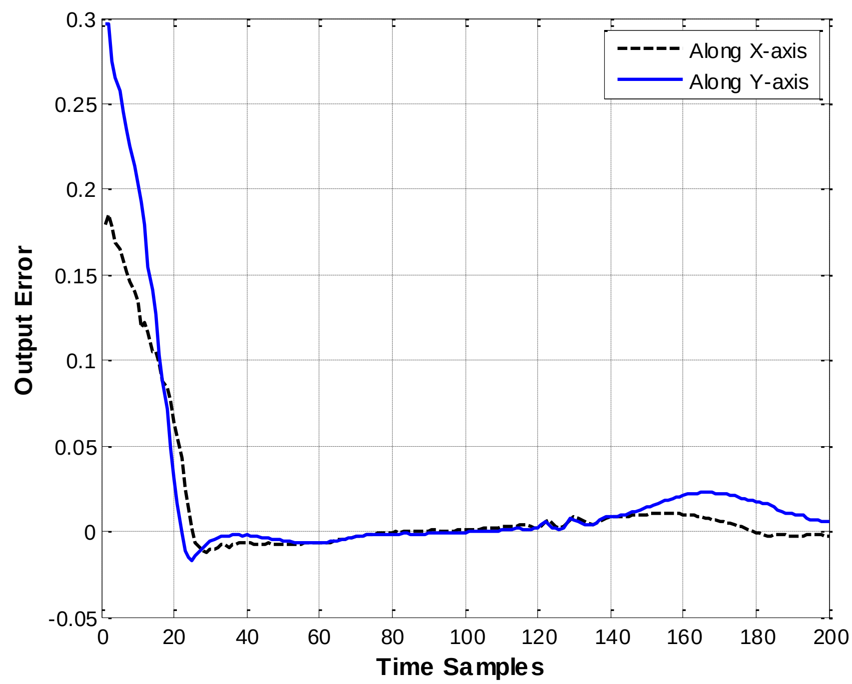

Figure 5.13d : Output Error under Varying Reference – Algorithm 1

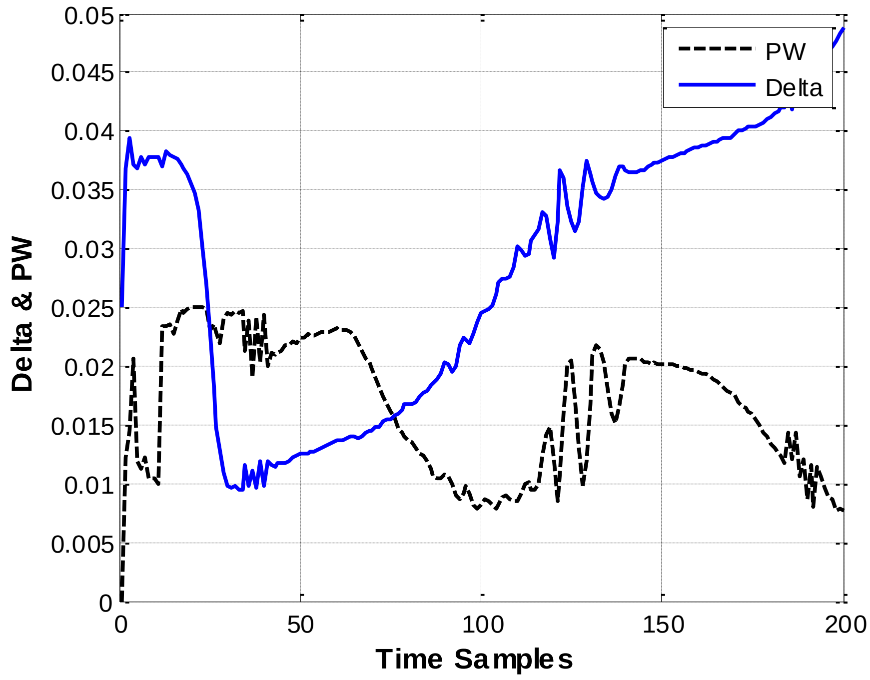

Figure 5.13e : Delta & PW under Varying Reference – Algorithm 1

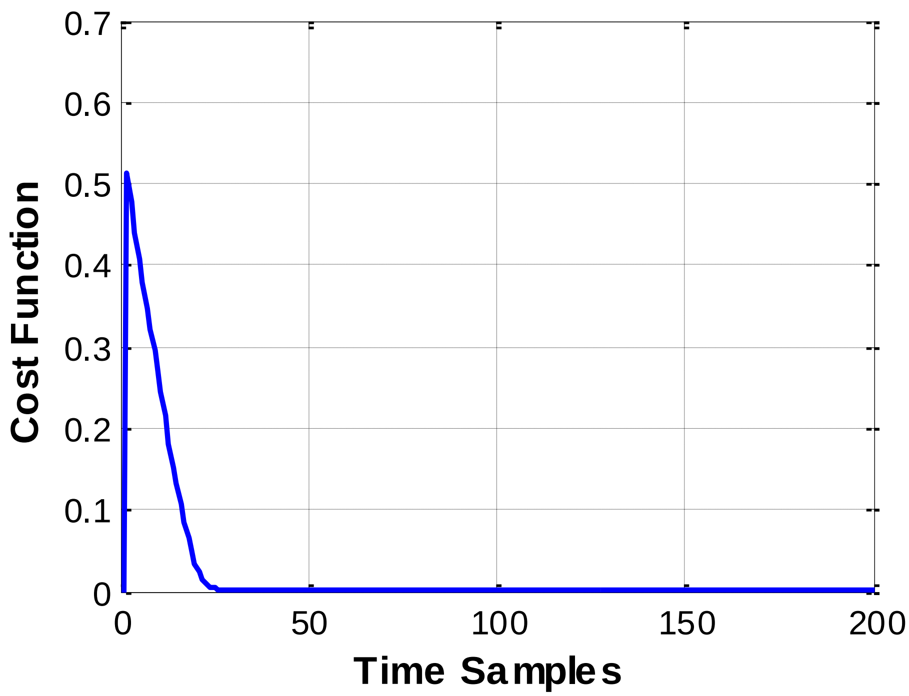

Figure 5.13f : Cost Function vs Time – Algorithm 1

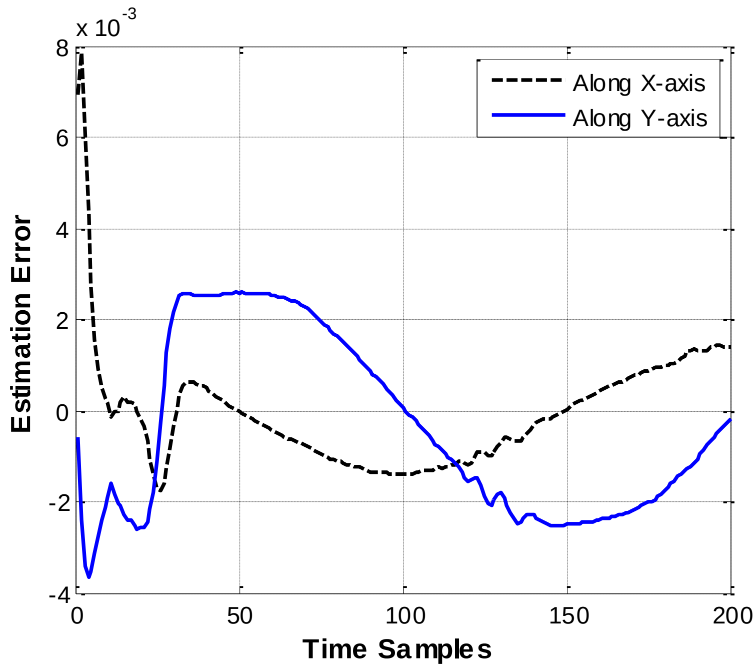

Figure 5.13g : Estimation Error under Varying reference – Algorithm 1

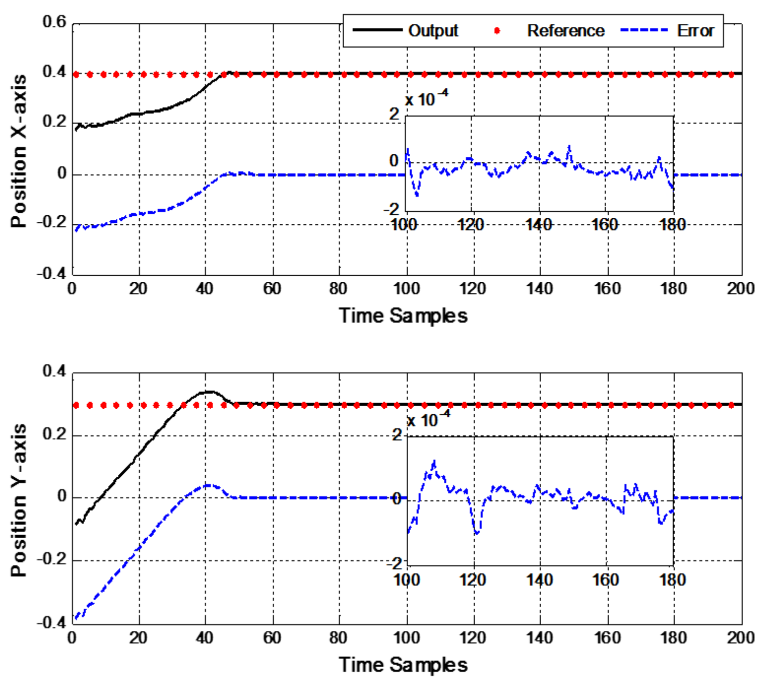

Figure 5.14a : Stabilization under Fixed Reference – Algorithm 2

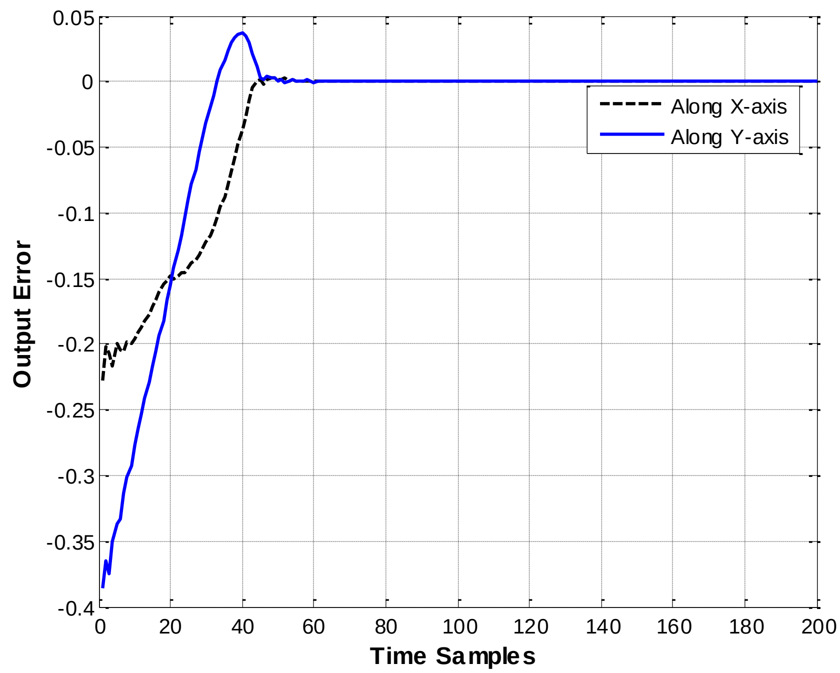

Figure 5.14b : Output Error under Fixed Reference – Algorithm 2

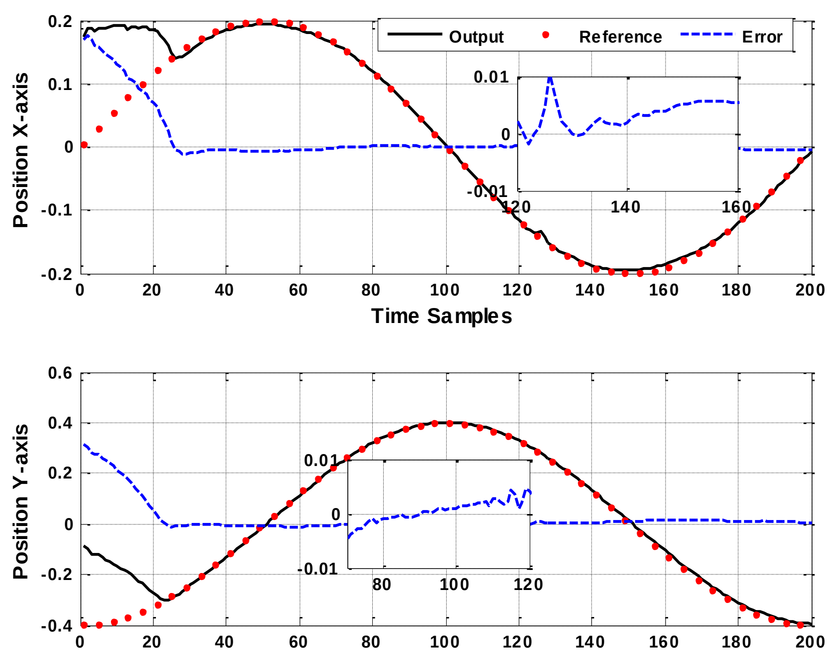

Figure 5.14c : Stabilization under Varying Reference – Algorithm 2

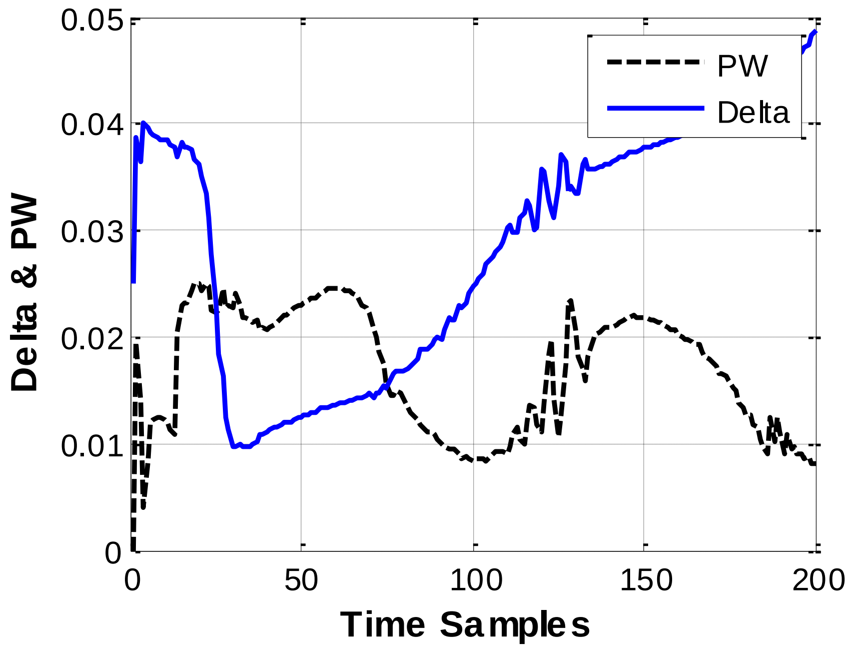

Figure 5.14d : Delta & PW under Varying Reference – Algorithm 2

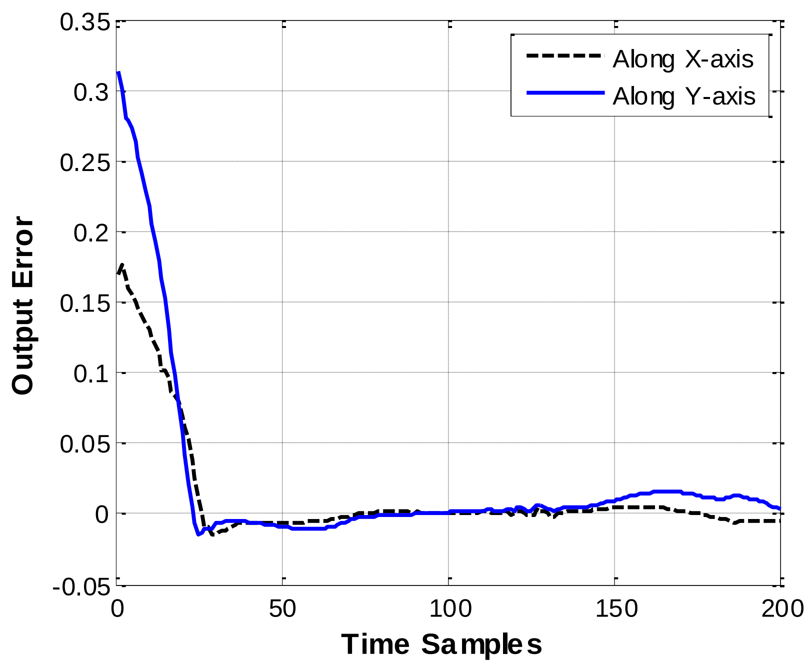

Figure 5.14e : Output Error under Varying Reference – Algorithm 2

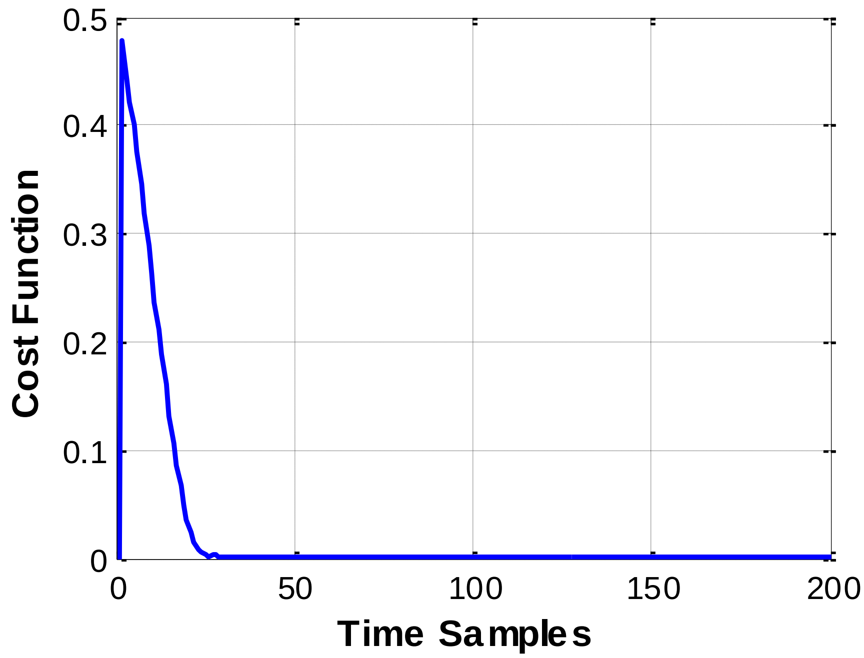

Figure 5.14f : Cost Function vs Time– Algorithm 2

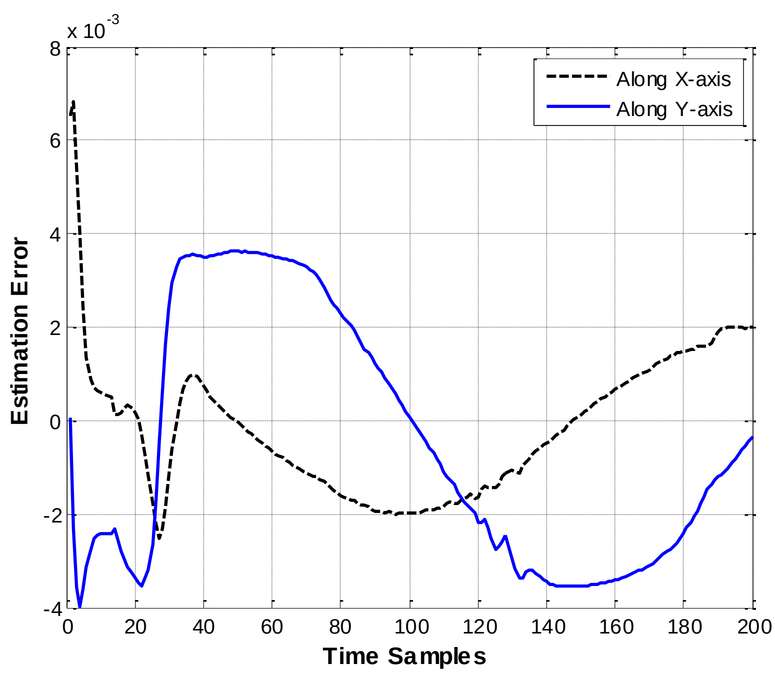

Figure 5.14g : Estimation Error under Varying reference – Algorithm 2

5.11 Comparison with existing Techniques

In order to compare the performance of proposed algorithms with existing techniques, Dominik Stahl's [1] technique is applied for orientation control of a drill machine described in section 5.9. They [1] used two particle filters , one for the state estimation and the other for estimation of control input for the system. However, for fair comparison, the first particle filter which is used for state estimation is not used. Rather state estimation was carried out through output feedback by using the same observer as developed for the algorithm 1 & 2. Stahl [1] used following multivariate Gaussian density for drawing of control input's transition pdf.

$$b_j(s_j|\bar{x}_j,\bar{u}_j) = \frac{1}{(2\pi)^{n/2}|R|^{-1/2}}\exp(\|s_j - \bar{x}_j\|_R^2) \tag{5.15}$$

Where s_j, $\bar{x}_j$ and u_j denotes the reference trajectory, states and input respectively. This prior knowledge about the control input is to be provided by the user. In case, this information is not accurately known, the performance of the algorithm will be seriously affected. Whereas, our technique uses particles to characterize the probability density function.

Similarly the weights of the particles are updated based on the prior knowledge using following typical Bayesian theory :-

$$w_j^{(i)} = w_{j-1}^{(i)}\frac{b_j(\mathrm{s}_j \mid \bar{x}_j^{(i)},\bar{u}_j^{(i)})\bar{a}_j(\xi_j \mid \xi_{j-1}^{(i)})}{q_j(\xi_j^{(i)} \mid \mathrm{s}_j,\xi_{j-1}^{(i)})} \tag{5.16}$$

Where $\xi_j^{(i)} = (\bar{x}_j^{(i)}, \bar{u}_j^{(i)}, \tilde{u}_j^{(i)})$. Whereas, we are proposing weight assignment procedure, in which each particle has been assigned a weight on the basis of the cost function as described in Figure 5.4.

The simulation was performed using the same parameters of section 5.10 so that a fair comparison can be made. The simulation results are shown in Figure 5.15. The Stahl's algorithm gets trapped into local minima and the cost function could not be minimized. In Figure 16 a comparison is made to compare the tracking performance of proposed algorithms with Stahl[1] by subjecting to a difficult varying reference. Algorithm I & II tracks the difficult varying signal whereas Stahl[1] could not track the signal.

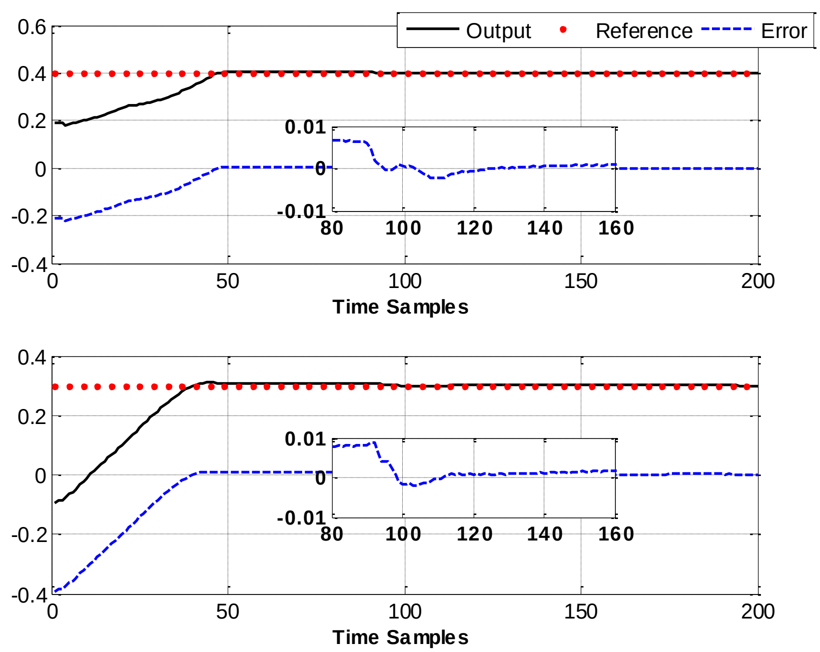

Figure 5.15a : Stabilization under Fixed Reference – Stahl [1]

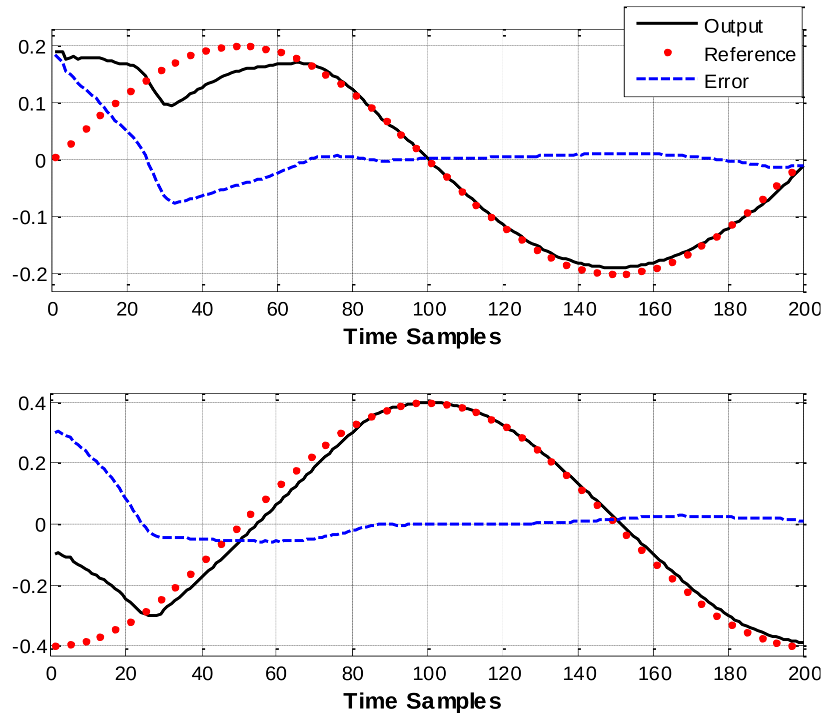

Figure 5.15b : Stabilization under Varying Reference – Stahl [1]

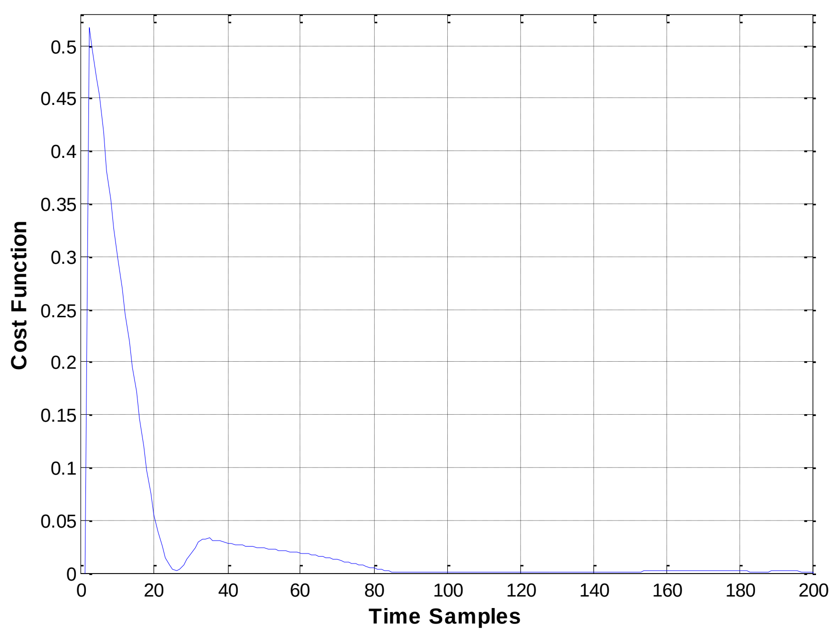

Figure 5.15c: Cost Function vs Time – Stahl [1]

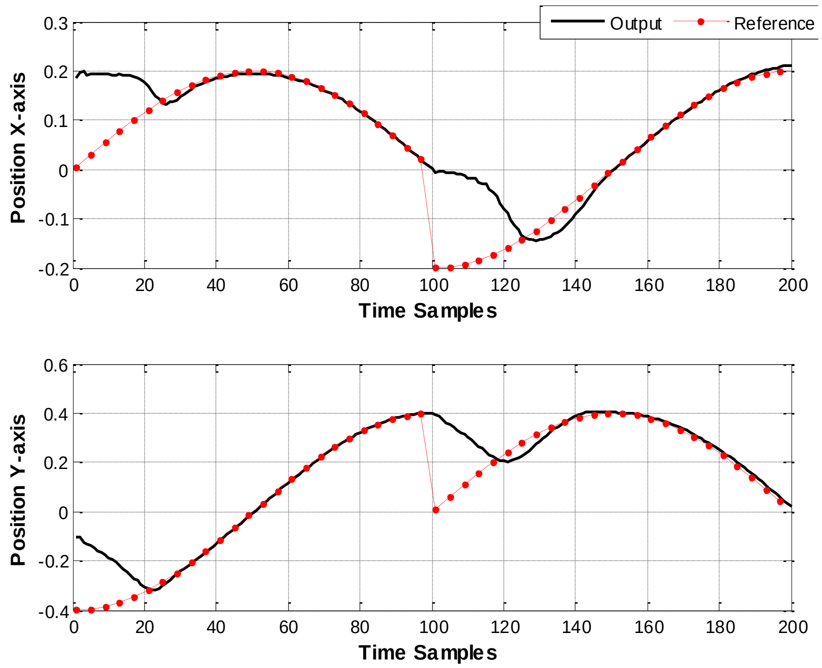

Figure 5.16a : Stabilization under Varying Reference – Algorithm 1

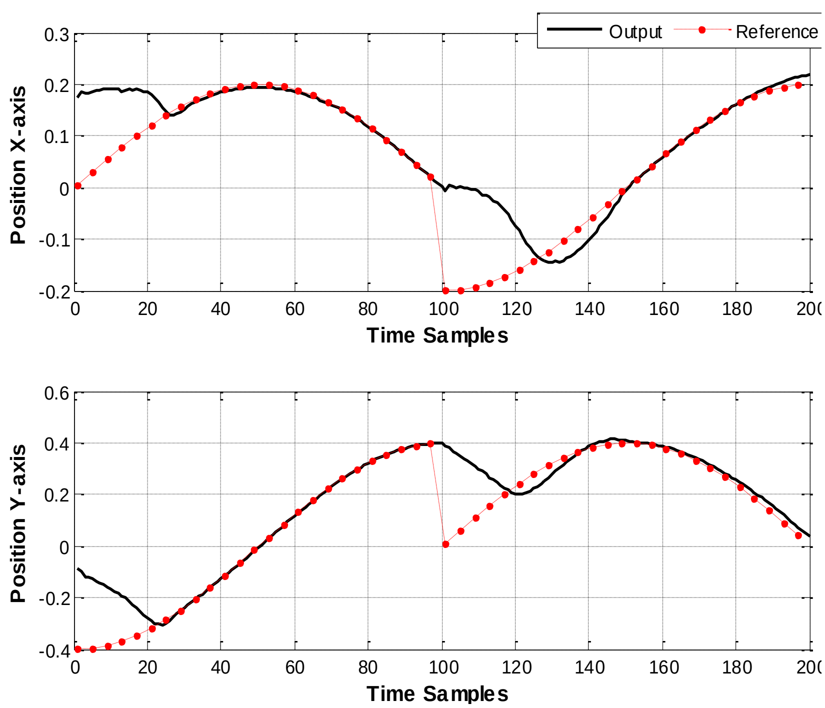

Figure 5.16b : Stabilization under Varying Reference – Algorithm 2

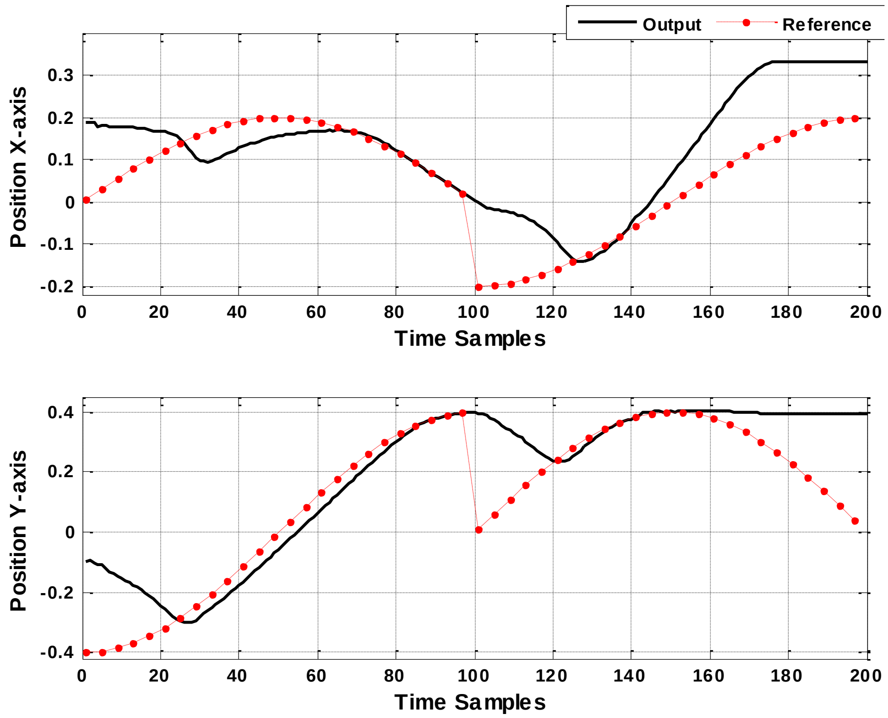

Figure 5.16c : Stabilization under Varying Reference – Stahl [1]

5.12 Monte Carlo Simulations

The robustness of the Particle controller for both the algorithms has been verified by introducing parametric perturbation in the system model. The particle controller is designed for nominal system parameters, whereas system is simulated for over 2000 times by introducing random disturbances in the parameters. The algorithm-1 withstand up to ±20% disturbance in system model (Figure 5.17) whereas the algorithm-2 withstand up to ±10% disturbance in system model (Figure 5.18). Both algorithms remained stable with minor variations in settling time and the tracking of target was achieved. The upper and lower bounds for the angular positions along X-axis and Y-axis are plotted. It can be seen that stabilization for desired fixed as well as varying reference is achieved with perturbed parameters as well. This demonstrates the robustness of the proposed controller.

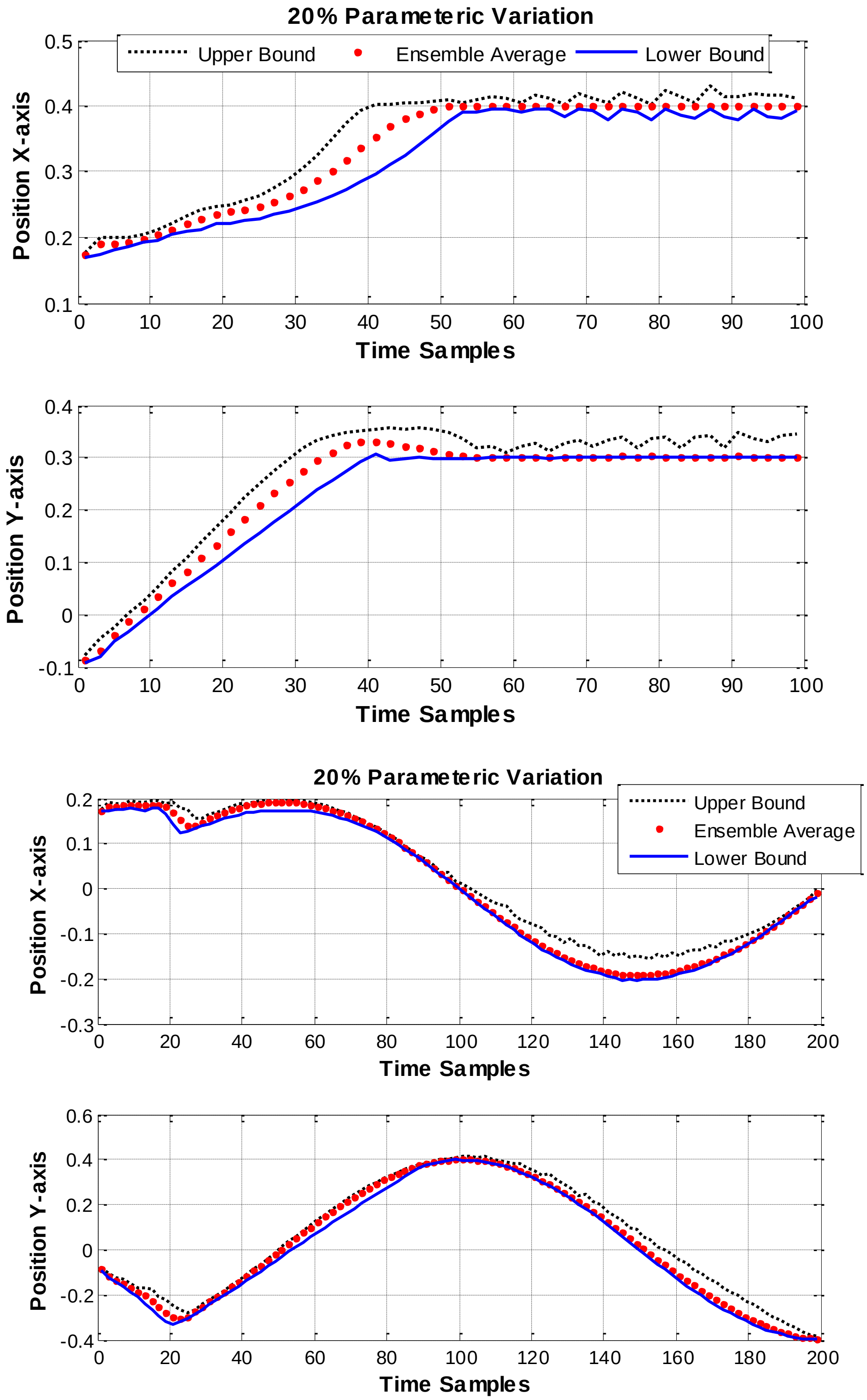

Figure 5.17: Monte Carlo Simulations – Algorithm 1

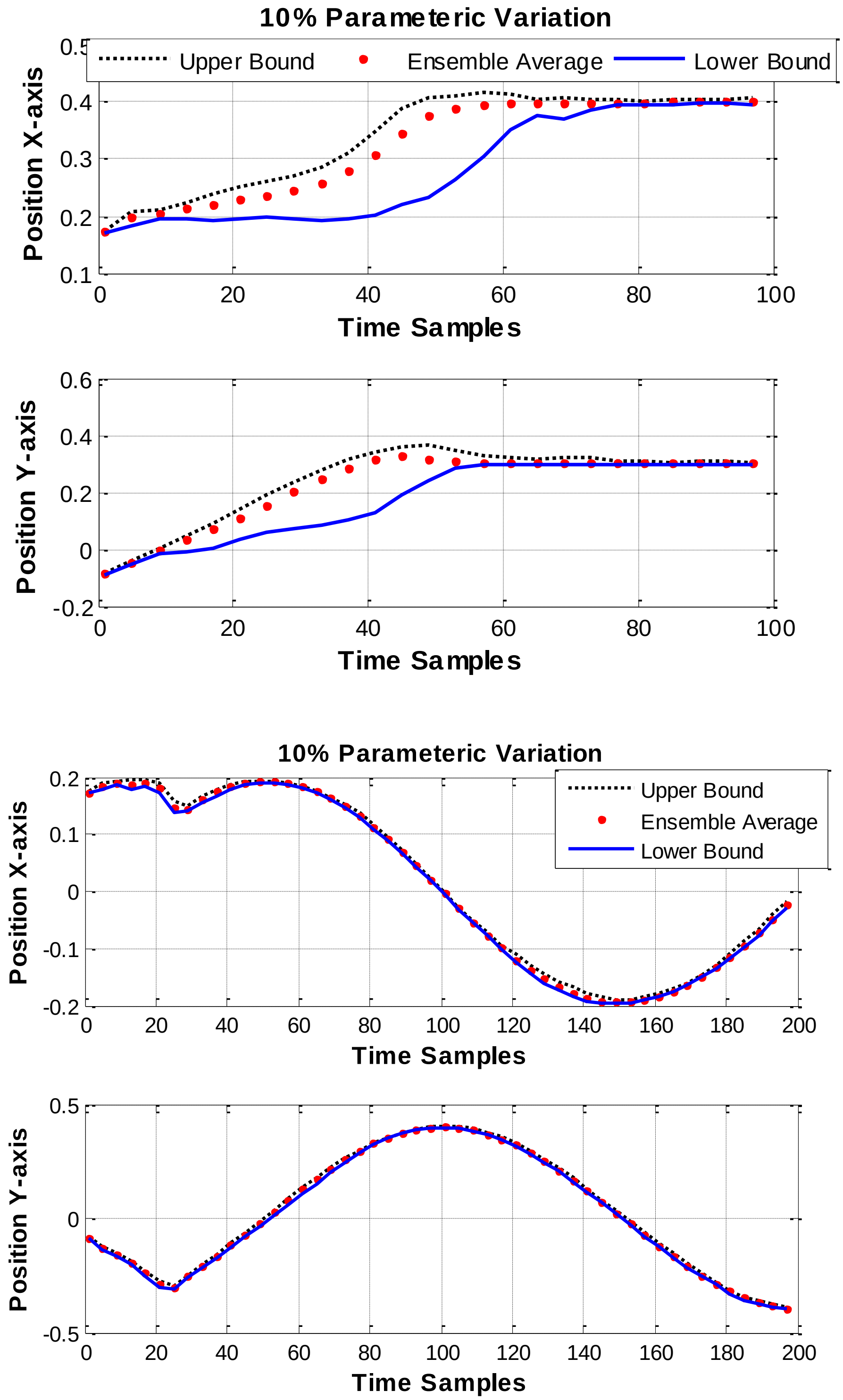

Figure 5.18: Monte Carlo Simulations – Algorithm 2

5.13 Discussion

Both the proposed algorithm for particle controller tracks the fixed as well as time varying reference. The algorithm 1 is based on current information but is difficult to implement in real time. The algorithm 2 is predictive in nature and suits real time implementation. The algorithm 1 is more robust than the other one as it can with stand ±20% perturbations in the nominal model. A comparison with existing technique Stahl[1], it is evident that they get trapped in local minima, and they do not have a mechanism to get out of local minima e.g. guard particles as used by proposed techniques. Moreover, using proposed "refined sampling", the tracking error can be further minimized which is not in the case of existing techniques. Also Stahl[1] could not track a difficult tracking reference (Figure 5.16). The searching of global minima using Monte Carlo methods proves to be better, faster and real time implementable when compared with the EMC technique of Chapter 4. It is also highlighted that the difficulty level is increased for particle controller as it is subjected to constrained actuation type III.

5.14 Comparison of Proposed Techniques

Table II & Table III shows the comparison of proposed techniques. In Table II, comparison of simulation time of proposed techniques is shown. The PEA & EMC techniques were subjected to Type II constraints whereas, Type III constraints were applied on actuation for Particle Controller techniques. Table III compares the proposed techniques on basis of robustness, tracking error, type of computation and probability to trap in local minima

Techniques	Constraint on actuation	Simulation Time / Real Time
PEA	Type II	3.22
EMC-RPA		96.75
EMC-MIP		405.5
Current Particle Controller	Type III	7.6
Predictive Particle Controller		3.9
Stahl[1]		4.03

Table II : Comparison of Simulation Time

Techniques	Robustness	Computation	Tracking error	Probability to trap in local minima
PEA	Medium	Single Step	High	Not Applicable
EMC-RPA	High	Iterative	Very Low	Very Low
EMC-MIP	Very High	Iterative	Very Low	Very Low
Current Particle Controller	Very High	Parallel	Low	Very Low
Predictive Particle Controller	High	Parallel	Low	Very Low
Stahl[1]	Low	Parallel	High	High

Table III : Comparison of Proposed Techniques

CHAPTER 6

CONCLUSION AND FUTURE SUGGESTIONS

6.1 Conclusion

A generalized framework of sampled data tracking problem is developed for a class of multi-input multi-output (MIMO) systems. This is applicable to a wide variety of systems belonging to the class of nonlinear systems with constrained input. Both classical (Optimal control) as well as proposed techniques (particle controller) have been used to design control law for such class of systems. These techniques are applied to a challenging example of two-axis orientation control of a gyroscopic system with constrained input.

The solution provided by [13] deals with problem where the pulse width of control input is fixed while its magnitude is proportional to the amount of control force required. Whereas, in this thesis we deal with a more difficult problem where the pulse amplitude is fixed and its width and position are allowed to vary. Due to the given constraints, the solution based on discrete time equivalent model is not possible. However, control signal generated by technique [13] can be transformed into a pulse equivalent area (PEA) signal. The proposed technique [27] has shown satisfactory results in achieving the desired orientation for the nominal as well as for the perturbed system with 10% and 25% variation in parameters. The main advantage of PEA is that it is easily implementable in real time due to its simplicity. However, precise control cannot be achieved through this technique specially in tracking applications.

To overcome approximation of PEA, an error minimized control (EMC) derived from the theory of MPC is developed. Controller design is improved by introducing output feedback. The problem of getting trapped in local minima has been addressed by designing two novel techniques. The non-causality issue has also been addressed by special sliding adjustment. The scheme is effective for fixed references as well as for tracking problems.

Extensive monte-carlo simulations show that the EMC technique gives satisfactory performance under both nominal and parameter variations. However the real time implementation is difficult due to intensive computational load which is required for extensive search of global minima. Iterative nature of the solution worsens the situation.

To overcome the practical limitation of EMC, Monte Carlo methods have been explored for fast searching of global minima and its real time implementation. Literature review revealed that the focus of researchers in designing control effort for nonlinear feedback systems has been restricted to a class of optimal control problems related to nonlinear stochastic discrete-time systems only. Another significant difference is that our technique uses particles to characterize the probability density function as opposed to existing techniques, which draw particles from the presumed probability density function.

New concepts of weight assignment process for non-dependence on apriori probability density function and refined sampling for precise searching of global minima have been introduced and successfully implemented. Two algorithms have been developed. First one is based on current information but is difficult to implement in real time. The other one is predictive in nature and suits real time implementation. Both the algorithms show somewhat similar results. However, the former algorithm proved to be more robust than the later. Extensive monte carlo simulations shows better transient response and tracking performance than EMC technique. A comparison with existing techniques reveals that proposed algorithm can recover if get trapped in local minima. They do not depend on prior knowledge for updating of weights of the particles.

In summary the thesis can be concluded as follows:-

- The sampled data tracking control problem for a class of multi-input multi-output (MIMO) nonlinear systems with constrained input requires development of novel control schemes since the classical nonlinear control design techniques experience limitations on account of definition of arbitrary control law for such systems
- To this account PEA based technique has been proposed for such systems
- Development of EMC for precise tracking problems has also been explored. Two algorithms are proposed for recovery from local minima and sliding adjustment to avoid non-causality
- Two algorithms based on Monte Carlo Methods are developed having following novel features :-
    - Uses particles to characterize the probability density function
    - Non-dependence on apriori probability density function for updating of weights
    - Refined sampling for precise searching of global minima
    - Use of Guard particles to recover from local minima trapping

6.2 Future Suggestions

The proposed control philosophy is expected to find applications in wide variety of challenging problems. Some suggested problems are control of systems with backlash, coulomb friction, control of artificial hand, Control of humanoid etc.

There are also possibilities of extensions in the proposed algorithms themselves. One interesting option is dynamic particles that will have the ability to generate continuous time trajectories for the input. This will be useful in regulator problem.

In addition, Particle controller suits parallel computing and can thus be embedded using FPGAs or ASICs. This will help in real time implementation.

REFERENCES

[1] Dominik Stahl, Jan Hauth, "PF-MPC: Particle filter-model predictive control", Systems & Control Letters, 60(8):632–643, August 2011.

[2] M. Sanjeev Arulampalam, Simon Maskell, Neil Gordon, and Tim Clapp , "A Tutorial on Particle Filters for Online Nonlinear/Non-Gaussian Bayesian Tracking", IEEE Transactions On Signal Processing, Vol. 50, No. 2, February 2002.

[3] A. Greenfield and A. Brockwell, "Adaptive control of nonlinear stochastic systems by particle filtering," in Proceedings of the Conference on Control and Automation, 2003.

[4] C. Andrieu, A. Doucet, S. S. Singh, and V. B. Tadic, "Particle methods for change detection, system identification, and control," Proceedings of the IEEE, vol. 92, 2004.

[5] L. Blackmore, "A probabilistic particle control approach to optimal robust predictive control" In Proceedings of the AIAA Guidance Navigation and Control Conference, 2006.

[6] C. Andrieu, A. Doucet, S.S. Singh, V.B. Tadić, Particle methods for change detection, system identification, and control, Proceedings of the IEEE 92 (3) (2004) 423–438.

[7] S.K. Botchu, S. Ungarala, Nonlinear model predictive control based on sequential Monte Carlo state estimation, in: 8th International IFAC Symposium on Dynamics and Control of Processs Systems, Preprints, 3: Jun 2007, pp. 31–36.

[8] J.P. de Villiers, S.J. Godsill, S.S. Singh, Particle predictive control, Journal of Statistical Planning and Inference (2011).

[9] N. Kantas, J.M. Maciejowski, A. Lecchini-Visintini, Sequential Monte Carlo for model predictive control, in: L. Magni, et al. (Eds.), Nonlinear Model Predictive Control, in: LNCIS, vol. 384, Springer-Verlag, Berlin, Heidelberg,2009, pp. 263–273.

[10] J. Hol, T. Schön, F. Gustafsson, On resampling algorithms for particle filters. Technical report, Department of Electrical Engineering, Linköping University, January 2007.

[11] N. J. Gordon; D. J. Salmond; A. F. M. Smith, "Novel approach to nonlinear/non-Gaussian Bayesian state estimation", IEE Proceedings F - Radar and Signal Processing Year: 1993, Volume: 140, Issue: 2, Pages: 107 – 113.

[12] Morales-Menendez, N. de Freitas, and D. Poole, "Real-time monitoring of complex industrial processes with particle filters," in Proceedings of Neural Information Processing Systems (NIPS), 2002.

[13] M. B. Malik, F. M. Malik, and K. Munawar, "Orientation control of a 3-d under-actuated drill machine based on discrete-time equivalent model", International

Journal of Robotics & Automation, vol. 27, no. 4, 2012, DOI: 10.2316/Journal.206.2012.4.206-3324.

[14] E. Chalupa, "Numeric control drilling jig-multiple-axis aerospace drilling machine", US Patent #6419426, issued July 2002.

[15] T.F. Coleman, Li.Yi, " An interior, trust region approach for nonlinear minimization subject to bounds", SIAM Journal on Optimization, Vol. 6, pp. 418–445, 1996.

[16] H. Nisar, A.S. Malik, T.S.Choi, "Multiple initial point prediction based block motion estimation algorithm", IEEE Symposium on Consumer Electronics, pp 1-6, 2007.

[17] Lei Fan, Xiyang Liu, Liping Jia, "A minimum elimination escape function method for multimodal optimization problems", in Tenth International Conference on Computational Intelligence and Security" pp.312-216, 2014.

[18] Peter M. Djuric et.all, "Particle filtering", IEEE Signal Processing Magazine, pp 19-38, Sep 2003

[19] Hassan K. Khalil, Nonlinear systems, 3rd edition, Prentice Hall, 2002.

[20] Alberto Isidori, Nonlinear control systems, 3rd edition, Springer-Verlag, 2001.

[21] Wilson J. Rugh, Linear system theory, Prentice Hall, 1996.

[22] Gene F. Franklin, J. David Powell and Michael L. Workman, Digital Control of Dynamic Systems, 3rd edition, Addison-Wesley, 1998.

[23] Stevens, B.L., Lewis, F.L., "Aircraft control and simulation", Second edition, USA,Wiley, 2003.

[24] Savet, P.H., "Gyroscopes theory & design with applications to instrumentation, guidance and control", McGraw-Hill, 1961.

[25] Longuski, J. M., "Solution of euler's equations of motion and eulerian angles for near symmetric rigid bodies subject to constant moments", AIAA/AAS Astrodynamics conference, AIAA-80-1642, Massachusetts, USA, August 11 -13, 1980.

[26] Erwin Kreyszig, Advanced engineering mathematics, 8^{th} edition, John-Wiley and Sons, 1983.

[27] A. Ali and M. B. Malik, "Pulse Equivalent Area based Orientation of a Class of Under-Actuated System under Constraints", Accepted, Under publishing in Mehran University Research Journal Of Engineering & Technology.

[28] H. Nisar, A.S. Malik and T.S.Choi, "Multiple initial point prediction based block motion estimation algorithm", IEEE Symposium on Consumer Electronics, pp 1-6, 2007.

[29] Lei Fan, Xiyang Liu and Liping Jia, "A minimum elimination escape function method for multimodal optimization problems", Tenth International Conference on Computational Intelligence and Security" pp.312-216, 2014

[30] J.E. Dennis, “Nonlinear least-squares state of the art in numerical analysis”, Academic Press, pp. 269-312, 1977.

[31] T.F. Coleman and Li.Yi, “ An interior, trust region approach for nonlinear minimization subject to bounds”, SIAM Journal on Optimization, Vol. 6, pp. 418–445, 1996.

[32] David G. Luenberger, “Observers for multivariable systems”, IEEE Trans. on Automat. Contr., Vol. AC-11, pp. 190-197, Apr. 1966.

[33] David G. Luenberger, “An introduction to observers”, IEEE Trans. on Automat. Contr., Vol. AC-16, No. 6, pp. 596-602, Dec. 1971.

[34] Prashant G.Mehta, Sean. P. Meyn, “A feedback particle filter based approach to optimal control with partial observations”,52nd IEEE conference on decision and control, 10Dec2013, Florence, Italy

[35] A. M. Dabroom and H. K. Khalil, “Output Feedback Sampled Data Control of Nonlinear Systems Using High-Gain Observers”, IEEE Trans. Automatic. Contrl,vol. 46, No 11, Nov. 2001.

[36] S.W. Jeon, S. Jung, “ Novel analysis of limit cycle for PWM signal of PD control system”, IEICE Electronic Express, Vol 6, No. 11, pp 787-793, 2009.

[37] A. Ali and M. B. Malik, “Pulse Equivalent Area based Orientation of a Class of Under-Actuated System under Constraints”, In Press, Mehran University Research Journal Of Engineering & Technology.

[38] A. Ali, M.Laiquat and M. B. Malik, “Control of Under-Actuated System with input Constraints”, Pakistan Journal of Engineering and Applied Sciences, Vol 19, pp 51-62, July 2016.

[39] C. Criens, F. Willems, M. Steinbuch, “Under actuated air path control of diesel engines for low emissions and high efficiency”, Proceedings of the FISITA 2012 World Automotive Congress, Vol. 189, pp 725-737, 2013.

[40] W. Dong, G. Y. Gu, X. Zhu, H. Ding, “Solving the boundary value problem of an under-actuated quadrotor with subspace stabilization approach” in Journal of Intelligent & Robotic Systems, 2014. DOI 10.1007/s10846-014-0161-3.

[41] N. P. I. Aneke, “Control of under actuated mechanical systems”, PhD Dissertation, Netherlands, 2003.

[42] Y. Sagara, N. Hori, “Experimental verification of roll-angle control using air-jet pulse actuation”, The 2nd International Conference on Computer and Automation Engineering (ICCAE), Vol. 5, pp. 418-422, 2010.

[43] Jun He, Feng Gao, Dan Zhang, “Design and performance analysis of a novel parallel servo press with redundant actuation”, International Journal of Mechanics and Materials in Design, Vol. 10, Issue 2, pp 145-163, 2014.

[44] R. E. Andeen, “The principle of equivalent areas”, Transactions AIEE, Vol.79, pp. 332-336, 1960.

[45] T. Suzuki, T. Ueno, N. Hori, "Experimental verification of PEA-based PWM control using on-off type air-jet thrusters", Proceedings of the International Conference on Information and Automation, Sri Lanka, 2005.

[46] T. Sakamoto, N. Hori, "New PWM schemes based on the principle of equivalent areas", IEEE International Symposium on Industrial Electronics, L'Aquila, Italy, pp. 505-510, 2002.

[47] Y. Sagara, N. Hori, "Experimental verification of roll-angle control using air-jet pulse actuation", The 2nd International Conference on Computer and Automation Engineering (ICCAE), Vol. 5, pp. 418-422, 2010.

[48] F. Farivar et.all, "Synchronization of Under actuated Unknown Heavy Symmetric Chaotic Gyroscopes via Optimal Gaussian Radial Basi Adaptive Variable Structure Control", in IEEE Transactions on control systems technology, Vol.. 21, No. 6, pp. 2374-2379, 2013.

[49] G. He, Z.Geng, "Dynamics and robust control of an under actuated torsional vibratory gyroscope actuated by electrostatic actuator", IEEE/ASME Transactions on Mechatronics, 2014, DOI: 10.1109/TMECH.2014.2350535.

[50] T. Ieko, Y. Ochi, K. Kanai, N. Hori, and P. N. Nikiforuk, "Design of a pulse-width-modulation spacecraft attitude control system via digital redesign,", Proc. of IFAC World Congress, Beijing, pp. 355-360,1999.

[51] Doucet, N. de Freitas, K. Murphy, and S. Russell, “Rao-Blackwellised particle filtering for dynamic Bayesian networks,” in Proceedings of the Conference on Uncertainty in Artificial Intelligence (UAI), 2000.

[52] J. Gordon, D. J. Salmond, and A. F. M. Smith, “Novel approach to nonlinear/non-Gaussian Bayesian state estimation,” IEE Proceedings - F, vol. 140, no. 2, pp. 107–113, Apr. 1993.

[53] Blackmore, S. Funiak, and B. C. Williams, “Combining stochastic and greedy search in hybrid estimation,” in Proceedings of 20th National Conference on Artificial Intelligence (AAAI05), 2005.

[54] Rahat Ali, Mohammad Bilal Malik, Fahad Mumtaz Malik and Atif Qayyum “Linear Sampled-Data Reconstruction Observers”, under review in IEEE Transactions on Automatic Control.

[55] Maopeng Ran, Qing Wang and Chaoyang Dong, “Stabilization of a class of nonlinear systems with actuator saturation via active disturbance rejection control”, Automatica, Volume 63, January 2016, Pages 302–310.

[56] Qing Wang, Maopeng Ran and Chaoyang Dong, “An analysis and design method for a class of nonlinear systems with nested saturations”, International Journal of Control, Volume 89, Issue 8, Pages 1711-1724.